

**ACUTE KIDNEY INJURY IN ZEBRAFISH LARVAE AS A REGENERATION MODEL
FOR DRUG DISCOVERY**

by

Lauren Brilli Skvarca

B.S. in Biomedical Engineering, Washington University in St. Louis, 2009

Submitted to the Graduate Faculty of the
School of Medicine in partial fulfillment
of the requirements for the degree of
Doctor of Philosophy

University of Pittsburgh

2015

UNIVERSITY OF PITTSBURGH

SCHOOL OF MEDICINE

This dissertation was presented

by

Lauren Brilli Skvarca

It was defended on

June 30, 2015

and approved by

Carlton M. Bates, MD, Professor, Pediatrics

Jeffrey L. Brodsky, PhD, Professor, Biological Sciences

Thomas R. Kleyman, MD, Professor, Medicine

Donghun Shin, PhD, Assistant Professor, Developmental Biology

Dissertation Advisor: Neil A. Hukriede, PhD, Associate Professor, Developmental Biology

Copyright © by Lauren Brilli Skvarca

2015

ACUTE KIDNEY INJURY IN ZEBRAFISH LARVAE AS A REGENERATION MODEL FOR DRUG DISCOVERY

Lauren Brilli Skvarca

University of Pittsburgh, 2015

Acute kidney injury (AKI) is a serious disorder for which there are limited clinical treatments. The Hukriede lab utilizes zebrafish as a screening model to identify small molecules that promote expansion of renal progenitor cells (RPCs) in the embryo, with the hypothesis that these compounds might also be effective AKI therapeutics by enhancing innate renal regenerative processes. This approach identified 4-(phenylthio)butanoic acid (PTBA), a novel class of histone deacetylase inhibitors (HDACi) that promotes RPC proliferation in zebrafish embryos by stimulating retinoic acid (RA) signaling. To evaluate the therapeutic potential of PTBA-class HDACi, we used a nephrotoxic model of gentamicin-induced AKI in zebrafish larvae that demonstrates the same hallmarks of renal injury and regeneration as the mammalian kidney. In this model, we show that m4PTB, the esterified version of PTBA, enhances post-AKI recovery by increasing dedifferentiation and proliferation of renal tubular epithelial cells (RTECs). To evaluate whether RA signaling also mediates m4PTB's effects in this AKI model, we used *Tg(12XRARE:EGFP)* larvae to show that RA signaling increases rapidly after AKI, and that this response is critical for RTEC-dependent regeneration. Finally, we show that although m4PTB does not directly stimulate RA signaling in zebrafish larvae, blocking the RA pathway abrogates m4PTB's effects on RTEC proliferation. These studies indicate that enhanced AKI recovery following m4PTB treatment requires intact RA signaling, and provide mechanistic insight into the signaling pathways involved in kidney regeneration post-AKI. Given the significant

healthcare burden posed by AKI, these are critical initial steps in order to improve the treatment options available to patients.

TABLE OF CONTENTS

PREFACE.....	XIV
1.0 INTRODUCTION.....	1
1.1 DEVELOPMENT AND FUNCTION OF THE VERTEBRATE KIDNEY ..	1
1.1.1 Overview of vertebrate kidney development	1
1.1.2 Kidney structure and function	5
1.2 ACUTE KIDNEY INJURY	5
1.2.1 Definition and epidemiology	5
1.2.2 Pathophysiology	6
1.2.2.1 Renal tubular epithelial component	6
1.2.2.2 Vascular component	8
1.2.2.3 Inflammatory component.....	9
1.2.3 Treatment and outcome	10
1.3 HISTONE DEACETYLASE INHIBITORS AND KIDNEY DISEASE	12
1.3.1 Overview.....	12
1.3.2 HDAC function	12
1.3.3 HDAC classification	13
1.3.4 Available HDAC inhibitors.....	14
1.3.5 Toxicities and limitations of HDACi therapy.....	16

1.3.6	HDACi attenuate fibrosis and inflammation in kidney disease	17
1.3.7	HDACi in acute kidney injury.....	20
1.4	RETINOIC ACID SIGNALING.....	22
1.4.1	Pathway overview	22
1.4.2	Role in renal development	23
1.4.3	Role in renal disease and regeneration	24
1.4.4	RA signaling and HDACs	26
1.5	LARVAL ZEBRAFISH AS A MODEL SYSTEM.....	27
1.5.1	General strengths of the zebrafish model system	27
1.5.2	Zebrafish larvae as an AKI model	28
1.5.3	Zebrafish larvae as a drug discovery model	28
2.0	CHARACTERIZATION OF THE ACUTE KIDNEY INJURY ENVIRONMENT IN ZEBRAFISH LARVAE	30
2.1	HYPOTHESIS	30
2.2	RESULTS	30
2.2.1	Gentamicin induces renal failure in zebrafish larvae	30
2.2.2	Gentamicin injection induces renal tubular injury	33
2.2.3	Renal tubular regeneration after gentamicin-AKI.....	37
2.2.4	Immune response during gentamicin-AKI.....	40
2.3	METHODS.....	47
2.3.1	Zebrafish husbandry	47
2.3.2	Gentamicin microinjection	47
2.3.3	Histological analysis	48

2.3.4	RNA isolation and quantitative RT-PCR.....	49
2.3.5	EdU labeling.....	49
2.3.6	Live zebrafish confocal imaging.....	50
2.4	DISCUSSION.....	51
3.0	HISTONE DEACETYLASE INHIBITOR M4PTB ENHANCES RECOVERY AFTER AKI IN ZEBRAFISH LARVAE.....	55
3.1	HYPOTHESIS	55
3.2	RESULTS.....	55
3.2.1	Establishing dosing with m4PTB in zebrafish larvae.....	55
3.2.2	Post-injury m4PTB treatment increases survival after gentamicin-AKI.	58
3.2.3	m4PTB treatment increases PT cell proliferation post-AKI.....	59
3.2.4	m4PTB increases tubular cell dedifferentiation post-AKI	62
3.2.5	m4PTB treatment does not affect the innate immune response.....	64
3.3	METHODS.....	66
3.3.1	Zebrafish husbandry	66
3.3.2	Gentamicin microinjection	66
3.3.3	MTD assay.....	66
3.3.4	Histone hyperacetylation assay	67
3.3.5	Histological analysis	67
3.3.6	Survival assay with m4PTB	68
3.3.7	EdU labeling.....	68
3.4	DISCUSSION.....	68

4.0	INTERSECTION OF M4PTB AND THE RETINOIC ACID PATHWAY IN	
	AKI	73
4.1	HYPOTHESIS	73
4.2	RESULTS	74
4.2.1	RA signaling increases in the pronephros after gentamicin injection	74
4.2.2	RA signaling is activated in injured tubular epithelial cells.....	76
4.2.3	Inhibition of RA signaling impairs survival after AKI.....	77
4.2.4	Inhibition of RA signaling impairs tubular regeneration after AKI.....	79
4.2.5	Short-term ATRA treatment increases survival during AKI	81
4.2.6	Mechanism of m4PTB action requires intact RA signaling	81
4.3	METHODS	86
4.3.1	Zebrafish husbandry	86
4.3.2	Gentamicin microinjection, chemical treatments, and heat shock	86
4.3.3	In situ hybridization	87
4.3.4	DN-RARα protein analysis	87
4.3.5	Histological analysis	88
4.3.6	RNA isolation and quantitative RT-PCR.....	88
4.3.7	Live confocal zebrafish imaging.....	88
4.3.8	Analysis of GFP fluorescence intensity.....	88
4.4	DISCUSSION.....	89
5.0	GENERAL DISCUSSION	93
	APPENDIX A	97
	APPENDIX B	99

BIBLIOGRAPHY	101
---------------------------	------------

LIST OF TABLES

Table 1: Histology summary of antibodies and conditions.	99
Table 2: qRT-PCR primer sequences.	99
Table 3: Raw qRT-PCR data for zebrafish studies.	100

LIST OF FIGURES

Figure 1: Schematic of mammalian embryonic kidney development.	3
Figure 2: Schematic of pronephric kidney development in zebrafish.	4
Figure 3: Cellular hallmarks of AKI.	8
Figure 4: Characteristic design of HDAC inhibitors.	16
Figure 5: Summary of HDACi therapies used in renal disease models.....	18
Figure 6: Gentamicin injection induces edema and death in zebrafish larvae.....	32
Figure 7: Zebrafish larvae show morphological hallmarks of AKI after gentamicin injection....	34
Figure 8: Renal tubular cells express Kim1 after gentamicin injury in zebrafish larvae.....	36
Figure 9: Renal tubular cells express Pax2a after gentamicin injury in zebrafish larvae.	38
Figure 10: Proliferation of PT cells after gentamicin-AKI.	39
Figure 11: Neutrophils infiltrate the kidney after gentamicin-AKI in zebrafish larvae.	41
Figure 12: Gentamicin injury results in increased renal neutrophils.	43
Figure 13: Dispersion of the neutrophil niche in the pronephric kidney after AKI.....	44
Figure 14: Gentamicin injury results in increased renal macrophages.	46
Figure 15: MTD and m4PTB-induced hyperacetylation in zebrafish larvae.....	57
Figure 16: Edema and PT cell polarity after gentamicin-induced AKI at 2 dpi.	58
Figure 17: m4PTB treatment increases larval survival after AKI.	59

Figure 18: m4PTB treatment increases PT cell proliferation.	61
Figure 19: m4PTB expands the Pax2a-positive population of PT cells post-AKI.	63
Figure 20: m4PTB treatment does not affect post-AKI neutrophil or macrophage infiltration. ..	65
Figure 21: RA signaling is increased in zebrafish larval kidneys after AKI.	75
Figure 22: RA signaling increases in renal epithelial cells after AKI.	76
Figure 23: RA signaling is activated in Kim1-positive renal epithelium.	77
Figure 24: Ro41-5353 treatment inhibits RA signaling and impairs survival after AKI.....	78
Figure 25: Blocking the RA pathway impairs tubular proliferation after AKI.....	80
Figure 26: Effect of ATRA on survival after AKI depends on treatment duration.	81
Figure 27: m4PTB does not synergize with ATRA to drive RARE:EGFP expression.....	82
Figure 28: Time course of DN-RAR α activation after heat shock.	83
Figure 29: m4PTB treatment does not activate DN-RAR α expression.	84
Figure 30: DN-RAR α induction impairs m4PTB-mediated RTEC proliferation.....	85
Figure 31: Anatomic orientation on transverse sections of zebrafish larvae.	97
Figure 32: Fluorescence western raw images.	98

PREFACE

*“Alone we can do so little; together we can do so much.”
-Helen Keller*

To all who provided help, support, and guidance:

to John Shannon and James Bridges, my first mentors in science...

to Neil Hukriede, my graduate thesis advisor...

to the fish community at the University of Pittsburgh...

to all current and former members of the Hukriede lab, particularly Chiara Cianciolo Cosentino, Jessica Fall, and Clara Woods...

to our collaborators, particularly Mark de Caestecker...

to the DLAR staff and administrative staff of the Medical Scientist Training Program, Graduate School of Medicine, and Department of Developmental Biology...

to the members of my thesis committee...

to my friends and family...

and to my husband Andrew...

Thank you.

Commonly used terms and abbreviations:

3G8	unknown antigen marking the apical brush border of the pronephric tubule
AKI	acute kidney injury
ATRA	all-trans retinoic acid
BMP	bone morphogenic protein
DMSO	dimethyl sulfoxide
DPF	days post fertilization
DPI	days post injection
EDU	5-ethynyl-29-deoxyuridine
EGFP	enhanced green fluorescent protein
GENT-AKI	zebrafish larvae injected with gentamicin
GFR	glomerular filtration rate
HAT	histone acetyl transferase
HDAC	histone deacetylase
HDACI	histone deacetylase inhibitor
HPF	hours post fertilization
HPI	hours post injection
IR-AKI	ischemia reperfusion acute kidney injury
KIM1	kidney injury molecule 1
M4PTB	methyl-4-(phenylthio)butanoate
MCP1	monocyte chemotactic protein 1
MTD	maximum tolerated dose
N-COR	nuclear receptor corepressor

PCNA	proliferating cell nuclear antigen
PT	proximal tubule
PTBA	4-(phenylthio)butanoic acid
PTU	1-phenyl-2-thiourea
RA	retinoic acid
RALDH	retinaldehyde dehydrogenase
RAR	retinoic acid receptor
RARE	retinoic acid response element
RPC	renal progenitor cell
RTEC	renal tubular epithelial cell
SAHA	suberoylanilide hydroxamic acid
SMRT	silencing mediator for retinoid and thyroid receptors
TGF- β	transforming growth factor-beta
TNF- α	tumor necrosis factor-alpha
TSA	trichostatin A
TUNEL	terminal deoxynucleotidyl transferase dUTP nick end-labeling
UUO	unilateral ureteral obstruction
VPA	valproic acid

1.0 INTRODUCTION

1.1 DEVELOPMENT AND FUNCTION OF THE VERTEBRATE KIDNEY

1.1.1 Overview of vertebrate kidney development

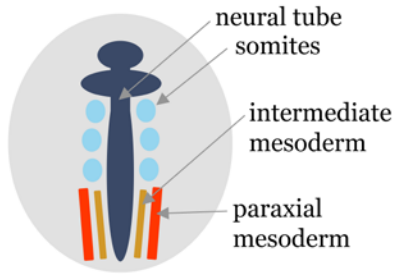
Three kidney structures form successively during embryonic development: the pronephros, mesonephros, and metanephros. The pronephros, the simplest of these structures, is nonfunctional in mammals but functions as the larval kidney of fish and amphibians^{1, 2}. The mesonephros serves as the embryonic kidney of mammals and the mature kidney of fish and amphibians^{1, 2}. Although transient, these structures are critical for proper development of the metanephric kidney, which is the adult kidney of mammals, birds, and reptiles².

In mammals, the kidney arises from the primary nephric duct (Wolffian duct), a set of bilateral epithelial tubes derived from Lhx1/Pax2/Pax8-positive cells of the intermediate mesoderm^{3, 4} (Figure 1A). As the nephric duct grows caudally in the embryo, a network of tubules develops from the surrounding mesenchyme¹. The rostral tubes of this network are rudimentary and comprise the pronephros, whereas the caudal tubes are more defined and comprise the mesonephros^{1, 2} (Figure 1B).

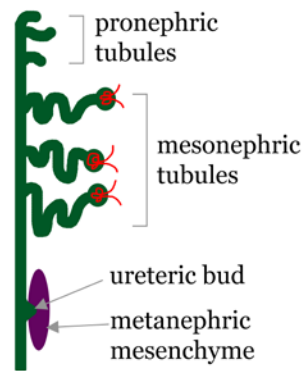
The metanephric kidney develops at the caudal end of the nephric duct, where an outgrowth of epithelial cells forms the ureteric bud. Interactions between cells of the ureteric bud

and surrounding metanephric mesenchyme governed by Ret/Gdnf signaling induce rounds of ureteric bud branching, which ultimately determines the number of nephrons, the functional units of the kidney⁵⁻⁸. Collections of Six2/Cited1-positive metanephric mesenchyme cells condense at the tips of the branching ureteric bud, undergo mesenchymal-to-epithelial transition, and form renal vesicles. The renal vesicle then forms the comma-shaped body, followed by the s-shaped body (Figure 1C). These final structures form the nephron and are patterned such that the proximal end forms the glomerulus, and the distal end forms the connecting tubule, which connects to the ureteric bud-derived collecting duct (Figure 1D). Foxd1-positive metanephric mesenchyme gives rise to the cortical renal stroma, and Flk1-positive cells contribute to the renal vasculature⁹. Nephron formation concludes by gestational week 36 in humans and continues through 10 days after birth in mice¹⁰.

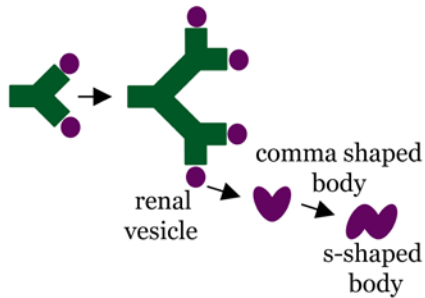
A. Specification of the renal field



B. Growth of the Wolffian duct and outgrowth of the ureteric bud



C. Branching of the ureteric bud and nephron development



D. Segmentation of mature nephrons

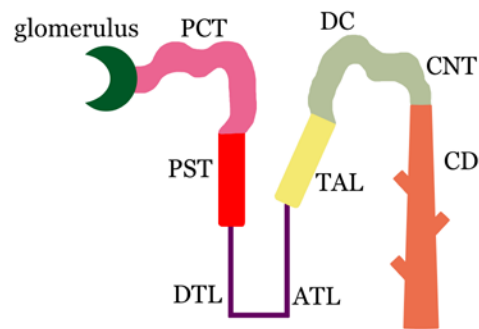
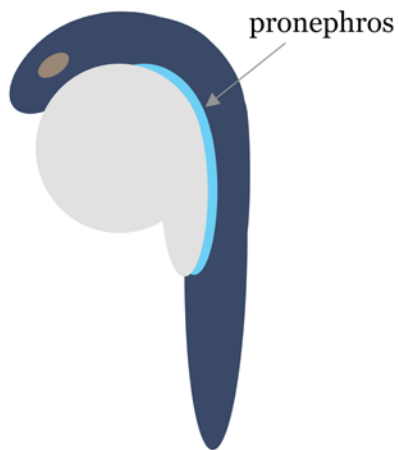


Figure 1: Schematic of mammalian embryonic kidney development.

(A) Specification of the kidney field from intermediate mesoderm. (B) Formation of the pronephros and mesonephros, and budding of the ureteric bud from the Wolffian duct. (C) Iterative branching of the ureteric bud and early development of nephrons from renal vesicles. (D) Depiction of mature nephron segments: proximal convoluted tubule (PCT), proximal straight tubule (PST), descending and ascending thin limb (DTL, ATL), thick ascending limb (TAL), distal convoluted (DC), connecting tubule (CNT), collecting duct (CD).

Analogous to mammalian renal development, the kidney of lower vertebrates including zebrafish is derived from a population of *pax2a/pax8/lhx1a*-positive renal progenitor cells (RPCs) in the intermediate mesoderm (Figure 1A)^{2, 11}. These progenitors undergo mesenchymal-to-epithelial transition to form the pronephros (Figure 2A), which consists of two glomeruli fused at the midline located between the neural tube and spinal cord, and two tubules located above the yolk^{2, 11}. RPCs are patterned such that anterior cells give rise to proximal nephron segments and posterior cells give rise to distal segments (Figure 2B)¹². Epithelialization of the pronephros is complete by 24 hours post fertilization (hpf), and the glomerulus is fully vascularized by 4 days post fertilization (dpf)². Unlike in mammals, the pronephros functions as the larval and juvenile kidney in zebrafish until formation of the mesonephric kidney, which begins at 11 dpf¹³. Developmental studies in animal models including zebrafish embryos have been instrumental in advancing our understanding of the cellular and molecular events that control kidney organogenesis^{1, 8-10, 14}.

A. Formation of the pronephros



B. Segmentation of pronephric nephrons

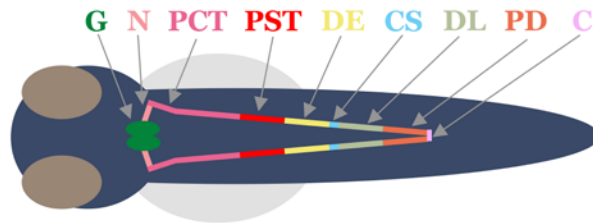


Figure 2: Schematic of pronephric kidney development in zebrafish.

(A) RPC progenitors in the embryo define the pronephros. (B) The mature pronephros consists of two glomeruli (G) fused at the midline, and two bilateral nephrons patterned into distinct segments: neck (N), proximal convoluted tubule (PCT), proximal straight tubule (PST), distal early (DE), corpuscle of Stannius (CS), distal late (DL), and pronephric duct (PD). These segments terminate at the cloaca (C).

1.1.2 Kidney structure and function

The kidney performs several critical functions. These include blood filtration to remove metabolic waste, regulation of fluid and electrolyte balance, and maintenance of bone density. Accomplishing these functions requires the coordination of 26 cell types comprising the metanephric kidney, which are organized into a sophisticated set of vascularized nephron filtering units that drain into a collecting system for urine excretion¹⁵. Nephrons consist of a glomerulus, the location of blood filtration, and an epithelial tubule that alters filtrate content. The tubule is divided into distinct segments characterized by unique expression profiles of transport proteins that determine function. In general, proximal segments are responsible for fluid reabsorption from the filtrate, whereas distal segments and collecting duct fine-tune the composition of the filtrate. Each human kidney contains on average 900,000 nephrons, with greater than 10-fold variation existing in the adult population¹⁶. Low nephron number is associated with both renal and cardiovascular disease^{16, 17}, pointing to the importance of understanding the mechanisms of kidney development, injury, and repair.

1.2 ACUTE KIDNEY INJURY

1.2.1 Definition and epidemiology

Acute kidney injury (AKI) is the rapid decline in renal function as defined by changes in serum creatinine, glomerular filtration rate (GFR), and urine output^{18, 19}. AKI is common, occurring in

3-20% of hospitalized patients^{20, 21} and in 11-67% of ICU patients²²⁻²⁵, with rates continuing to rise²⁶. Rather than a single condition, AKI represents a spectrum of diseases, with increased severity correlating with worsened outcome and higher mortality^{22, 27-29}. Ultimately, AKI accounts for at least \$10 billion in US healthcare costs²⁸ and results in 2 million deaths annually worldwide³⁰.

1.2.2 Pathophysiology

Leading causes of AKI include sepsis, heart failure, major surgery, and nephrotoxins²⁹⁻³¹. In reality, the etiology is generally multifactorial and involves combinations of these factors³⁰. Since renal biopsy is rarely indicated in AKI patients, the mechanisms underlying pathophysiology have been largely defined using rodent animal models³². Perhaps the most well-characterized model is ischemia reperfusion AKI (IR-AKI), in which investigators temporarily clamp the renal artery resulting in organ ischemia. Although not a perfect model, especially in recapitulating aspects of sepsis-induced AKI^{30, 33, 34}, ischemia is an important component of AKI regardless of initial insult³⁵. Given the scarcity of human kidney tissue, the IR-AKI model has been pivotal in advancing our understanding of AKI pathophysiology in humans. These studies have identified key players during AKI events that interact in three main compartments: the tubular epithelium, vascular endothelium, and cells of the immune system. These components are described individually below.

1.2.2.1 Renal tubular epithelial component

In IR-AKI, kidney hypoperfusion triggers endothelial vasoconstriction, which exacerbates local ischemia and ultimately depletes ATP in renal tubular epithelial cells (RTECs)³⁶⁻³⁸. Due to a high

metabolic workload and location in the kidney, epithelial cells in the proximal tubule (PT) are particularly susceptible to ischemic injury, but distal tubular cells are also affected³⁹. Epithelial damage is manifested by loss of the apical brush border, disrupted apical-basal cell polarity, and weakened cellular junctions^{35, 37}. Severely injured cells undergo cell death, with various populations exhibiting autophagy, apoptosis, or necrosis⁴⁰⁻⁴³, leaving bare patches of basement membrane. These changes result in sloughing of cellular debris and contribute to obstruction of the tubular lumen, accumulation of fluid in the interstitial space, and activation of immune cells³⁷ (Figure 3A-B). Blocking apoptotic cell death by inhibiting either p53 or caspase signaling has been shown to be renoprotective and improves outcome after AKI⁴⁴⁻⁴⁷.

Since nephrogenesis halts shortly after birth in mammals^{48, 49}, recovery after AKI depends on the repair of damaged tubules. Injured RTECs dedifferentiate and proliferate to repopulate areas of lost cells⁵⁰ (Figure 3C). During these processes, cells reactivate developmentally-expressed genes and pathways^{14, 51}, including vimentin⁵², Pax2⁵³, Lhx1⁵⁴, and Wnt signaling^{55, 56}. These mechanisms comprise the kidney's post-injury regenerative potential.

In contrast to proliferation-mediated repair, maladaptive epithelial responses have also been observed after injury. A proportion of RTECs that attempt to proliferate do not successfully complete the cell cycle and arrest in G2/M⁵⁷. These arrested cells activate c-Jun N-terminal kinase (JNK) signaling, resulting in the secretion of profibrotic factors including transforming growth factor beta 1 (TGF- β 1) and connective tissue growth factor (CTGF)⁵⁷ (Figure 3D). These events have negative consequences for recovery. First, cell cycle arrest depletes the proliferative pool that replaces dead cells. Second, RTEC secretion of profibrotic factors activates fibroblasts and contributes to tissue scarring. What triggers these maladaptive responses remains poorly understood and actively investigated.

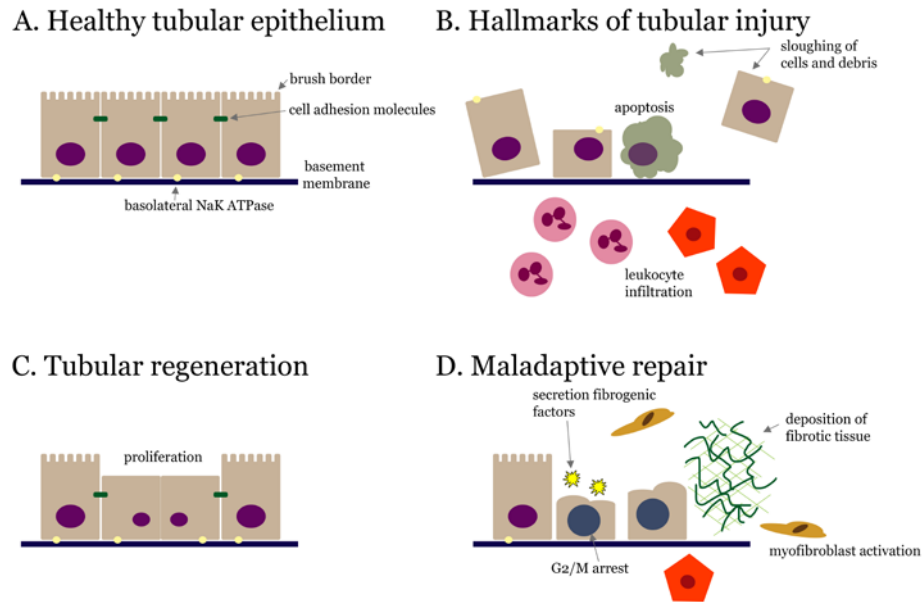


Figure 3: Cellular hallmarks of AKI.

(A) Healthy tubular epithelial cells, with intact cellular junctions and apical-basal polarity. (B) Characteristic cellular changes induced by AKI include loss of brush border and apical-basal polarity, sloughing of cellular debris, and influx of immune cells. (C) Epithelial proliferation response post-injury. (D) Some injured epithelial cells arrest in G2/M and secrete profibrotic factors, leading to scar tissue formation and maladaptive repair.

1.2.2.2 Vascular component

The vasculature performs several important functions to ensure adequate blood flow. Endothelial cells regulate vessel tone, maintain proper permeability, block cellular adhesion, and support anti-coagulation. AKI impairs all of these functions, and compared to the tubular epithelium, the renal vascular endothelium demonstrates minimal regeneration³⁸.

AKI rapidly disrupts endothelial cell-cell junctions, resulting in capillary leak within 2 hours post-injury⁵⁸. Injured endothelial cells also upregulate cell adhesion molecules including intercellular adhesion molecule 1 (ICAM-1) and E/P-selectins^{38, 59-61}. Combined, these changes facilitate the adhesion and transmigration of leukocytes. Finally, injured endothelial cells decrease production of anti-coagulation proteins, activating the clotting response³⁸. The net result of these changes is the occlusion of small vessels, which further exacerbates ischemia and

cellular injury. Ultimately, many of these small vessels are lost (“vascular dropout”), contributing to long-term hypoxia and predisposing the kidney to future injury. Strategies to preserve the renal endothelium have been shown to be beneficial in animal AKI models and include increasing vasodilation, enhancing anti-coagulation, and blocking leukocyte adhesion^{37, 38, 62}. These studies, however, provide only renoprotective benefits and may not be viable post-injury treatment options.

Additionally, the injured vascular system may contribute to renal fibrosis. In the uninjured kidney, pericytes surround and communicate with endothelial cells to regulate barrier function and vascular tone. Several studies suggest that during AKI, pericytes detach and differentiate into activated interstitial myofibroblasts. These cells generate fibrotic tissue around dying tubules⁶³⁻⁶⁶. Blocking pericyte detachment decreased fibrosis in a mouse unilateral ureteral obstruction (UUO) model, providing further evidence that pericyte activation results in fibrosis⁶⁷.

1.2.2.3 Inflammatory component

In the healthy kidney, the immune cell population is sparse and consists primarily of resident dendritic cells and macrophages that help maintain homeostasis^{68, 69}. Upon injury, RTECs increase expression of the toll-like receptors TLR2 and TLR4 and produce a milieu of pro-inflammatory cytokines, including tumor necrosis factor-alpha (TNF- α) and TGF- β 1, which attract leukocytes to the kidney^{70, 71}. As described above, injured endothelial cells are also key participants in leukocyte infiltration.

The innate immune response is activated rapidly, with neutrophils arriving within 30 minutes of IR-AKI injury⁷². These phagocytes clear pathogens and cellular debris, secrete tissue-remodeling factors, and attract macrophages. The role of neutrophils in AKI is up for debate. Some groups demonstrated amelioration of injury and preservation of endothelial barrier

function when neutrophil transmigration was inhibited^{59, 73}, while other studies reported no effect^{74, 75}. These findings are not surprising given the diversity of neutrophil functions, and warrant careful studies that evaluate timing and depletion efficiency in the context of a particular model.

Heterogeneous macrophage populations have been identified that participate in both tissue injury and repair^{76, 77}. Early in the course of injury, inducible nitric oxide synthase (iNOS)-positive M1-type macrophages infiltrate the kidney and perpetuate damage and epithelial apoptosis by secreting pro-inflammatory cytokines and producing reactive oxygen species (ROS)⁷⁷. Depletion of macrophages during this early phase decreases tubular cell death and prevents renal functional impairment^{78, 79}. Between 2 and 3 days after injury, environmental cues, for example phagocytosis of apoptotic cells, trigger suppression of M1 macrophages and promote M2 polarization^{77, 78}. M2 macrophages express arginase 1 and mannose receptor (MR) and are generally considered to promote tissue repair. These repair phase macrophages proliferate in situ⁸⁰, protect RTECs from apoptosis, and promote cell cycle progression^{56, 81, 82}. Several studies have demonstrated the importance of this phenotype switch. Failure to suppress the M1 phenotype leads to poor long-term outcome with increased fibrosis⁸³. Suppressing M2 proliferation or depleting macrophages late during repair when these cells predominate increases injury, impairs functional recovery, decreases epithelial proliferation, and increases fibrosis^{56, 78, 80, 84}. Directly administering M2-polarized cells is renoprotective during AKI⁸⁵.

1.2.3 Treatment and outcome

Effective AKI treatment relies on early diagnosis and identification of the underlying cause. There are currently no targeted clinical treatments that accelerate renal recovery or decrease

fibrosis when administered after injury. Treatment is supportive and includes discontinuation of nephrotoxic therapies, fluid resuscitation, and renal replacement therapy³⁰. Although the timing and intensity of these treatments remains controversial⁸⁶⁻⁸⁸, it is generally accepted that early intervention leads to higher patient survival⁸⁹.

Severe AKI that requires renal replacement therapy carries the highest mortality rate of up to 60%^{29, 90}, but even mild AKI is associated with increased risk of death^{91, 92}. It was previously believed that renal function returned to baseline after resolution of an AKI episode^{93, 94}, but accumulating evidence points to AKI as a significant risk factor for chronic kidney disease^{95, 96}.

Several mechanisms have been proposed to mediate the transition from AKI to chronic kidney disease. First, nephron loss during AKI exposes surviving nephrons to increased workload and increased cellular stress, thus decreasing future regenerative capability^{96, 97}. Second, severe AKI causes cell cycle arrest in G2/M phases and subsequent production of profibrotic factors that promote scar tissue formation⁵⁷. Third, it has been shown that persistence of the inflammatory response after AKI, in particular M1 macrophages, exacerbates fibrosis^{83, 98}. Finally, endothelial damage and vascular dropout during AKI lead to hypoxia, resulting in further inflammation and fibrosis^{66, 96, 97, 99}. Direct causality has not yet been established¹⁰⁰, but these factors may explain how cellular damage that occurs during AKI could lead to fibrosis and long-term renal impairment.

1.3 HISTONE DEACETYLASE INHIBITORS AND KIDNEY DISEASE

1.3.1 Overview

Although initially developed as chemotherapeutic agents, the discovery that histone deacetylase inhibitors (HDACi) can reduce fibrosis and attenuate injury-mediated damage in kidney disease models has opened the possibility of utilizing HDACi as therapeutics for AKI. Since histone deacetylases (HDACs) play multiple roles during both kidney organogenesis¹⁰¹ and the pathogenesis of kidney disease¹⁰², the continued development of isoform-selective HDACi has provided necessary tools to study the individual roles that HDACs play during these processes.

1.3.2 HDAC function

Acetylation and deacetylation of nucleosomal histone proteins serves as a post-translation modification that regulates transcriptional activity. This mechanism involves the interplay between the activity of two enzyme classes: (1) histone acetyltransferases (HATs), which promote an open chromatin configuration and transcriptional activation, and (2) HDACs, which generally promote chromatin condensation and transcriptional repression. Specifically, most HDACs remove acetyl groups from the ϵ -amino moiety of lysine residues located on N-terminal histone tails. This leaves the histone with a net positive charge, strengthening its electrostatic interaction with the DNA phosphate backbone resulting in transcriptional repression of associated genes.

As members of large multiprotein complexes, HDACs also target many non-histone proteins¹⁰³ and, in some instances, participate directly in gene activation^{104, 105}. For example,

HDACs positively regulate the oncogene c-Jun as well as the anti-apoptotic gene B-cell lymphoma 2 (Bcl-2)¹⁰⁵. Additionally, it has been demonstrated that HDACs are required for interferon-induced gene expression, which is critical for an antiviral immunological response¹⁰⁶. Therefore, the function of HDACs, either as corepressors or coactivators, appears to be context-dependent.

1.3.3 HDAC classification

To date, 18 mammalian HDAC proteins have been identified, and they are divided into four classes based on similarity to yeast orthologs¹⁰⁷. Class I, II, and IV enzymes depend on zinc for catalytic activity and contain a highly conserved deacetylase domain^{102, 108}. Class III enzymes (sirtuins) are structurally distinct from the other HDAC classes since the catalytic activity of these enzymes depends on NAD⁺ rather than zinc and histones are not their primary substrate^{102, 108}. Class I is comprised of HDACs 1, 2, 3, and 8. Class II is subdivided into class IIa, containing HDACs 4, 5, 7, and 9, and class IIb which contains HDACs 6 and 10. HDAC 11 is the sole member of Class IV because its catalytic domain resembles the active sites of both class I and class II enzymes¹⁰⁸.

Understanding HDAC substrate specificity, as well as identifying strategies for developing novel isoform-selective HDACi, depends on thoroughly distinguishing between and within HDAC classes^{102, 108, 109}. Class I HDACs are expressed ubiquitously, are localized to the nucleus, and interact with corepressor complexes to exert their function. HDAC1 and HDAC2 are recruited to the nucleosome remodeling and deacetylation (NuRD), corepressor for RE1 silencing transcription factor (Co-REST), and Sin3 corepressor complexes. HDAC3 is most often recruited to the silencing mediator for retinoid and thyroid receptors/nuclear receptor

corepressor (SMRT/N-CoR) complex¹¹⁰. Additionally, the active site of HDAC3 contains a unique tyrosine residue (Tyr198) not present in the active sites of other HDACs in its class, which may contribute to the substrate specificity of HDAC3¹¹¹. HDAC8 does not appear to be recruited to corepressor complexes and is the only class I HDAC with intrinsic enzymatic activity¹¹¹.

In contrast to class I, class II HDACs are thought to have tissue-specific roles, and are expressed in both the cytoplasm and the nucleus¹¹². Class IIa enzymes contain a mutation in the catalytic site, resulting in a 1,000-fold reduction in activity¹⁰⁸. Therefore alternative mechanisms, such as the recruitment of class I HDACs¹⁰⁸ or the interaction with corepressor complexes such as SMRT/N-CoR^{110, 113}, may be required to achieve activity. Additionally, it has been proposed that this class of HDACs might act as “receptors” rather than enzymes, since they often bind acetylated lysine residues without performing the deacetylation reaction¹¹⁴. While little is known about the function of the class IIb member HDAC10, the structure of HDAC6 is unique and consists of two catalytic domains and a zinc finger. Although α -tubulin was thought to be its primary target¹¹⁵, increasing evidence suggests that HDAC6 also plays key functions during cellular stress. By binding ubiquitin, HDAC6 senses the accumulation of misfolded proteins and subsequently activates the heat shock protein response¹¹⁶⁻¹¹⁸.

1.3.4 Available HDAC inhibitors

HDACi targeting class I and II HDACs generally follow a classic warhead-linker-cap structure (Figure 4). The warhead, or chelator, binds zinc in the HDAC catalytic site, rendering the enzyme inactive. The linker is a carbon chain that connects the warhead and cap and spans the length of the HDAC pocket. The cap, or surface-binding domain, interacts with residues on the

surface of the HDAC enzyme and contributes to isoform specificity of the inhibitor¹¹⁴. There are at least four categories of HDACi that adhere to this structure: short chain fatty acids, hydroxamic acids, aminobenzamides, and cyclic peptides. The short chain fatty acids are carboxylic acids that include valproic acid (VPA), butyric acid, phenylbutyrate (PBA), and 4-(phenylthio)butanoic acid (PTBA). These inhibitors are relatively weak and display some class I specificity. The hydroxamic acids are more broad-spectrum inhibitors capable of inhibiting class I and II HDACs, and include trichostatin A (TSA), suberoylanilide hydroxamic acid (SAHA), LBH-589, LAQ-824, and PXD-101. Aminobenzamides are class I-selective and include SNDX-275, MGCD0103, and MS-275. Finally, there are several cyclic peptides, such as depsipeptide (romidepsin/FK-228) and apicidin, which appear moderately selective for class I HDACs^{102, 119}. Although originally isolated as natural compounds, several synthetic analogues have now been created^{120, 121}.

Due to their pro-differentiation, anti-proliferative effects, HDACi have generated excitement in the cancer field as novel chemotherapeutic agents^{122, 123}. Traditionally, PBA has been used to treat disorders of the urea cycle due to its nitrogen scavenging effects since the 1990s¹²⁴. SAHA (vorinostat) was the first FDA-approved HDACi for the treatment of refractory cutaneous T-cell lymphoma¹¹⁹. In addition, about a dozen other compounds have entered clinical trials¹¹⁴ and in 2009, the FDA also approved FK-228 (romidepsin), for treatment of cutaneous T-cell lymphoma¹²⁵. Currently, vorinostat and romidepsin are the only two FDA-approved HDACi.

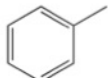
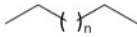
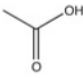
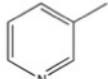
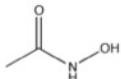
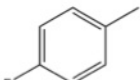
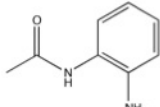
Component	Cap	Linker	Warhead
Example chemical structures	 Basic aryl ring		 Carboxylic acid
	 Aryl ring with substitution		 Hydroxamic acid
	 Aryl ring with modification		 Benzamide
Function	Surface interactions with HDAC protein	Channel spacer	Zinc chelating domain

Figure 4: Characteristic design of HDAC inhibitors.

The general structure of HDACi can be broken into three regions, each with a specific function: cap, linker, and warhead. Modifications can be introduced at each portion of the moiety, contributing to structural diversity¹²⁶.

1.3.5 Toxicities and limitations of HDACi therapy

From a global perspective, patients tolerate HDACi therapy quite well, and the maximum tolerated dose has yet to be reached in some regimens¹²³. Common side effects of vorinostat, romidepsin, and MS-275 include fatigue, nausea, and vomiting, although these are reversible upon treatment withdrawal^{123, 127}. More worrisome, however, are the cardiac and immunologic effects, such as QT prolongation, thrombocytopenia, and/or myelosuppression, following HDACi treatment. Specifically, QT prolongation was observed during clinical trials with romidepsin, although confounding factors were also identified in specific patient populations¹²⁵. Additionally, VPA is a teratogen known to cause neural tube and other birth defects¹²⁸. Although one study determined that TSA administered to pregnant mice did not harm either the mothers or

the pups¹²⁹, further studies are warranted to characterize the specific toxicity profiles associated with various HDACi.

1.3.6 HDACi attenuate fibrosis and inflammation in kidney disease

As described previously, the pathogenesis of many kidney diseases is characterized by dysregulation of cellular proliferation and infiltration by inflammatory cells, leading to irreversible fibrosis. While therapeutic options in the clinic are limited, HDACi are promising treatments for targeting both the profibrotic and inflammatory pathogenic aspects of kidney disease across many injury models^{130, 131}. These studies are summarized in Figure 5¹³²⁻¹³⁹.

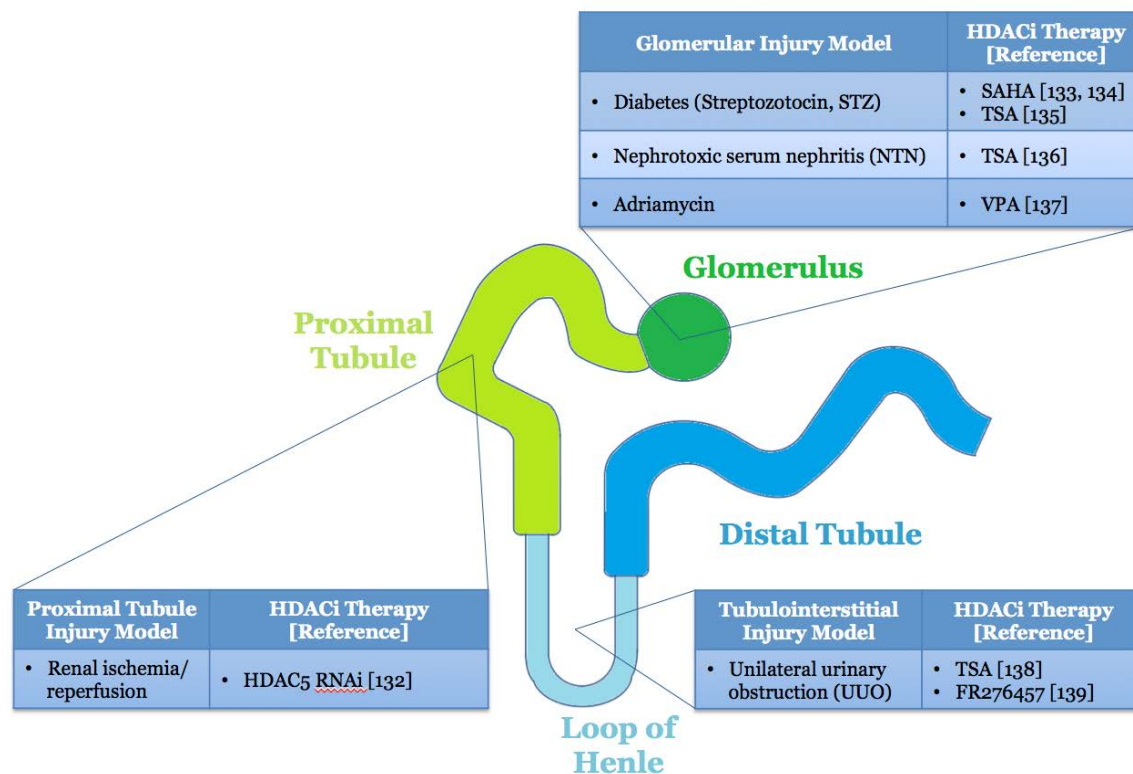


Figure 5: Summary of HDACi therapies used in renal disease models.

Several HDACi have been found to attenuate fibrotic, inflammatory, and proliferative features of renal disease in mammalian models. Studies are organized by location of damage in the nephron in the injury model¹²⁶.

To ameliorate renal fibrosis, researchers have focused their efforts on elucidating the mechanisms of TGF- β signaling. TSA treatment prevented TGF- β 1-dependent responses in cultured human RTECs¹⁴⁰. Cells treated with TSA still demonstrated Smad protein phosphorylation, which relays TGF- β 1 signaling to the nucleus, indicating that TSA blocks the defects of TGF- β 1 downstream of these factors. Co-treatment of human RTECs with TGF- β 1 and TSA prevented TGF- β -induced apoptosis by blocking caspase protein cleavage (also observed in an in vivo model¹³⁸). This effect was mediated by inhibiting extracellular signal-regulated kinase (ERK) activation. This latter finding is notable since recent studies have shown that epidermal growth factor receptor (EGFR) is required for sustained TGF- β -dependent fibrosis in a mouse model of angiotensin II-induced renal fibrosis¹⁴¹. Thus, this work proposes a dual therapeutic role for HDAC inhibition in preventing tubular interstitial fibrosis: (1) suppressing the profibrotic effects of TGF- β 1, and (2) mitigating renal tubular atrophy by protecting against tubular epithelial cell apoptosis.

Additional mechanisms have been proposed for attenuating tubular damage-mediated fibrosis through HDAC inhibition. In a mouse model of UUO, Pang et al. observed a decrease in fibrotic markers in TSA-treated kidneys¹³⁸. This was associated with decreased levels of phosphorylated signal transducer and activator of transcription 3 (STAT3). Since STAT3 has been implicated in the regulation of tubulointerstitial fibrosis following UUO¹⁴² and is a known HDAC target, these findings suggest HDACi may also decrease renal fibrosis by decreasing STAT3 signaling in this model of chronic kidney disease. Thus, HDACi are likely contributing in multiple ways to exert antifibrotic effects.

HDACi have also been implicated in the prevention of inflammatory infiltration after renal damage. Following UUO, there is an increase in both HDAC1 and HDAC2 in the tubular

epithelium. While treatment with TSA decreased fibrosis scores, it also decreased macrophage infiltration and expression of colony-stimulating factor 1 (*Csf1*), a secreted cytokine that promotes proliferation and survival of monocyte/macrophages. Similarly, TSA and VPA were able to attenuate TNF-induced *Csf1* expression in cultured rat RTECs¹⁴³. Work by another group demonstrated that treatment with FR276457, a hydroxamic acid derivative that inhibits both class I and II HDACs, resulted in decreased monocyte chemotactic protein 1 (MCP1) levels, a chemotactic cytokine that normally attracts macrophages to the kidney shortly after UUO¹³⁹. However, the role of macrophages in acute and chronic kidney injury is complex and involves both the detrimental effects of early, inflammatory M1 macrophages, and late, anti-inflammatory M2 macrophages that also enhance epithelial regenerative responses⁶⁸. Therefore HDACi may decrease pro-inflammatory M1 macrophages early, and/or promote expansion of anti-inflammatory and pro-regenerative M2 macrophages later in the course of disease.

1.3.7 HDACi in acute kidney injury

In addition to antifibrotic and anti-inflammatory effects, there is also evidence that epigenetic modulation through HDAC inhibition can promote regeneration after tissue injury by reactivating the expression of signaling machinery normally required during kidney organogenesis. In particular, bone morphogenic protein 7 (BMP7) is detected in the developing mammalian kidney and reactivated after renal ischemia⁵⁴. Further, exogenous BMP7 treatment is therapeutic in rodent kidney injury models¹⁴⁴⁻¹⁴⁶. Several groups have determined that this reactivation may be HDAC dependent.

Marumo et al.¹³² observed that exposure to transient renal ischemia resulted in histone hypoacetylation in mouse PT epithelial cells. This led them to investigate whether HDACs

played a role in modulating the kidney's response to ischemic injury. Recovery after reperfusion in vitro was associated specifically with decreased levels of HDAC5, and knockdown of HDACs 1, 2, or 5 induced expression of *Bmp7*. In vivo, fewer HDAC5-positive cells were observed in the PT after reperfusion, which correlated with histone hyperacetylation and induction of BMP7.

The role of HDACs and BMP7 was examined further in a mouse model of septic AKI¹⁴⁷. In this study, increased *Hdac2* and *Hdac5* and decreased *Bmp7* expression was observed in the kidney after cecal ligation and puncture. However, TSA treatment before surgery prevented *Hdac2* and *Hdac5* induction, and increased *Bmp7*. These changes were associated with enhanced functional recovery and decreased tubular damage, possibly through mitigating inflammation. Accordingly, TSA pre-treatment decreased *Tnfa* and *Mcp1* expression levels in the kidney. Therefore, the induction of BMP7 through HDAC2 or HDAC5 inhibition may prevent renal injury through effects on the inflammatory response.

Finally, Imai et al. showed that TSA treatment prevented proteinuria and blood urea nitrogen (BUN) elevation in nephrotoxic nephritis (NTN) mice¹³⁵. This global attenuation of renal injury was associated with activation of *Bmp7* expression in an uncharacterized side population of cells identified by flow cytometry. Although rather controversial, some believe this side population may constitute a population of intrarenal stem cells^{148, 149}. Since TSA treatment did not increase *Bmp7* expression in other renal cells, this population may serve as a source of BMP7 to promote renal regeneration. This suggests that pharmaceutical HDACi therapy may have the potential to stimulate the BMP pathway – or other developmental pathways – and promote regeneration, thus ameliorating kidney injury. Importantly, these changes in histone acetylation status and gene expression occur during the recovery phase after

reperfusion, implying that HDACi treatment – in contrast to the renoprotective strategies discussed above – may be a useful therapy after injury has occurred in the hospital setting.

1.4 RETINOIC ACID SIGNALING

1.4.1 Pathway overview

Vitamin A is essential for life and has been studied for almost 100 years¹⁵⁰. Cells metabolize vitamin A to several retinoids including all-trans retinoic acid (ATRA)¹⁵¹, which is the metabolite largely responsible for influencing expression of over 500 genes that regulate embryonic development, immunology, stem cell differentiation, and cancer biology¹⁵².

Retinoic acid (RA) levels are regulated by the spatiotemporal expression of enzymes responsible for its synthesis and degradation. Vitamin A enters the cell in its alcohol form as retinol, and is oxidized to retinaldehyde by alcohol/retinol dehydrogenase (ADH/RDH) enzymes, and subsequently to RA by retinaldehyde dehydrogenase (RALDH) enzymes^{151, 153}. In free acid form, RA can diffuse to nearby cells signaling in a paracrine fashion, where it is ultimately degraded by members of the cytochrome P450 family of enzymes, CYP26s^{151, 153, 154}. Together, these enzyme families establish a gradient of RA to exert tight control over signaling within specific tissues, which is critical since both RA deficiency and excess are detrimental to development and health^{155, 156}.

Intracellular RA binds to nuclear retinoic acid receptors (RARs), which heterodimerize with retinoid X receptors (RXRs)¹⁵⁷. In mammals, there are 3 RARs (α , β , and γ) and 3 RXRs (α , β , and γ)¹⁵⁸. These receptors pairs are transcriptional complexes that bind directly to retinoic acid

response elements (RAREs), consensus DNA sequence repeats located upstream of target genes¹⁵³. Since direct measurement of RA levels is technically difficult, the generation of transgenic animals that utilize RAREs to drive reporter gene expression has provided the scientific community with critical tools to study RA signaling dynamics¹⁵⁹⁻¹⁶².

In the absence of RA, gene expression is inhibited by RAR-RXR recruitment of corepressor complexes (SMRT/N-CoR), which include HDAC proteins^{153, 163}. RA binding induces a conformation change, resulting in the exchange of corepressors for coactivators including HATs that open chromatin for target gene transcription^{153, 163}. Generally, RA binding results in the activation of gene transcription; however, in rare cases ligand binding induces HDAC recruitment and gene silencing^{164, 165}.

1.4.2 Role in renal development

RA signaling plays several important roles during brain, heart, liver, lung, pancreas, limb, and kidney formation¹⁶⁶⁻¹⁶⁸. The requirement for proper development has been established by genetic deletions of pathway components in rodent models. These studies demonstrate that loss of RARs during embryogenesis results in an array of developmental defects, and deletion of RALDH2 enzyme alone is embryonic lethal^{156, 168}.

RA is important for the specification and patterning of the pronephric kidney field. During gastrulation, inhibition of RA signaling ablates the Lhx1-positive kidney progenitor cell population and prevents tubule formation in *Xenopus* embryos¹⁶⁹. Loss of RA signaling also decreases expression of pronephric kidney markers in mouse embryos¹⁶⁹. Conversely, exogenous RA treatment expands the kidney field in *Xenopus* and induces embryonic stem cells to express intermediate mesoderm markers^{169, 170}. These findings suggest that RA is critical for intermediate

mesoderm specification. Studies in zebrafish have demonstrated that RA signaling is also important in determining proximal-distal patterning of the pronephros. During somitogenesis, caudal transcription factors (*cdx*) establish clear expression domains of *raldh* and *cyp26* enzymes in the paraxial mesoderm, generating a gradient of RA availability¹⁷¹. Nephron progenitors exposed to higher RA levels become proximal tubule segments, whereas those exposed to lower RA levels become distal tubule segments¹⁷¹. Disruption of either *cdx* expression or RA signaling impairs segment identity^{171, 172}.

Finally, RA signaling induces growth and branching of the ureteric bud during metanephric kidney development¹⁷³. RA signaling in the renal stroma induces *Ret* expression in ureteric bud cells, which is critical for ureteric bud branching and nephron formation^{6, 7}. Consequently, loss of RA signaling during fetal development, induced by vitamin A deficiency or deletion of RARs, causes severe kidney malformations^{174, 175}. Even mild vitamin A reduction results in decreased nephron number at birth in rats¹⁷⁶. In humans, low maternal vitamin A intake during pregnancy is associated with decreased renal volume at birth¹⁷⁷, and this decreased nephron endowment is implicated in cardiovascular and renal disease in adult life^{16, 17}.

1.4.3 Role in renal disease and regeneration

RA mediates regenerative processes across many organ systems, often by reactivating developmental mechanisms that orchestrate organogenesis^{178, 179}. Classic studies of limb epimorphic regeneration in amphibians demonstrate that exogenous RA results in the super-regeneration of extra, mispatterned limbs¹⁷⁸. Later studies in zebrafish demonstrated that RA induces the dedifferentiation and proliferation of mesenchymal blastema cells by modulating fibroblast growth factor (FGF) and Wnt signaling, thus coordinating fin regeneration^{180, 181}. In

other organ systems, RA promotes neuron growth and decreases macrophage infiltration after axon damage¹⁸², ameliorates emphysema in rats potentially by stimulating alveolar epithelial proliferation¹⁷⁹, and regulates cardiomyocyte proliferation after cardiac injury in zebrafish¹⁸³. In these models, RA provides pro-proliferative and anti-inflammatory signals that positively affect tissue regeneration¹⁷⁹. It is important to point out that these effects are context-dependent, and in the cancer field, retinoids are commonly used as chemotherapeutic agents that arrest proliferation and induce differentiation of tumor cells^{184, 185}.

In the kidney, retinoids have largely been studied in glomerular diseases, which are characterized by podocyte injury and loss that leads to proteinuria and sclerotic lesions^{186, 187}. Across several rodent models of glomerular injury, RA treatment decreases proteinuria and sclerosis, impairs podocyte proliferation, and preserves glomerular structure and function¹⁸⁸⁻¹⁹². Recently, two studies provided mechanistic insight into the role of RA in glomerular disease by demonstrating that albumin binds and sequesters RA in podocytes, thereby preventing the proliferation and differentiation of podocyte progenitor cells^{193, 194}. Thus, proteinuria deprives podocyte progenitors of RA, leading to aberrant proliferation and ultimately to podocyte loss and sclerosis.

In addition to effects on podocytes, RA decreases infiltration of macrophages and T cells and reduces fibrosis in both glomerular and tubulointerstitial disease models^{188, 189, 191, 195}. These findings were correlated with reduced levels of MCP1^{188, 195}. These studies are consistent with the anti-inflammatory effects of retinoids described in other disease models and point to the promise of retinoid therapy across a variety of renal diseases^{179, 182}.

1.4.4 RA signaling and HDACs

In the classical model of RA signaling described above, RAR-RXR pairs exist in the absence of RA ligand bound in corepression complexes containing HDAC enzymes that condense chromatin and inhibit gene transcription^{153, 163}. These complexes are well known to contain HDAC3, but HDACs 1, 2, 4, 5, and 7 have also been shown to interact¹¹⁰. Thus, HDACi that block the activity of these corepressor-bound HDACs may activate RA target genes at endogenous RA levels lower than normally required to initiate gene transcription¹⁹⁶.

The link between RA signaling and HDAC inhibition is best characterized in the cancer field, which often utilizes combinatorial RA-HDACi chemotherapy to halt proliferation and drive differentiation and apoptosis in cancer cells^{184, 185}. Combinatorial therapy is particularly potent in the treatment of malignancies that have shown resistance to RA alone^{197, 198}. Data from renal cell carcinoma (RCC) cell lines suggest that retinoid-resistance is often due to loss of *RARβ2* expression¹⁹⁹. Treatment with MS-275 (entinostat) results in hyperacetylation of the *RARβ2* promoter and re-expression of this gene, restoring sensitivity of these lines to retinoids. When MS-275 is combined with 13-cis-retinoic acid, there is a significant inhibition of RCC tumor growth in mouse xenografts. Similar results have been obtained with TSA and RA²⁰⁰. Another possible mechanism involves the reactivation of Caspase-8 with HDAC8 inhibition, which then synergizes with RA to promote differentiation of neuroblastoma cancer cells^{201, 202}. Combinatorial RA-HDACi has been used in phase I clinical trials for patients with advanced solid tumors, including renal malignancies²⁰³. Taken together, these studies demonstrate how RA and HDACi synergize to influence gene expression as a potent cancer treatment strategy.

This link has also been shown by the Hukriede lab in the context of renal development. Treatment of zebrafish embryos with PTBA, a class I HDACi, expands the kidney field by

increasing proliferation of *lhx1a*-positive RPCs²⁰⁴. Injection of a construct encoding a dominant-negative RAR prevented kidney field expansion, suggesting that RPC proliferation depends on intact RA signaling²⁰⁴. Analogous to the cancer field, this study demonstrates that RA and HDACi treatment can also work together during embryonic development. Importantly, RA-HDACi drives cell cycle arrest and differentiation in cancer cells, but drives proliferation of RPCs during renal development, suggesting that the actions of RA and HDACi are context-dependent.

1.5 LARVAL ZEBRAFISH AS A MODEL SYSTEM

1.5.1 General strengths of the zebrafish model system

The zebrafish (*Danio rerio*) was pioneered as a model organ system by Dr. George Streisinger at the University of Oregon in the 1980s. Thirty years later, zebrafish are currently studied in over 950 labs worldwide (zfin.org; 6/16/2015). Zebrafish afford key advantages for biomedical research, including ease of maintenance, external fertilization and development, large clutch size, genetic tractability, and optical clarity during embryogenesis. Several organs in zebrafish possess a robust regeneration potential through adulthood, facilitating drug discovery in neural, endocrine, renal, and cardiac research. Importantly, the Sanger Institute completed sequencing of the entire zebrafish genome in 2013. This work identified zebrafish orthologs for 71% of all human genes, and orthologs for 82% of genes associated with human disease²⁰⁵. Thus, the zebrafish has become an influential model system to elucidate disease mechanisms and to identify new drug targets for these diseases in humans.

1.5.2 Zebrafish larvae as an AKI model

The larval pronephric kidney affords several advantages for AKI studies. First, the structure is simple consisting of only two nephrons. Second, segmentation is conserved between zebrafish and mammalian nephrons, demonstrating functional similarity¹². Third, the response to renal injury in the larva involves cellular repair within existing nephrons, whereas injury in the adult induces the formation of entire new nephrons²⁰⁶⁻²⁰⁸. Finally, zebrafish larvae possess an intact innate immune system with active, circulating neutrophils and macrophages observed at 3 dpf²⁰⁹. Although adaptive immunity does not develop until juvenile stages, zebrafish transgenic lines that mark specific leukocyte populations have been instrumental to studying the inflammatory component of infection and regeneration^{209, 210}. For these reasons, the larval zebrafish pronephric kidney is an apt model to study AKI.

1.5.3 Zebrafish larvae as a drug discovery model

Zebrafish embryos are small and develop rapidly, with many organ systems functioning by 2 dpf. These characteristics enable the use of zebrafish embryos as a high-throughput tool for drug discovery and toxicology screens. Embryos can be arrayed in multi-well plates, treated with compound libraries, and examined for effects on health, transgene expression, or other desired phenotypes to identify novel drug candidates²¹¹. For example in the kidney, automated imaging combined with detection algorithms can locate the embryo, map expression domains, and detect regional changes in *Tg(lhx1a:EGFP)* levels²¹². This assay can be used to identify small molecules that expand the RPC field during kidney development²¹².

Prior to this work, a chemical library screen was performed in the Hukriede lab that examined the effects of 1990 small molecules on zebrafish embryo development. From this screen, the PTBA class of novel HDACi was identified, and was shown to expand the kidney field by enhancing RPC proliferation²⁰⁴. These studies led to the main hypothesis of the work presented here: since PTBA increases RPC proliferation during kidney development, this class of compounds may hold promise as AKI therapeutics by similar signaling mechanisms.

Material modified and re-published with permission:

¹²⁶***Brilli LL**, *Swanhart LM, de Caestecker MP, Hukriede NA. HDAC inhibitors in kidney development and disease. *Pediatric nephrology*. 2013;28(10):1909-21. doi: 10.1007/s00467-012-2320-8. PubMed PMID: 23052657; PubMed Central PMCID: PMC3751322.

*Denotes equally contributing authors.

2.0 CHARACTERIZATION OF THE ACUTE KIDNEY INJURY ENVIRONMENT IN ZEBRAFISH LARVAE

2.1 HYPOTHESIS

Developing novel treatment strategies for AKI requires both a thorough understanding of the pathophysiologic mechanisms, and animal models that reliably recapitulate these complexities. Given the strengths of zebrafish as a drug discovery model, and since adult zebrafish generate new nephrons throughout life, we decided to develop a model of nephrotoxic AKI in zebrafish larvae. Due to the physiological and functional similarities between zebrafish pronephric and mammalian metanephric nephrons¹², we hypothesized that this AKI model would recapitulate many hallmarks of injury and regeneration.

2.2 RESULTS

2.2.1 Gentamicin induces renal failure in zebrafish larvae

We first determined the time course of renal injury in response to gentamicin, an aminoglycoside antibiotic that at high doses causes AKI in humans. Renal injury results from the disruption of mitochondrial function, which leads to PT cell damage and apoptosis^{213, 214}. Gentamicin was

delivered to zebrafish larvae by microinjection into the common cardinal vein at 2.5-3 dpf, resulting in edema at 2-3 days post-injection (dpi), consistent with compromised renal function as previously shown²⁰⁷. The percentage of edematous and dead larvae at 3 dpi increased with increasing injection dose (Figure 6A). Based on these findings, we developed a scoring system for gentamicin toxicity. Larvae with no pericardial edema or other phenotypic alterations were classified as “normal”; those exhibiting pericardial edema and low mortality rate were designated “moderate” larvae; those with generalized edema and higher mortality rate were designated “severe” (Figure 6B-E). To generate a high proportion of moderate/severe AKI, we used a working range of 5-8ng gentamicin, and selected surviving fish for subsequent experiments at 2 or 3 dpi with moderate/severe AKI (referred to as gent-AKI).

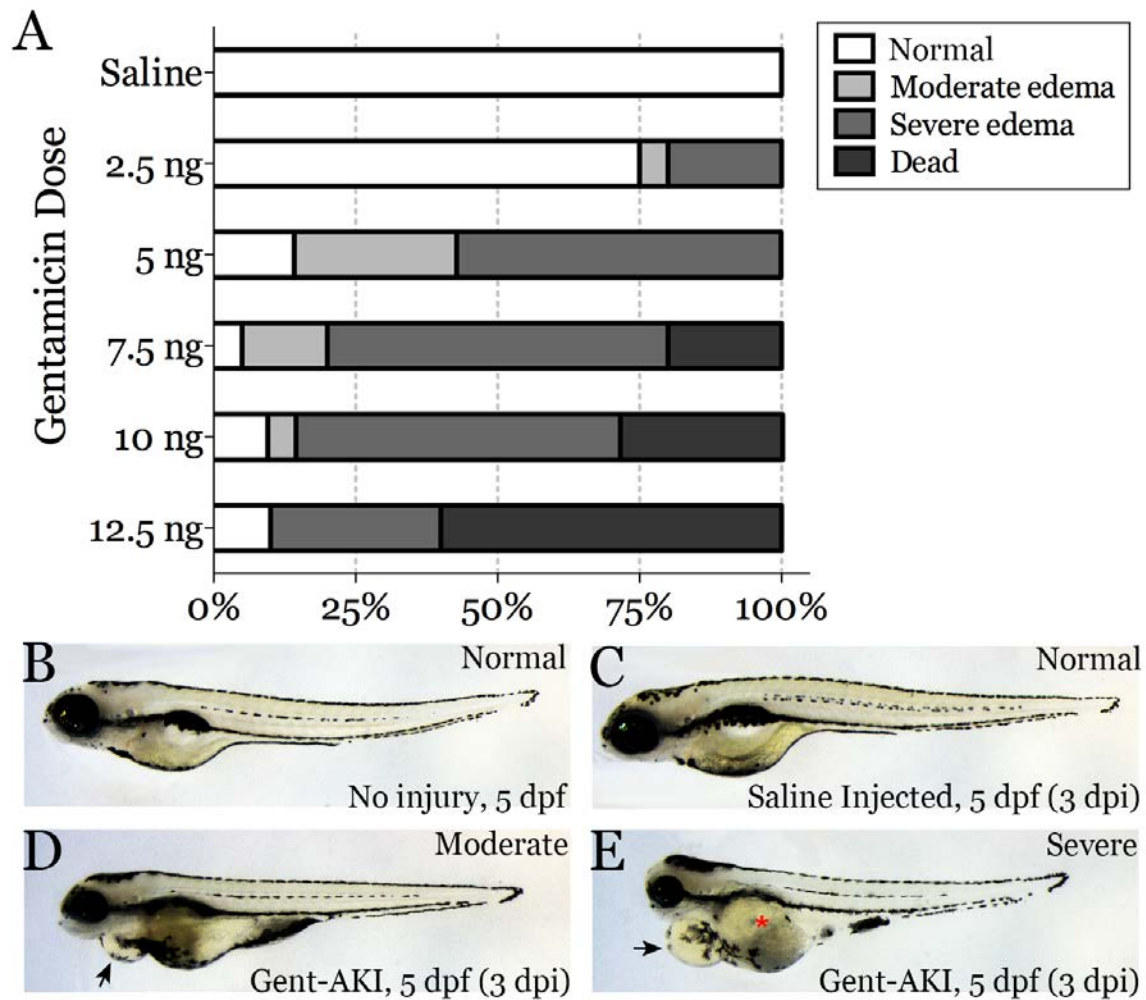


Figure 6: Gentamicin injection induces edema and death in zebrafish larvae.

(A) Gentamicin dose curve. Larvae were injected with increasing doses of gentamicin at 2.5 dpf, and the severity of AKI corresponding to injection dose was evaluated by scoring the proportion of larvae that displayed no edema, moderate phenotype, severe phenotype, or death at 3 dpi (n=5 experiments, 20-25 larvae/group). (B-E) Appearance of zebrafish larvae after gentamicin-induced AKI. Zebrafish larvae at 5 dpf (3 dpi) uninjected (B), injected with saline solution (C), or 5-7.5ng gentamicin (gent-AKI) with moderate phenotype displaying pericardial edema (black arrow) (D), and severe phenotype displaying both pericardial and general edema (red asterisk) (E). Experiments performed by C. Cosentino and L. Brilli Skvarca²¹⁵.

2.2.2 Gentamicin injection induces renal tubular injury

To visualize pronephric tubular injury caused by gentamicin in zebrafish larvae, we used the transgenic line *Tg(PT:EGFP)*, in which enhanced green fluorescence protein (EGFP) is expressed in the PT segments and neural crest cells. Compared to uninjured larvae, edematous gent-AKI larvae showed distension of the tubular lumen (Figure 7A-B) with epithelial cell flattening at 3 dpi (Figure 7C-D). Whereas uninjured larvae displayed few if any apoptotic cells, gent-AKI larvae showed increased terminal deoxynucleotidyl transferase dUTP nick end-labeling (TUNEL) staining in the PT (Figure 7E-F). To assess cell polarity, we performed whole mount immunofluorescence for the Na/K ATPase α -subunit (anti- α 6F), which is normally localized to the basolateral membrane. Na/K ATPase staining was properly distributed along the basolateral membrane of PT cells in uninjured larvae but was diffusely distributed throughout the cytoplasm in gent-AKI larvae, indicating loss of cell polarity. Gent-AKI larvae also showed extrusion of cellular debris into the tubular lumen (Figure 7G-H). Taken together, these data show clear similarities between gentamicin-induced pronephric injury in zebrafish larvae and mammalian AKI³⁵. (See Figure 31 in Appendix A for general anatomic orientation on transverse sections of zebrafish larvae.)

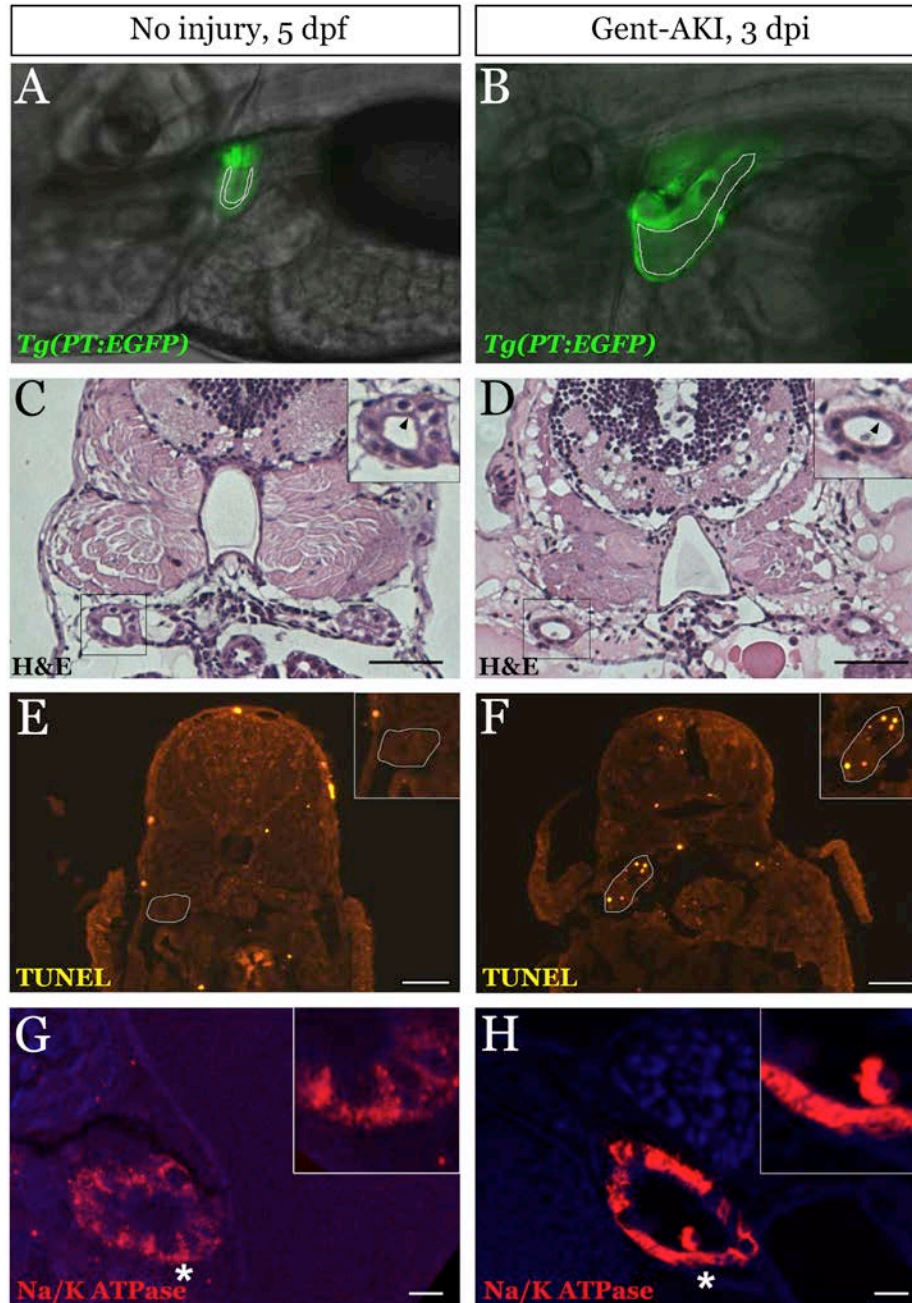


Figure 7: Zebrafish larvae show morphological hallmarks of AKI after gentamicin injection.

Uninjured larvae (A, C, E, G) or gent-AKI larvae (B, D, F, H) analyzed at 3 dpi. (A-B) Lateral view of *Tg(PT:EGFP)* larvae showing enlarged tubular lumen (white lines) in gent-AKI fish. PT cells are labeled with EGFP fluorescence (green). (C-D) Transverse sections stained with hematoxylin and eosin, showing flattening of epithelial cells and thinning of the brush border in gent-AKI larvae (arrowheads). Insets show higher magnification of the tubules. Scale bars, 10 μ M. (E-F) TUNEL staining for apoptotic cells is increased in gent-AKI larvae. Insets show a higher magnification of the tubule outlined in white. Scale bars, 5 μ M. (G-H) Immunofluorescence for Na/K ATPase on transverse sections of the PT demonstrates loss of basolateral expression and cell sloughing after gentamicin-induced injury. Insets show higher magnification of the region marked with asterisk. Scale bars, 10 μ m. Experiments performed by C. Cosentino and L. Brilli Skvarca²¹⁵.

We also evaluated whether zebrafish larvae expressed kidney injury molecule 1 (Kim1), a transmembrane glycoprotein that is expressed in injured PT cells in mammals²¹⁶. Kim1 is currently being evaluated as a biomarker of tubular injury in humans²¹⁷⁻²¹⁹. Since Kim1 has not previously been used as a marker of renal tubular injury in zebrafish, we first evaluated expression and localization of Kim1 in larval zebrafish after gentamicin-induced AKI. *kim1* mRNA expression increased in trunk tissue of zebrafish larvae in a dose-responsive manner within 24 hours of gentamicin injection and remained elevated at 2 dpi (Figure 8A-B). Since gentamicin induces selective injury to PT cells^{215, 220}, we used the transgenic reporter line *Tg(PT:EGFP)* to show that Kim1 protein is expressed in EGFP-positive PT cells in zebrafish larvae at 1 and 2 days after injury (Figure 8C). These data provide further comparison between tubular injury induced by gentamicin in zebrafish larvae and mammalian AKI.

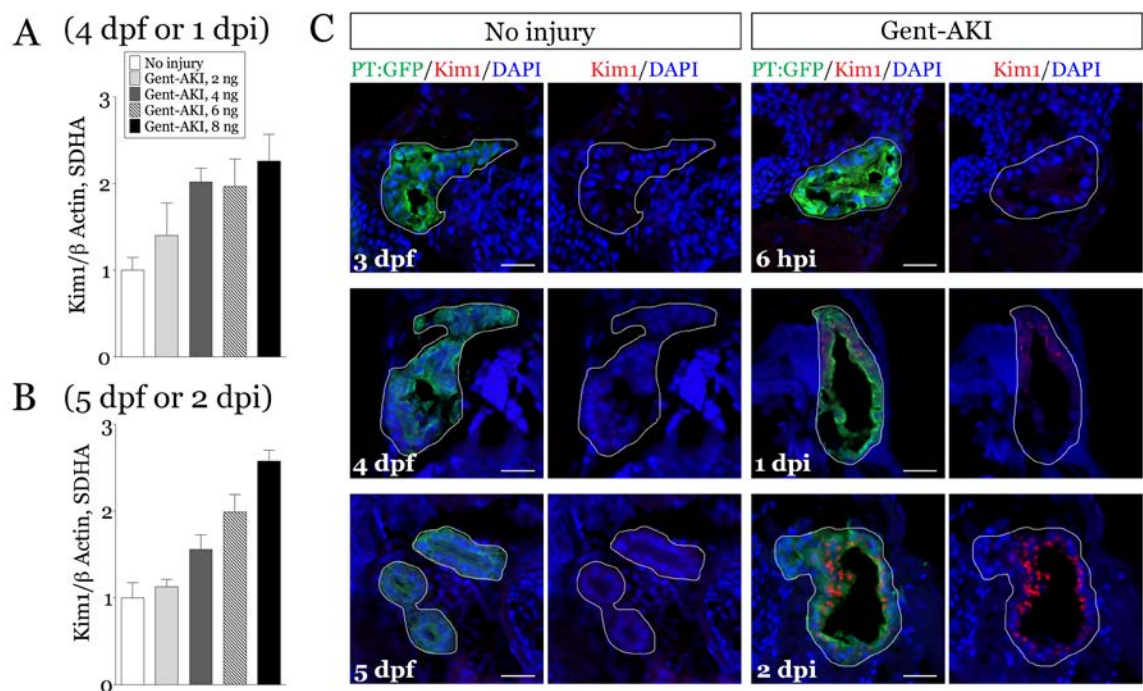


Figure 8: Renal tubular cells express Kim1 after gentamicin injury in zebrafish larvae.

(A-B) An injury dose curve was performed by injecting wildtype larvae with a single dose of 2, 4, 6, or 8ng gentamicin at 3 dpf. We then performed qRT-PCR to examine effects on *kim1* mRNA expression in dissected trunk tissue at 1 and 2 dpi. Graph is one representative experiment, shown as mean \pm SD for 3 technical replicates (n=4-7 experiments, 15 larvae/group). Expression normalized to β -actin and *sdha*. Experiments performed with technical assistance from J. Fall. (C) *Tg(PT:EGFP)* fish were injected with 8ng gentamicin at 3 dpf followed by immunofluorescence staining on transverse cryosections for Kim1 (red) and GFP (green) at 6 hours post injection (hpi), 1 dpi, and 2 dpi. Tubules are outlined in white. Scale bars, 20 μm^{221} .

2.2.3 Renal tubular regeneration after gentamicin-AKI

Kidney regeneration in mammals is characterized by dedifferentiation and proliferation of surviving RTECs that reactivate genes normally required during organogenesis⁵⁴. To confirm these findings in our model, we investigated whether PT cells expressed Pax2a post-AKI, a transcription factor reactivated after injury in mammalian AKI models^{53, 54, 222, 223}. We detected increased numbers of Pax2a-positive PT cells in the kidneys of gentamicin-injected larvae at 2 dpi (Figure 9). This observation is consistent with a dedifferentiation response occurring in the injured tubules of gent-AKI larvae^{50, 53, 54, 222, 223}.

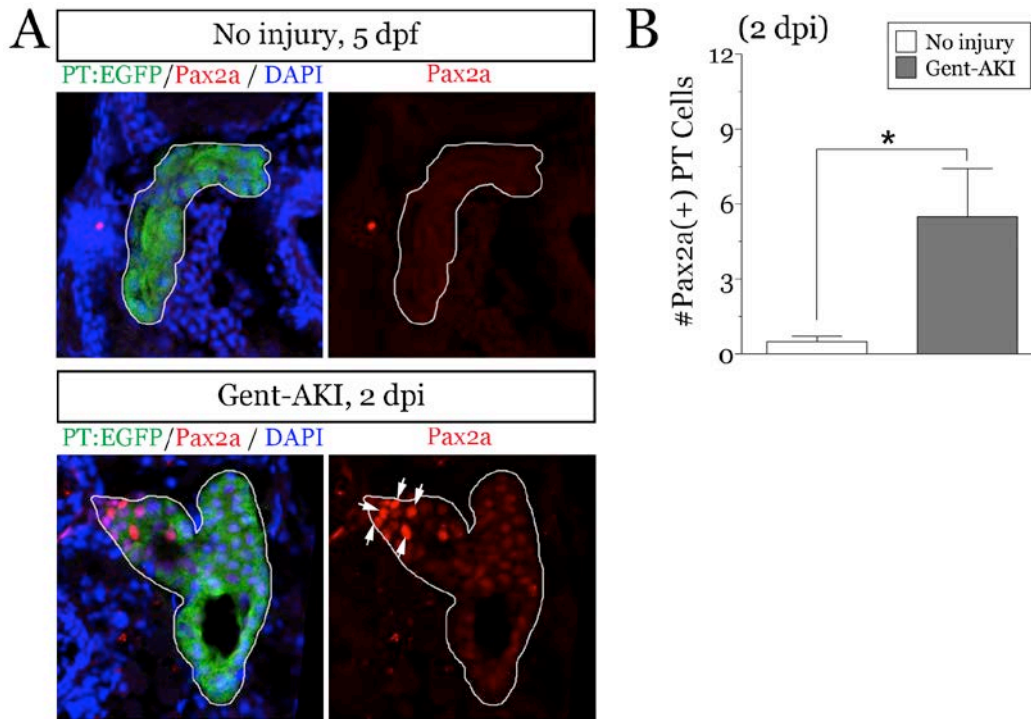


Figure 9: Renal tubular cells express Pax2a after gentamicin injury in zebrafish larvae.

(A) Transverse cryosections of uninjured or gent-AKI *Tg(PT:EGFP)* fish immunostained with anti-GFP (green) and anti-Pax2a (red, white arrows), and counterstained with DAPI (blue). Tubules are outlined in white. (B) Pax2a-positive cells were quantified in the PT by examining serial sections (n=10 tubules/group). Data expressed as mean \pm SEM. 2-tailed T Test, *P<0.05.

We evaluated the tubular proliferation response in this AKI model by quantifying the number of PT cells in the S-phase of the cell cycle after gentamicin injection. To do this, we treated zebrafish larvae with the thymidine analogue 5-ethynyl-29-deoxyuridine (EdU) followed by immunofluorescence microscopy. At 3 dpi, EdU was colocalized with 3G8 staining, which marks the apical brush border of PT cells²²⁴ (Figure 10A). Baseline proliferation index, defined as the number of EdU-positive cells divided by the number of DAPI-positive PT cells at 5 dpf, for control larvae was 3.5%, which increased after gentamicin-induced AKI to 7.3% (Figure 10B). These data suggest that PT cells in the pronephric kidney of zebrafish larvae undergo dedifferentiation and proliferation after gentamicin-induced injury, analogous to the regenerative epithelial response in mammalian AKI models.

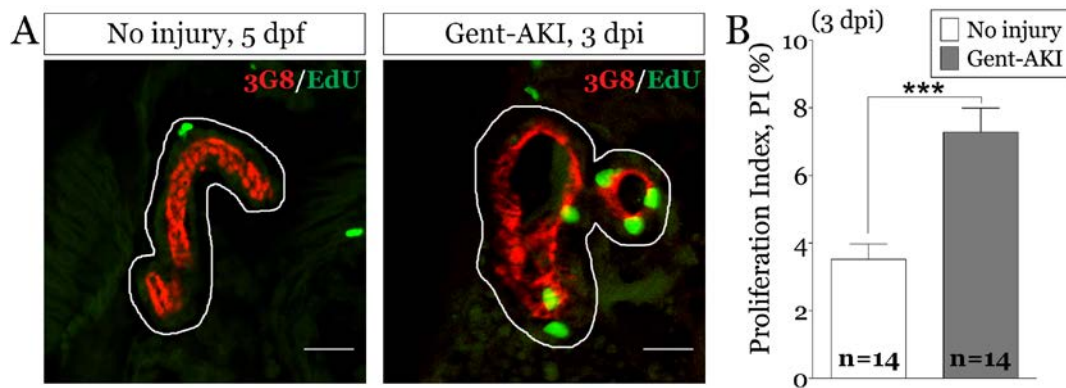


Figure 10: Proliferation of PT cells after gentamicin-AKI.

(A) Uninjured and gent-AKI larvae were incubated with the thymidine analogue EdU (green) at 3 dpi, and transverse sections were counterstained with 3G8 antibody (red) to mark the PT apical brush border. White lines outline the tubules. Scale bars, 20 μ m. (B) Quantitative analysis of proliferating PT cells shows a significant increase in the percentage of 3G8, EdU-positive cells between uninjured ($3.5\% \pm 0.46$) and gent-AKI fish ($7.3\% \pm 0.71$). “n” indicates the number of tubules analyzed per group. Data are expressed as mean \pm SEM; 2-tailed T test: *** $P < 0.0005$ ²¹⁵.

2.2.4 Immune response during gentamicin-AKI

In mammals, AKI results in the rapid influx of leukocytes, including neutrophils and macrophages^{72, 76-79}. Since the innate immune response is functional in zebrafish by 3 dpf²⁰⁹, we determined whether neutrophils and macrophages also infiltrate the pronephric kidney after gentamicin-AKI.

To evaluate the neutrophil response in this model, we first performed live time-lapse confocal imaging in *Tg(cdh17:mCherry); Tg(lyz:EGFP)* double transgenic fish after gentamicin injection. These fish mark kidney tubular epithelial cells in red (mCherry)²¹² and neutrophils in green (EGFP)^{225, 226} (Figure 11A). We captured z-stack images of the PT region over 17 hours beginning at 24 hpi. lyz:EGFP-positive neutrophils moved rapidly in uninjured fish, with few cells accumulating near the PT (Figure 11B). In contrast, neutrophils in gent-AKI fish moved slowly and remained close to the mCherry-positive kidney epithelium (Figure 11B). These results suggest that neutrophils migrate to the PT during gentamicin-AKI in zebrafish larvae.

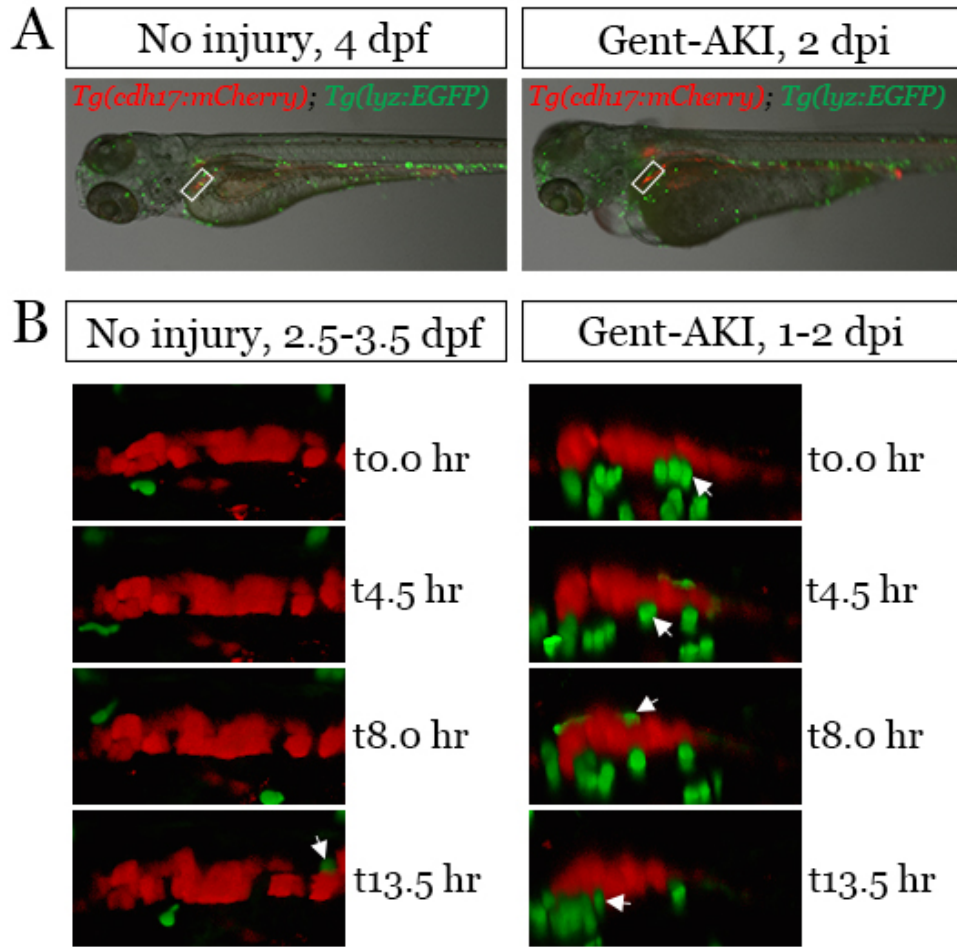


Figure 11: Neutrophils infiltrate the kidney after gentamicin-AKI in zebrafish larvae.

(A) Images of *Tg(cdh17:mCherry); Tg(lyz:EGFP)* double transgenic fish at 4 dpf or 2 dpi, depicting the global neutrophil population (green) and the pronephric tubules (red). White box indicates the PT region shown in the images below. (B) Single frame 3D projections of the PT region of *Tg(cdh17:mCherry); Tg(lyz:EGFP)* double transgenic fish captured at the indicated time point by time-lapse confocal microscopy. White arrows indicate examples of lyz:EGFP-positive neutrophils located near the kidney epithelium. Magnification 20X.

In order to quantify this response in *Tg(lyz:EGFP)* fish, we fixed samples at time points after gentamicin injection. We performed immunofluorescence microscopy and counted the number of lyz:EGFP-positive neutrophils adjacent to the PT epithelium by examining serial sections (Figure 12A). At 4 dpf (1 dpi), there was no change in the number of renal neutrophils after gentamicin injection. However, gent-AKI larvae showed significantly more renal neutrophils at both 5 dpf (2 dpi) and 6 dpf (3 dpi) compared to uninjured controls (Figure 12B). These data suggest that neutrophils infiltrate the pronephric kidney of zebrafish larvae after gentamicin-AKI between 1 and 2 dpi.

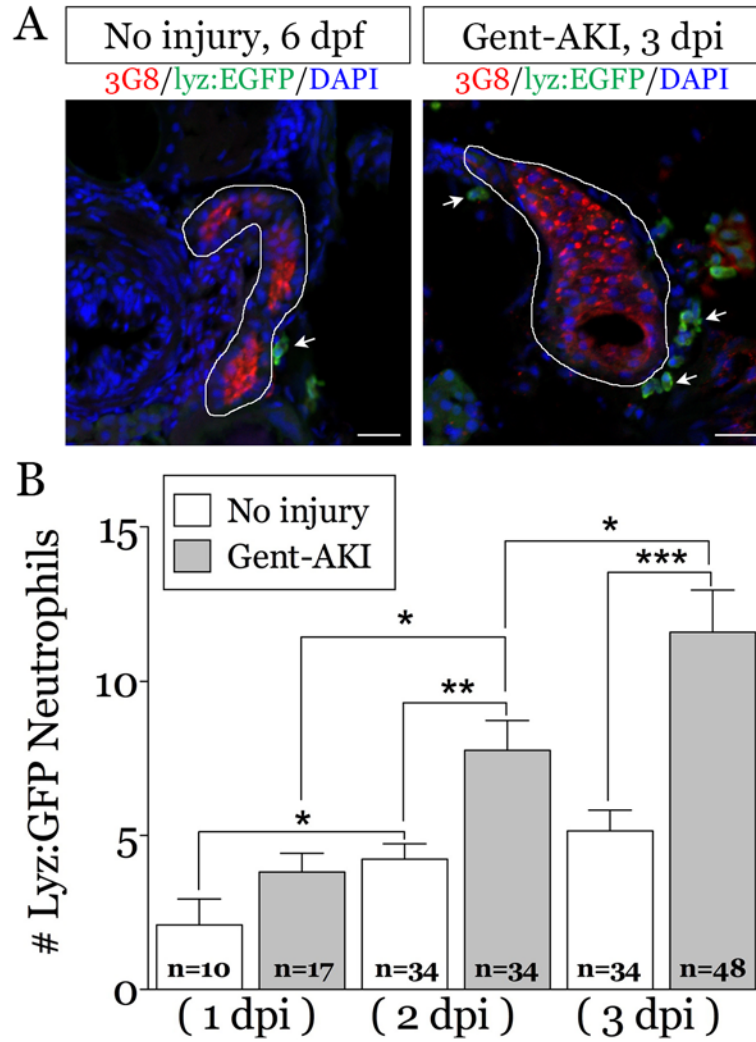


Figure 12: Gentamicin injury results in increased renal neutrophils.

(A) Uninjured and gent-AKI *Tg(lyz:EGFP)* larvae were fixed at 1, 2, and 3 dpi, and transverse sections were counterstained with anti-3G8 (red) to mark the PT apical brush border and anti-GFP (green) to mark neutrophils (examples, white arrows). White lines outline the tubules. Scale bars, 20 μ m. (B) Quantitative analysis shows a significant increase in the number of renal neutrophils at 2 and 3 dpi. Data are expressed as mean \pm SEM; 2-tailed T test: * $P < 0.05$, ** $P < 0.005$, *** $P < 0.0005$. “n” represents the number of tubules analyzed per group.

The glomerular hematopoietic niche may provide a nearby source for these infiltrating neutrophils during injury. Beginning at 4 dpf during larval development, the glomerulus is seeded with hematopoietic cells that migrate from the caudal venous plexus in the tail²²⁷. Consistent with these observations, we detected neutrophil clusters medial to the PT on 2-3 sections beginning at 5 dpf (Figure 13A). These medial clusters were less prominent or absent in many gent-AKI fish at 2 and 3 dpi, with neutrophils distributed on the lateral sides of the PT (Figure 13B). Whether AKI triggers decreased neutrophil migration from the tail, inhibits proliferation in the glomerulus, or stimulates migration from the niche to the PT requires further study.

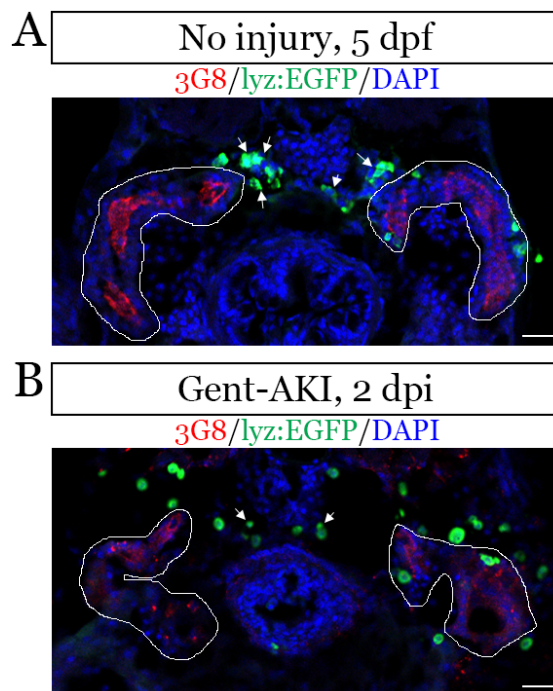


Figure 13: Dispersion of the neutrophil niche in the pronephric kidney after AKI.

Uninjured (A) or gent-AKI (B) *Tg(lyz:EGFP)* fish stained with anti-3G8 and anti-GFP antibodies. Arrows indicate neutrophils in the hematopoietic niche near the glomerulus. White lines outline the tubules. Scale bars, 20 μ m.

We performed similar histological studies using the macrophage reporter line *Tg(mpeg1:dendra2)*²²⁸ crossed with *Tg(PT:EGFP)* to quantify the macrophage response during

larval zebrafish gentamicin-AKI (Figure 14A). Compared to uninjured fish, gent-AKI larvae showed increased numbers of renal macrophages at 3 dpi (Figure 14B). Globally, macrophages in gent-AKI fish were also larger in size at both 2 and 3 dpi (2 dpi: 187 pixel² in uninjured vs. 259 pixel² in gent-AKI, 2-tailed T test $P < 0.0001$; 3 dpi: 184 pixel² in uninjured vs. 252 pixel² in gent-AKI, 2-tailed T test $P < 0.0001$; at least 325 cells per group). This observation is consistent with increased cell size due to phagocytosis also described in mouse IR-AKI²²⁹. Taken together, these data indicate that a robust innate immune response occurs after gentamicin-induced AKI in zebrafish larvae.

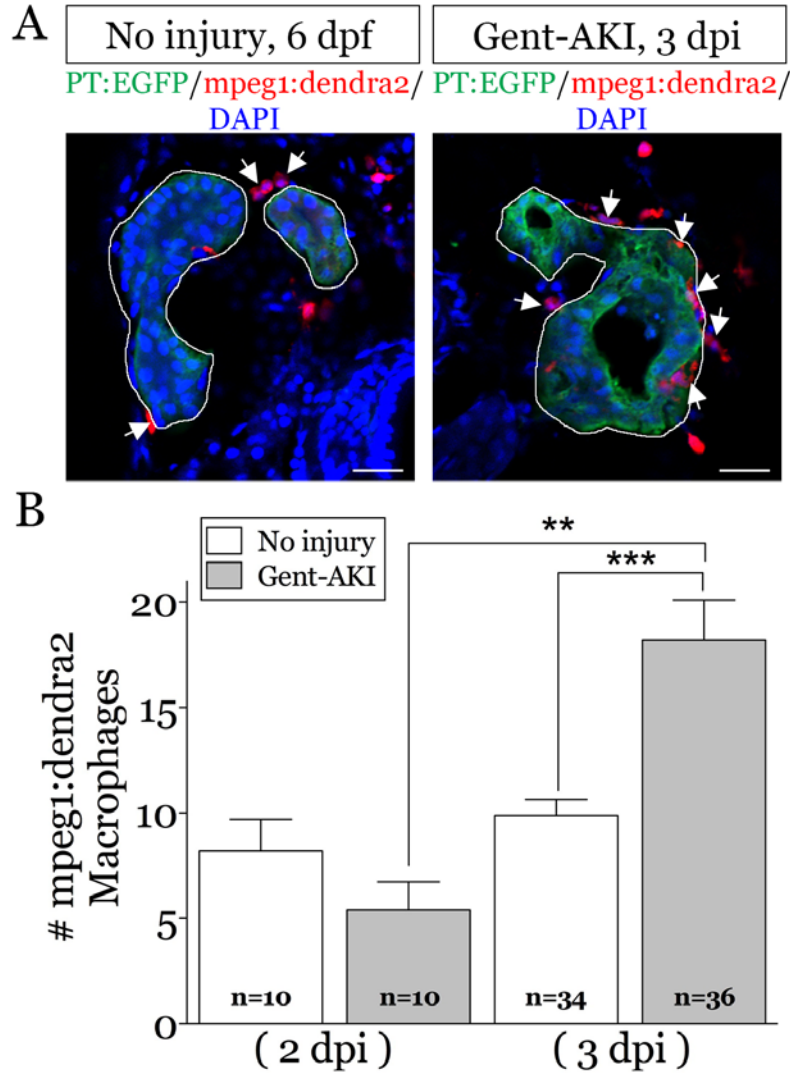


Figure 14: Gentamicin injury results in increased renal macrophages.

(A) Double transgenic *Tg(PT:EGFP); Tg(mpeg1:dendra2)* larvae were fixed at 2 and 3 dpi, and transverse sections were counterstained with anti-GFP (green) to mark the PT and anti-Dendra2 (red) to mark macrophages (examples, white arrows). White lines outline the tubules. Scale bars, 20 μ m. (B) Quantitative analysis shows a significant increase in the number of renal macrophages at 3 dpi. Data are expressed as mean \pm SEM; 2-tailed T test: ** $P < 0.005$, *** $P < 0.0005$. “n” represents the number of tubules analyzed per group.

2.3 METHODS

2.3.1 Zebrafish husbandry

All studies were approved by the University of Pittsburgh Institutional Animal Care and Use Committee. Zebrafish adults and embryos were maintained under standard conditions as described²³⁰. Embryos were used from Pitt AB wildtype as well as the following published transgenic lines: *Tg(lyz:EGFP)*²²⁵ and *Tg(mpeg1:dendra2)*²²⁸. The *Tg(PT:EGFP)* transgenic line was isolated serendipitously during the generation of *Tg(sox10:EGFP)* fish for an unrelated project. The *sox10* promoter (a gift from Robert Kelsh) was placed upstream of the EGFP sequence using Gateway Toolkit plasmids and the pDestTol2pA2 vector and injected into 1-cell stage embryos together with Tol2 transposase mRNA. Founder fish were identified by incrossing and stable *Tg(PT:EGFP)* embryos were raised. *Tg(cdh17:mCherry)* was generated in conjunction with and displays pronephric mCherry expression analogous to the published line *Tg(cdh17:EGFP)*²¹². For in vivo imaging, embryos were kept in E3 medium containing 0.003% 1-phenyl-2-thiourea (PTU) after 24 hours post fertilization.

2.3.2 Gentamicin microinjection

Zebrafish larvae were injected with a single dose of gentamicin at 2.5 or 3 dpf, as previously described²⁰⁶. Briefly, larvae were anesthetized in tricaine/E3 medium (5 mM NaCl, 0.33 mM CaCl₂, 0.33 mM MgSO₄, and 0.17 mM KCl) and injected with 1nl gentamicin (Sigma-Aldrich)

diluted in saline, delivered into the common cardinal vein. 10 kDa lucifer yellow or rhodamine dextran (Invitrogen) was included in the gentamicin injection solution at 1 mg/ml to verify successful microinjection. After injection, larvae were incubated in 50 µg/ml penicillin/streptomycin diluted in E3 medium.

2.3.3 Histological analysis

Immunofluorescence microscopy was performed on cryosections as described previously². Briefly, larvae were fixed in 4% paraformaldehyde and treated with a 10-30% sucrose/PBS gradient before embedding in tissue freezing medium (Ted Pella). Transverse sections were generated at a thickness of 12-14 µm. Slides were blocked with 10% goat serum in PBST, followed by primary antibody and secondary antibody incubations. The following primary antibodies were used: anti-3G8, anti-Pax2a, anti-GFP, anti-Kim1, anti-Dendra2. The following secondary antibodies were used: goat anti-mouse Cy3, goat anti-rabbit or goat anti-mouse alexa fluor 488, goat anti-rat alexa fluor 594, donkey anti-rabbit alexa fluor 568, and goat anti-chicken alexa fluor 555. Incubation with 4', 6-diamidino-2-phenylindole (DAPI, Vector Laboratories) was used to counterstain nuclei. Whole mount immunofluorescence was performed with anti-α6F antibody to detect Na/K ATPase, followed by JB4 embedding and microtome sectioning, as previously described²⁰⁶. For detection of apoptotic cells, TUNEL staining was performed on cryosections using the In Situ Cell Death Detection Kit (Roche), according to the manufacturer's instructions. Sections were examined by confocal microscopy (Zeiss LSM 700). Conditions for histology are summarized in Table 1, Appendix B.

To quantify Pax2a-positive cells in *Tg(PT:EGFP)* fish, we imported serial images containing PT:EGFP-positive kidney staining into ImageJ 1.46r software (NIH). The ROI tool

was used to outline the pronephric kidney in the green channel, and then the “Analyze Particle” function was used to quantify the number of Pax2a-positive cells in the red channel. Background removal and threshold values were held constant between groups for each experiment. Particle size range was 80 to infinity. Per nephron, 3 images were analyzed skipping one section between images. Similar ImageJ analysis was performed in *Tg(PT:EGFP); Tg(mpeg1:dendra2)* fish to quantify macrophage cell size. For these images, there was no background removal, mpeg1:dendra2 channel threshold was 53 to 255, and particle size range was 60 to infinity.

2.3.4 RNA isolation and quantitative RT-PCR

Samples for RNA isolation were generated by cutting zebrafish larvae at the hindbrain to isolate trunk tissue. 10 to 15 larvae were pooled and homogenized per sample. RNA was isolated using the RNeasy Micro kit (Qiagen), and cDNA was generated using the SuperScript First Strand kit (Invitrogen). qRT-PCR was performed as described previously²⁰⁴. Exon-spanning primers were designed using Beacon Designer version 8.13 to detect *kim1* mRNA. Primer sequences are listed in Table 2, Appendix B. Expression was normalized to *β-actin* and *sdha* mRNAs, as described²⁰⁴. qRT-PCR was repeated using cDNA samples from 3-7 different experiments. Raw data for each replicate is listed in Table 3 in Appendix B. Data shown in graphs are from one representative experiment with 3 technical replicates.

2.3.5 EdU labeling

To label proliferating cells in zebrafish, larvae were treated with EdU using the Click-iT Imaging Kit (Invitrogen), adapted by S. Eckerle and J. Holzschuh for cryosections²³¹. Larvae were

incubated in EdU solution (10 mM EdU and 5% DMSO in E3 medium) for 30 minutes at 4°C and allowed to recover in E3 for one hour at 28.5°C before fixation. Staining was performed using alexa fluor 488 followed by immunostaining with anti-3G8. To calculate the proliferation index, we determined the average number of cells in the PT (as marked by 3G8) of control larvae at 5 dpf (311 ± 7 cells, mean \pm SEM, n=20 nephrons). To determine the numerator, we counted the number of EdU-positive cells in one nephron per larvae within the 3G8 region.

2.3.6 Live zebrafish confocal imaging

24 hours after gentamicin injection, zebrafish larvae were anesthetized in 160 mg/ml tricaine (Sigma-Aldrich), embedded in a thin layer of 0.5% low-melt Sea Plaque agarose (Cambrex), and covered with E3 medium plus PTU to prevent pigment development. Image stacks were acquired using a Leica TCS SP5 multiphoton microscope (Leica Microsystems, Wetzlar, Germany) with an HCX IRAPO L 20X/0.95 water immersion objective, non-descanned detectors and a custom built motorized stage (Scientifica, East Sussex, UK). Sequential stack scanning was performed bidirectionally with a resonant scanner (16000 Hz, phase set to 1.69) with 32x line averaging and a zoom of 1.7x. EGFP and mCherry were excited with a Mai Tai DeepSee Ti:Sapphire laser (Newport/Spectra Physics, Santa Clara, CA) at 900 and 561 nm, respectively. Using the “Mark and Find” function, (x,y) coordinates and z-series parameters (step size 1.48 μ m) were defined for individual embryos. Images were captured every 27 minutes for 17 hours. Maximal projections were compiled in series to generate time-lapse movies using LAS AF Version: 3.0.0 build 8134 and Metamorph software. Still images were captured from these movies to generate panels in Figure 11.

2.4 DISCUSSION

We have shown that gentamicin induces renal failure in zebrafish larvae, with histological features consistent with mammalian AKI. In this model, RTECs express the renal injury marker Kim1, lose epithelial character, and subsequently undergo dedifferentiation and proliferation. Phagocytes also invade the pronephric kidney in the post-AKI environment. These studies highlight the pathophysiologic similarities between gentamicin-AKI in zebrafish larvae and mammalian AKI models. Combined with the general strengths of zebrafish, including large clutches, rapid development, and live imaging, these features validate larval gentamicin-AKI as an excellent model for studying AKI mechanisms and identifying therapeutic targets.

Another strength of this model lies in its clinical relevance. In humans, gentamicin is an effective antibiotic treatment for gram-negative infections, but it also causes renal impairment in up to 25% patients²¹⁴. Gentamicin directly injures PT cells and induces cell death in a subset of these cells. Comparably in our zebrafish AKI model, gentamicin induces dose-dependent renal injury in a proportion of larvae and causes apoptosis in a subpopulation of PT cells. In contrast, other AKI models completely ablate entire tubular cell populations or nephron segments. These models, including directed laser injury in zebrafish²³² and diphtheria-toxin-mediated PT damage in mice²³², cause massive cell death and therefore do not fully recapitulate the clinical AKI injury environment.

Although gentamicin-AKI is clinically relevant, microinjection is time consuming and technically challenging. Since gentamicin is cationic, it must be delivered directly into the circulatory system of each fish; larvae treated with gentamicin in the embryo media do not develop AKI in our hands. It would therefore be advantageous to develop an alternative AKI model that also causes partial RTEC loss but does not require manipulation of individual larvae.

To achieve this goal, the Hukriede lab is currently developing a transgenic line that utilizes the thyroid-stimulating hormone beta subunit (*tsh β*) promoter and the Gal4-UAS system to drive mosaic nitroreductase expression in PT and pituitary cells²³³. In this model, metronidazole treatment would induce apoptosis only in the subset of PT cells that express nitroreductase, resulting in patchy apoptosis. This tool will provide a complimentary genetic model to gentamicin-AKI that will greatly facilitate future studies.

Despite serious renal impairment, most patients survive after AKI; however, gentamicin-AKI in the zebrafish larval model is ultimately lethal. Despite epithelial regeneration, over 50% of fish die within 3 days after high-dose gentamicin injection. Severely injured larvae develop massive general edema, which likely damages other organs and compromises long-term survival. Failure of recovery may be partially explained by the simplicity of the system. Since the pronephric kidney consists only of 2 nephrons, there are significantly fewer reserves compared to the metanephric kidney. Additionally, unlike rodents, serum creatinine or GFR measurements are so far not possible in zebrafish due to small intravascular blood volume. However, two other techniques have been described. Fluorescent beads can be injected into the circulatory system, and uptake by the PT can be examined by live imaging². Additionally, Zhou and Hildebrandt generated a transgenic line that expresses fluorescent-tagged vitamin D binding protein (VDBP), the closest zebrafish protein to mammalian albumin²³⁴. This group evaluated glomerular filtration using ELISA to detect VDBP in the embryo media, analogous to proteinuria, in an inducible transgenic zebrafish model of podocyte injury. These studies provide alternative methods for general functional assessments in zebrafish AKI models. Since we show that zebrafish larvae express Kim1 in the PT following gentamicin injection, Kim1 levels could be compared as a biomarker of renal injury. Since our qRT-PCR assay does not specifically

measure renal *kim1*, more accurate evaluation of renal injury would require either pronephric dissection or quantification of Kim1 immunofluorescence in the kidney. Developing other functional markers would greatly enhance the power of the zebrafish AKI model.

Although this work characterizes many aspects of nephrotoxic AKI in zebrafish larvae, future studies are needed to evaluate whether this model recapitulates other traits of mammalian AKI. First, it is not known whether RTECs in zebrafish undergo maladaptive repair through G2/M arrest. Addressing this question would require careful cell cycle analysis post-AKI. So far, our attempts to identify and optimize antibodies for phospho-histone-H3, which marks cells in G2/M phases, for use in zebrafish have been unsuccessful. If G2/M arrest occurs in zebrafish, a following question is whether these cells would have similar negative consequences for renal fibrosis in this model. In preliminary studies, we did not find foxD1-positive cells in the pronephric kidney, and there are currently no reports of a renal stroma population in the zebrafish kidney. Thus, even if G2/M arrest does occur during zebrafish AKI, it may have less significant effects on outcome.

Further studies are also needed to characterize the immune response more completely. Here, we used immunofluorescence in the *Tg(mpeg1:denra2)* line to examine renal macrophage numbers during AKI. Increased macrophages could result from migration or proliferation in situ. Live imaging experiments would facilitate cell tracking to determine definitively whether macrophages migrate to the kidney, whereas EdU studies would determine if renal macrophages proliferate after AKI. In rodent AKI models, current evidence suggests that M1 macrophages migrate to the kidney early in the course of injury, whereas expansion of the M2 population occurs later by proliferation within the kidney⁸⁰. More fundamentally, it is not yet known whether macrophages in zebrafish larvae polarize into M1/M2 phenotypes. Promisingly, a few

groups have identified macrophages in zebrafish that express TNF α (M1 marker) and/or arginase 1 (M2 marker)²⁰⁹. The Hukriede lab is currently optimizing immunofluorescence staining to assess whether mpeg1:dendra2-positive cells coexpress M1 and/or M2 markers during AKI. Finally, we have adapted macrophage depletion strategies from mouse for use in the larval zebrafish AKI model. This technique involves microinjection of clodronate-containing liposomes which induce macrophage apoptosis, and will allow us to evaluate the role of these potential macrophage subpopulations after AKI. These studies will provide further insights into the injury environment of gentamicin-AKI in zebrafish larvae.

Material modified and re-published with permission:

²¹⁵*Cianciolo Cosentino, C, *Skrypnyk, NI, ***Brilli, LL**, Chiba, T, Novitskaya, T, Woods, C, West, J, Korotchenko, VN, McDermott, L, Day, BW, Davidson, AJ, Harris, RC, de Caestecker, MP, Hukriede, NA: Histone deacetylase inhibitor enhances recovery after AKI. *Journal of the American Society of Nephrology : JASN*, 24: 943-953, 2013.

²²¹*Chiba, T, *Skrypnyk, NI, ***Skvarca, LB**, Penchev, R, Zhang, KX, Rochon, ER, Fall, JL, Paueksakon, P, Yang, H, Alford, CE, Roman, BL, Zhang, MZ, Harris, RC, Hukriede, NA, de Caestecker, MP: Retinoic acid signaling coordinates macrophage-dependent injury and repair after AKI. *Journal of the American Society of Nephrology : JASN*, In press, 2015.

*Denotes equally contributing authors.

3.0 HISTONE DEACETYLASE INHIBITOR M4PTB ENHANCES RECOVERY AFTER AKI IN ZEBRAFISH LARVAE

3.1 HYPOTHESIS

Since gentamicin injection in zebrafish larvae recapitulates the major hallmarks of mammalian AKI, we next evaluated the potential of this model as a drug discovery tool to develop new AKI therapies. Previously in the Hukriede lab, a chemical library screen identified the PTBA class of novel HDACi based on its ability to increase RPC proliferation during renal development in zebrafish embryos²⁰⁴. The analogue methyl-4-(phenylthio)butanoate (m4PTB) is a prodrug in the PTBA class that shows greater activity in vivo due to esterification of the free acid²⁰⁴ (Figure 15A). Based on the embryonic phenotype, we hypothesized that m4PTB would improve outcome post-AKI by increasing the RTEC proliferation response in this larval zebrafish model.

3.2 RESULTS

3.2.1 Establishing dosing with m4PTB in zebrafish larvae

To establish an effective working concentration of m4PTB in zebrafish larvae, we first determined the maximum tolerated dose (MTD), defined as the maximum concentration at which

there were no signs of significant toxicity or death²³⁵. Cohorts of 15-20 larvae were incubated with 1% DMSO (vehicle control treatment) in E3 medium with or without m4PTB at increasing concentrations for 24 hours from 4 to 5 dpf. Using this approach, the MTD for m4PTB in zebrafish larvae was established at 8 μ M, which represents the highest effective dose well tolerated by zebrafish larvae (Figure 15B).

To further rationalize the working dose of m4PTB, we performed western blot analysis to evaluate *in vivo* histone H4 acetylation, a marker of HDACi activity. We treated 4 dpf larvae with increasing concentrations of m4PTB and generated protein extracts from whole fish at different time points after treatment. There was a marked upregulation of H4 acetylation after 6 hours, detectable at the lowest concentration of m4PTB used (2 μ M); however, only the 8 μ M MTD dose showed H4 acetylation at 12 hours, and none of the concentrations induced H4 hyperacetylation after 24 hours of treatment (Figure 15C). These data indicate that m4PTB induces short-term changes in histone acetylation status for 6 to 12 hours. Further supporting our choice for working concentration, 4 μ M m4PTB treatment resulted in a general increase in hyperacetylation, including in the pronephric kidney (Figure 15D-G). Since both 4 μ M and 8 μ M induced comparable H4 acetylation after 6 hours, we chose 4 μ M m4PTB as our working concentration in AKI survival studies.

Over the course of the experiments presented here, the Hukriede lab used m4PTB synthesized either by Lee McDermott (University of Pittsburgh, Drug Discovery Institute) or by Enamine (www.enamine.net). Similar compound analysis was performed on each new batch to inform the batch-specific working dose for subsequent experiments. This dose ranged from 0.5 to 4 μ M.

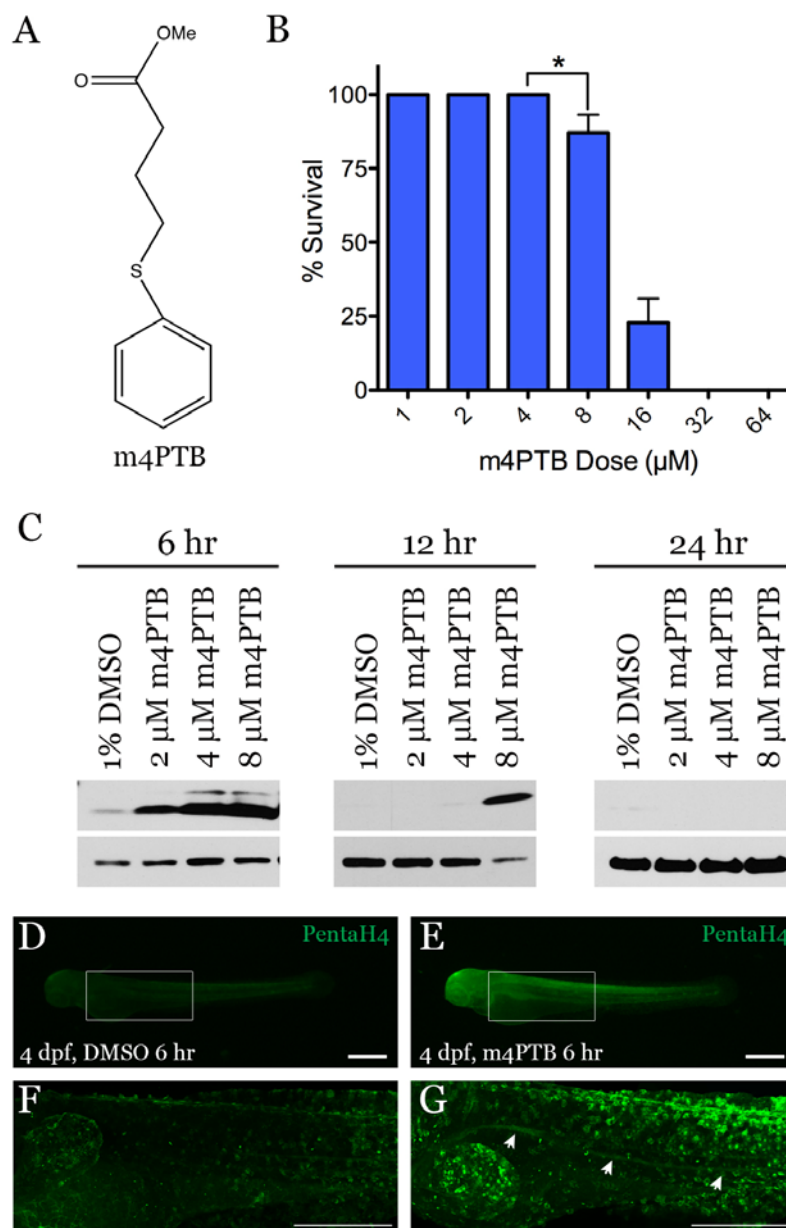


Figure 15: MTD and m4PTB-induced hyperacetylation in zebrafish larvae.

(A) Structure of m4PTB. (B) MTD assay. Larvae were treated with m4PTB at 4 dpf and scored for health and survival at 5 dpf. Asterisk indicates dose at which significant death was observed ($n=91$ fish), Fisher's exact test: $*P<0.05$. MTD assay performed with technical assistance from C. Woods. (C-G) Acetylation of histone H4. (C) Western blot examining the acetylation state of histone H4 (top panel) isolated from larvae treated at 4 dpf with 1% DMSO, 2 μ M, 4 μ M or 8 μ M m4PTB for 6, 12, or 24 hours. Western blot for α -tubulin as a loading control (bottom panel). (D-E) Whole mount immunostaining for acetylated histone H4 at 4 dpf after 6-hour treatment with 1% DMSO or 4 μ M m4PTB demonstrates global hyperacetylation. (F-G) Confocal images of boxed regions in D and E show hyperacetylation in the pronephric kidney (arrowheads) after m4PTB treatment. Scale bars, 300 μ m²¹⁵.

3.2.2 Post-injury m4PTB treatment increases survival after gentamicin-AKI

We sought to determine whether m4PTB treatment enhanced renal recovery in the zebrafish gentamicin AKI model. Since our goal was to establish a post-injury treatment regimen, we wanted to initiate m4PTB treatment after larvae clearly demonstrated renal injury. We previously showed robust upregulation of renal Kim1 expression at 2 dpi (Figure 8), so we assessed whether larvae showed further evidence of renal injury at this time point. Gent-AKI larvae that displayed pericardial edema and darkened yolks at 2 dpi (Figure 16A-B) also showed histological loss of renal tubular cell polarity (Figure 16C-D). In combination, these findings indicate that gentamicin induces renal damage by 2 dpi, and allowed us to identify injured larvae by examining for gross phenotypic changes. Thus, in subsequent experiments we treated larvae with m4PTB for 24 hours beginning at 2 dpi.

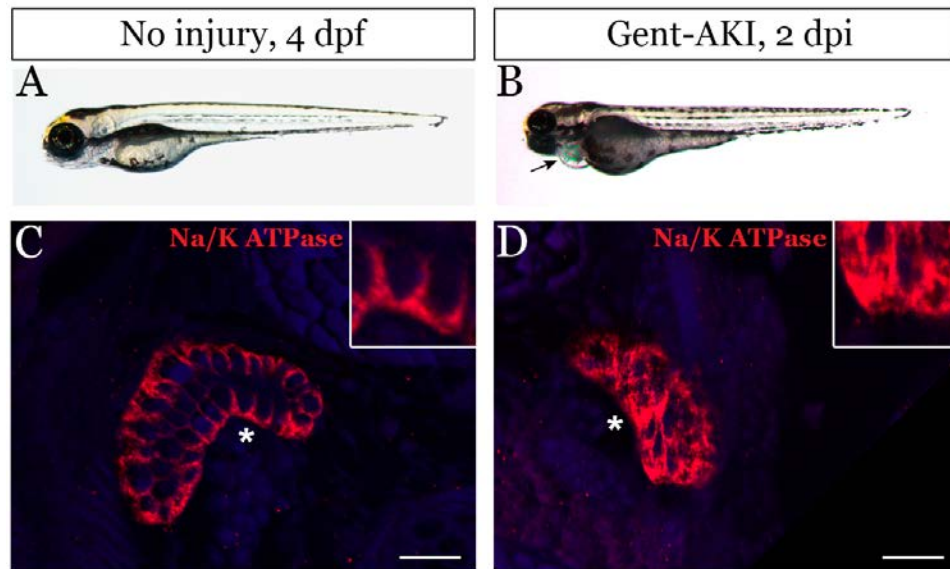


Figure 16: Edema and PT cell polarity after gentamicin-induced AKI at 2 dpi.

(A) Uninjured and (B) gentamicin-injected edematous larvae at 4 dpf or 2 dpi (arrow, pericardial edema). (C-D) Loss of cell polarity at 2 dpi. Transverse sections of the PT in control larvae showing normal distribution of the Na/K ATPase antibody (C), whereas gent-AKI larvae display a clear disruption of cell polarity (D). Insets show higher magnification of the PT (asterisk). Scale bars, 20 μ m. Experiments performed by C. Cosentino and L. Brilli Skvarca²¹⁵.

Having established an effective working dose and post-AKI treatment window for m4PTB, we next treated gent-AKI larvae with a single dose of either 1% DMSO or 4 μ M m4PTB from 2 to 3 dpi and monitored survival rates. Compared to vehicle, gent-AKI larvae treated with m4PTB showed significantly increased survival at 5 and 6 dpi, from 58% to 79% and from 55% to 74%, respectively (Figure 17). These results show that short-term, delayed m4PTB treatment enhances overall recovery after AKI in this model.

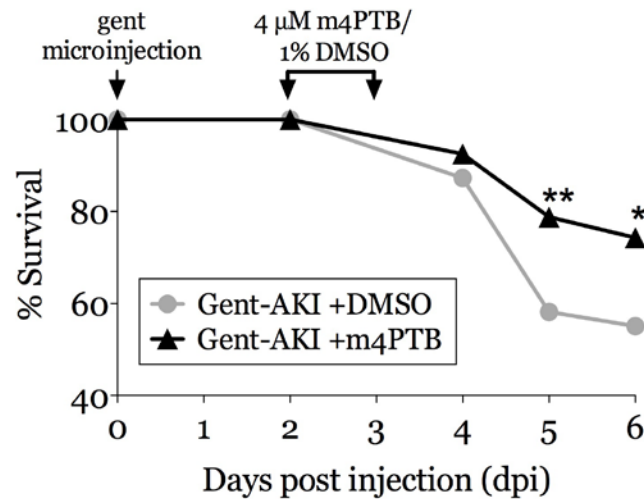


Figure 17: m4PTB treatment increases larval survival after AKI.

Gent-AKI larvae were treated with either 1% DMSO vehicle or 4 μ M m4PTB at 2 dpi, and survival rate was evaluated at 4, 5, and 6 dpi: 4 dpi, 87% (n=69/79 fish) in vehicle-treated larvae versus 93% (n=74/80 fish) in m4PTB-treated larvae; 5 dpi, 58% (n=46/79 fish) in vehicle-treated larvae versus 79% (n=63/80 fish) in m4PTB-treated larvae; 6 dpi, 55% (n=38/69 fish) in vehicle-treated larvae versus 74% (n=52/70 fish) in m4PTB-treated larvae. Data pooled from 3 independent survival assay experiments. Fisher's exact test: *P<0.05, **P<0.005. Experiments performed by C. Cosentino and L. Brilli Skvarca²¹⁵.

3.2.3 m4PTB treatment increases PT cell proliferation post-AKI

Since m4PTB increases RPC proliferation in zebrafish embryos²⁰⁴, we determined whether enhanced post-AKI survival after treatment with m4PTB was associated with increased RTEC proliferation. We injected fish with gentamicin at 2.5 dpf, followed by 1% DMSO or m4PTB

treatment at 2 dpi. To evaluate cell proliferation, we treated larvae with EdU at 3 dpi and assayed for EdU-positive cells in the PT marked by anti-3G8 staining (Figure 10 and Figure 18). In uninjured larvae, the percentage of EdU-positive PT cells increased from 3.5% in DMSO-treated controls to 7.1% in m4PTB-treated fish. In gent-AKI larvae, the proliferation index was also increased from 7.3% in DMSO-treated controls to 10.7% in m4PTB-treated fish (Figure 10 and Figure 18). There was no significant change in the number of apoptotic cells at 3 dpi between DMSO and m4PTB treatment groups (DMSO: 4.56 ± 1.4 cells; m4PTB: 4.06 ± 1.0 cells; TUNEL labeling in 3G8-positive PT cells, mean \pm SEM). Therefore, the increased proliferative response after treatment with m4PTB suggests that enhanced recovery in this zebrafish AKI model results from increased PT cell regeneration and repair of injured tubules.

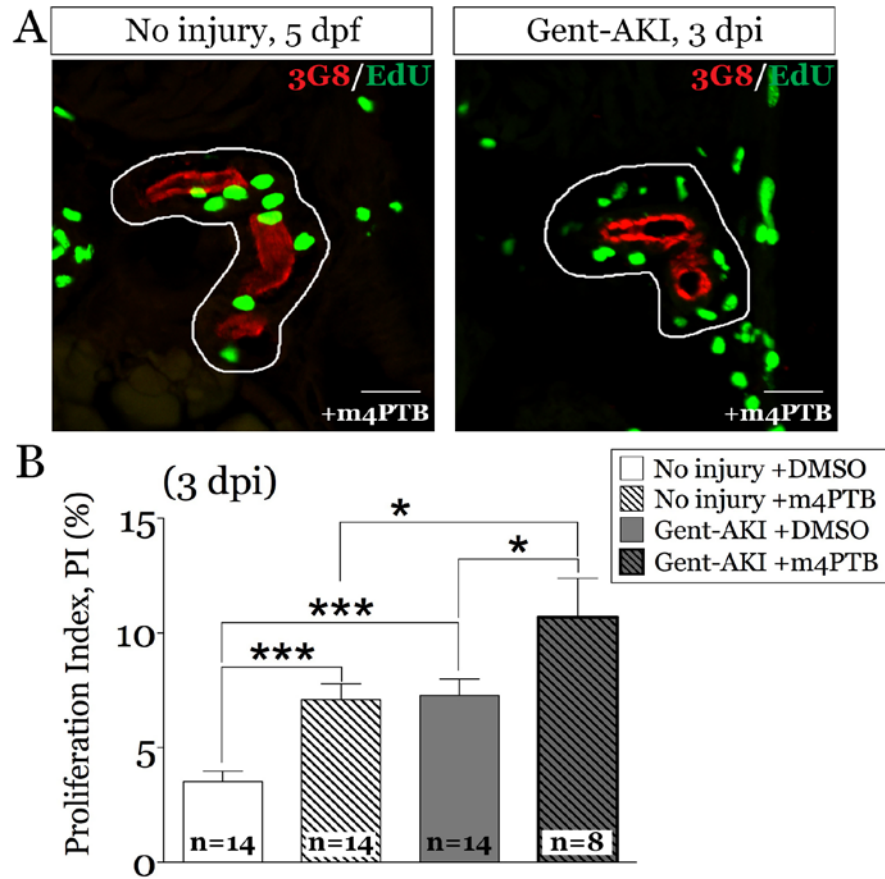


Figure 18: m4PTB treatment increases PT cell proliferation.

(A) Uninjured and gent-AKI fish were treated with 1% DMSO (Figure 10) or 4 μ M m4PTB at 4 dpf (2 dpi). At 5 dpf (3 dpi), larvae were incubated with EdU (green), and transverse sections were counterstained with 3G8 antibody (red) to mark the apical brush border of the PT. White lines outline the tubules. Scale bars, 20 μ m. (B) Quantitative analysis of proliferating proximal tubule cells. Cell counting analysis shows a significant increase in the percentage of 3G8, EdU-positive cells in m4PTB-treated larvae at 5 dpf in uninjured fish (3.5% \pm 0.46 versus 7.1% \pm 0.68) and at 3 dpi in gent-AKI fish (7.3% \pm 0.71 versus 10.7% \pm 1.7). “n” indicates the number of fish analyzed per group. Data are expressed as mean \pm SEM; 2-tailed T test: *P<0.05; ***P<0.0005²¹⁵.

3.2.4 m4PTB increases tubular cell dedifferentiation post-AKI

Several mechanisms could explain m4PTB-induced RTEC proliferation, including accelerated cell cycle progression and/or increased dedifferentiation. To examine the latter possibility, we injected *Tg(PT:EGFP)* fish with gentamicin at 3 dpf, followed by DMSO or m4PB treatment at 2 dpi. We then quantified the number of Pax2a-positive cells in the PT at 3 dpi, since Pax2a is reactivated after injury in mammalian AKI models^{53, 54, 222, 223}. Compared to uninjured larvae, gent-AKI larvae had a greater number of Pax2a-positive cells (4.1 ± 0.6 cells vs. 9.5 ± 1.3 cells), which was almost doubled by 24-hour m4PTB treatment (18.0 ± 2.8 cells) (Figure 19). These results point to an increased dedifferentiation response, and suggest that m4PTB's effects on tubular epithelial proliferation are due in part to stimulating dedifferentiation.

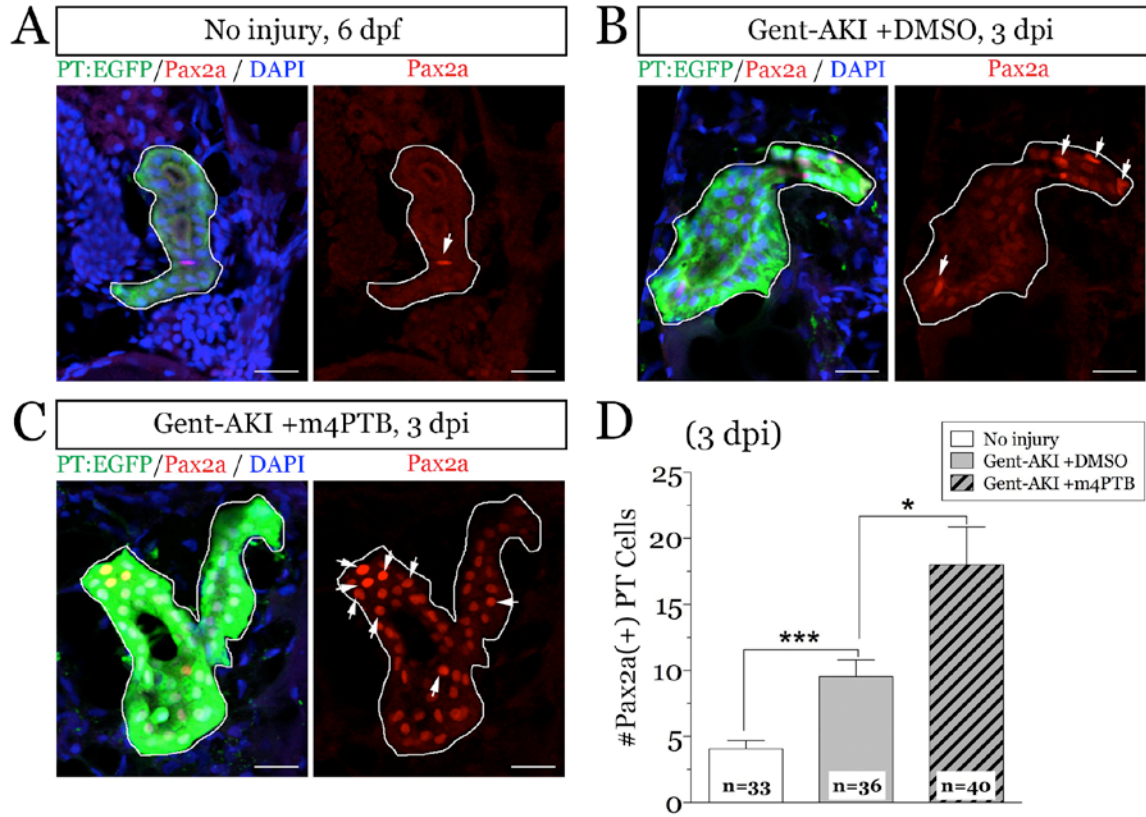


Figure 19: m4PTB expands the Pax2a-positive population of PT cells post-AKI.

(A-C) Transverse cryosections of uninjured or gent-AKI *Tg(PT:EGFP)* fish treated with 1% DMSO vehicle or 1-2 μ M m4PTB, immunostained with anti-GFP (green) and anti-Pax2a (red, white arrows), and counterstained with DAPI (blue). Tubules are outlined in white. Scale bars, 20 μ m. (D) Pax2a-positive cells were quantified in the PT by examining serial sections. Data expressed as mean \pm SEM. 2-tailed T test, *P < 0.05, ***P < 0.0005. “n” indicates the number of tubules analyzed per group.

3.2.5 m4PTB treatment does not affect the innate immune response

HDACi have been shown to improve long-term outcomes in mammalian AKI partly due to their anti-inflammatory properties^{139, 143}. Therefore, we assessed whether post-injury treatment with m4PTB also affected the innate immune response in this model. We injected *Tg(lyz:EGFP)* or *Tg(mpeg1:denra2)* fish with gentamicin at 3 dpf, followed by DMSO or m4PTB treatment at 2 dpi. We then quantified renal neutrophils and macrophages, respectively, by immunofluorescence staining at 3 dpi. There was no significant change in the number of neutrophils or macrophages between treatment groups (Figure 20). Thus, the mechanism by which m4PTB ameliorates AKI in zebrafish larvae does not involve modulating the innate immune response.

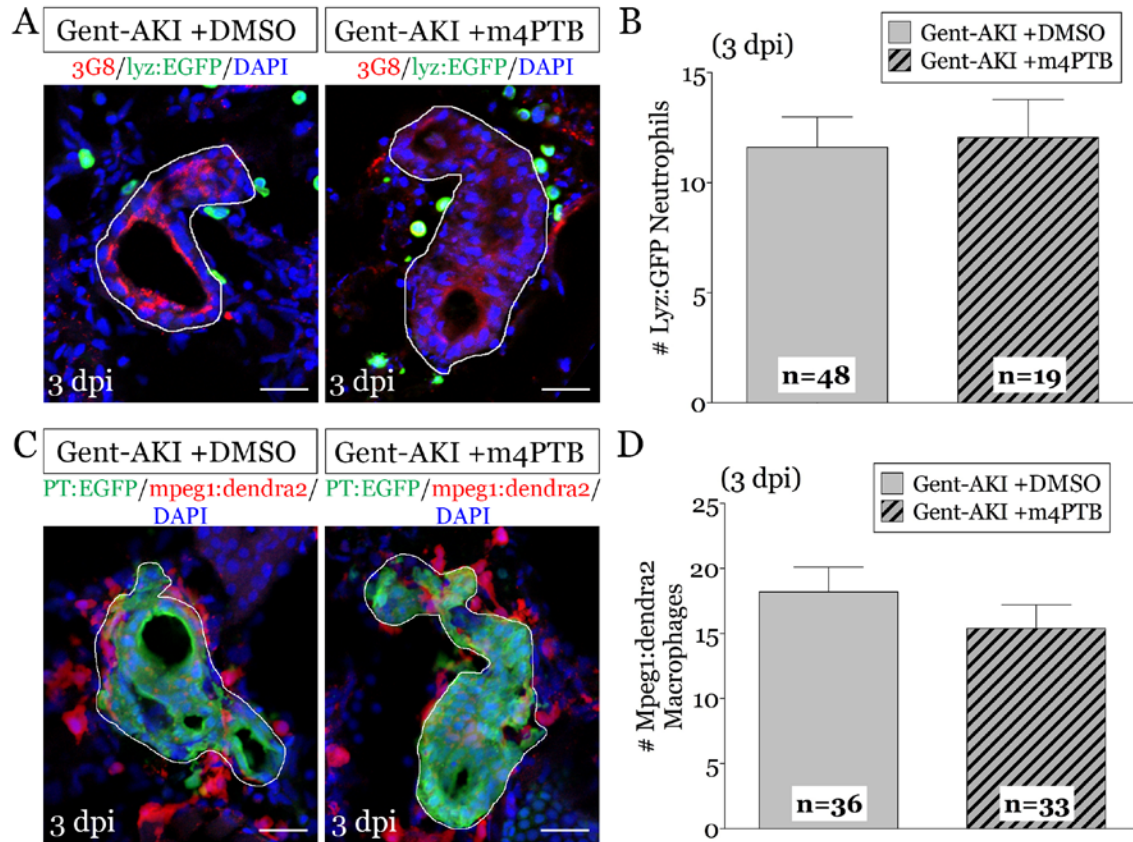


Figure 20: m4PTB treatment does not affect post-AKI neutrophil or macrophage infiltration.

(A) *Tg(lyz:EGFP)* larvae were injected with gentamicin at 3 dpf and treated with either DMSO or m4PTB at 2 dpi. Larvae were fixed at 3 dpi and stained with anti-3G8 and anti-GFP antibodies. (B) Quantitative analysis shows no significant difference in the number of renal neutrophils after treatment. (C) Double transgenic *Tg(PT:EGFP); Tg(mpeg1:dendra2)* larvae were injected with gentamicin at 3 dpf and treated with either DMSO or m4PTB at 2 dpi. Larvae were fixed at 3 dpi and stained with anti-GFP and anti-Dendra2 antibodies. (D) Quantitative analysis shows no significant difference in the number of renal macrophages between groups. Data are expressed as mean \pm SEM; 2-tailed T test: not significant. White lines outline the tubules. Scale bars, 20 μ m. “n” represents the number of tubules analyzed per group.

3.3 METHODS

3.3.1 Zebrafish husbandry

Zebrafish husbandry was performed as described in Chapter 2.

3.3.2 Gentamicin microinjection

Gentamicin microinjection was performed as described in Chapter 2.

3.3.3 MTD assay

Cohorts of 15-20 zebrafish larvae were arrayed in individual wells of a 12 well plate and incubated with treatment solution containing 1% DMSO diluted in E3 medium, \pm m4PTB at increasing concentrations. m4PTB was synthesized as previously described²⁰⁴. Treatment was initiated at 4 dpf and continued for 24 hours at 28.5°C. At 5 dpf, larvae were examined for signs of toxicity, including slowed heartbeat, impaired tail circulation, impaired touch response, edema, and death. The MTD was determined as the maximum m4PTB concentration that did not result in mortality or generalized toxicity in \geq 50% fish. Each assay was performed in triplicate with mixed clutches for every new synthesis batch of compound. Working doses were established between 0.5 and 4 μ M between batches.

3.3.4 Histone hyperacetylation assay

Cohorts of 20 larvae were treated with increasing concentrations of m4PTB at 4 dpf and harvested for western blot after 6, 12, or 24 hours, or for immunofluorescence after 6 hours. For western blot analysis, larvae were pooled and transferred to cold PBST +0.1% tricaine for 10 minutes. This solution was removed, and 1x Laemmli buffer (Biorad) plus 5% 2-mercaptoethanol was added. SDS-PAGE and western blotting were performed as described previously²⁰⁴, with the following modifications. Proteins were separated on 4-20% polyacrylamide gradient gels (Biorad). Membranes were incubated at 4°C overnight with 1:1,000 rabbit anti-acetylated H4 Lysine 5/8/12 and 16 antibodies (pan H4 acetylation, PentaH4, Millipore), or 1:1,000 anti- α -tubulin antibody (Sigma-Aldrich) in PBST containing 5% nonfat milk.

Whole mount immunofluorescence examining global histone hyperacetylation was performed with PentaH4 antibody (1:250) as previously described for α 6F antibody²⁰⁶, with an additional incubation with 100 μ g/ml proteinase K included before the blocking step. Larvae were imaged by confocal microscopy (Zeiss LSM 700) by stitching z-stack images consisting of 58, 4 μ m optical sections.

3.3.5 Histological analysis

Histology was performed as described in Chapter 2. Conditions for histology are summarized in Table 1, Appendix B.

3.3.6 Survival assay with m4PTB

For survival studies, m4PTB was used at a treatment concentration one-half the maximum tolerated dose (4 μ M). Larvae were soaked in treatment solution containing 1% DMSO \pm m4PTB diluted in E3 medium beginning 48 hours after gentamicin injection (2 dpi). After 24 hours at 3 dpi, treatment solution was removed and replaced with E3 medium. Larvae were assayed for death at 4, 5, and 6 dpi. Survival rates were compared using a 2-tailed Fisher's exact test.

3.3.7 EdU labeling

EdU labeling and proliferation analysis was performed as described in Chapter 2.

3.4 DISCUSSION

This work shows that post-injury treatment with the novel HDACi m4PTB increases recovery after gentamicin-AKI in zebrafish larvae. m4PTB enhances recovery in this model by stimulating RTEC dedifferentiation and proliferation, without affecting the innate immune response. m4PTB treatment also expands the population of *lhx1a*-positive RPCs by increasing proliferation in the embryo²⁰⁴, suggesting that m4PTB acts by a common mechanism during renal development and regeneration. Taken together, these studies demonstrate how compound screens in zebrafish embryos can be used to identify new drug targets that show promise as novel therapeutics in kidney disease models.

To evaluate whether our results in zebrafish translate to mammalian AKI, our collaborators in the lab of Mark de Caestecker at Vanderbilt University evaluated the therapeutic potential of m4PTB in mouse IR-AKI. In this model, m4PTB treatment accelerated renal functional recovery, increased the proportion of proliferating S-phase RTECs, and decreased long-term fibrosis²¹⁵. These studies provide evidence that m4PTB also ameliorates AKI after IR-AKI in mice by comparable mechanisms to gentamicin-AKI in zebrafish larvae. More generally, they show how modeling AKI in zebrafish can identify new therapies that translate well in mammals.

Despite many similarities between zebrafish and mouse AKI, the effects of HDAC inhibition on the immune response may differ depending on the particular AKI model and compound. After treating mice with the potent nephrotoxin aristolochic acid, Novitskaya et al. observed a reduction in macrophages after m4PTB treatment, which correlated with increased functional recovery and decreased fibrosis²³⁶. This is consistent with other reports of beneficial, anti-inflammatory properties of more broad-spectrum HDACi in kidney disease models^{97, 237}. In zebrafish gentamicin-AKI, however, we saw no change in the number of infiltrating neutrophils or macrophages after m4PTB treatment. One possible explanation for this difference could be the timing of evaluating the leukocyte response. In the Novitskaya study, m4PTB's effects on expression of macrophage markers and macrophage numbers were most robust late in injury, at days 14-21 after injury. Early in the course of injury at 4-7 dpi, several macrophage markers remained unchanged. These findings indicate that early m4PTB treatment may promote a healthy repair environment, mitigating inflammation as a long-term benefit.

We also noted differences in how m4PTB affected the dedifferentiation and proliferation response after AKI in mice versus zebrafish. In mouse, microarray studies identified a greater

than 2-fold expression increase of several G2/M transitional regulators after m4PTB treatment, including Cyclin B1, Cyclin B2, Cdca3, Polo Like Kinase 1, and Checkpoint Kinase 1. These expression changes led the de Caestecker lab to evaluate the proportion of proliferating RTECs in the S, G2, or M phases of the cell cycle. m4PTB treatment increased S-phase proliferation with a concomitant decrease in the number of cells in G2/M. Further supporting these results, Thus in mouse AKI, m4PTB alleviates cell cycle arrest by promoting cell cycle progression. Given the role of G2/M arrested cells in advancing renal fibrosis, these results may explain why m4PTB-treated mice ultimately developed less fibrotic tissue. In zebrafish, we also observed increased S-phase proliferation by EdU incorporation after m4PTB treatment, but we did not evaluate other phases of the cell cycle. As discussed in Chapter 2, it is not currently known whether RTECs undergo G2/M arrest after AKI in zebrafish. Therefore, to fully assess translatability, further studies are warranted to evaluate m4PTB's effects on cell cycle regulation in zebrafish.

Conversely in zebrafish AKI, we observed a greater number of Pax2a-positive RTECs after m4PTB treatment. This indicates that m4PTB stimulates RTEC dedifferentiation, which could also explain the increased proliferative response. Immunofluorescence microscopy studies demonstrating colocalization of Pax2a and EdU in RTECs would more definitively determine whether m4PTB-stimulated RTEC dedifferentiation leads to increased proliferation and tubular repair. It has been shown in mouse AKI that proliferating RTECs are both Pax2- and Kim1-positive²²², suggesting that the injured cell population is responsible for the regeneration response. Kim1, however, has not been quantified on the cellular level. Theoretically, it would be feasible to quantify Kim1 immunofluorescence in order to examine whether m4PTB decreases Kim1 levels in dedifferentiated cells, effectively creating a mildly-injured RTEC

population that contributes to repair. Further, we could examine whether m4PTB treatment promotes RTEC health by performing Na/K ATPase staining and examining for restored apical/basal polarity. These studies are ongoing in the Hukriede lab.

More generally, these results indicate that m4PTB has both pro-dedifferentiation and pro-proliferation effects on cell populations in zebrafish and mice – observations that contrast with the pro-differentiation, anti-proliferation profile of many HDACi in the cancer field. Several studies, however, demonstrate that HDACi have different and even paradoxical effects in cancer cells compared to non-cancerous cells. For example, HDACi that are highly toxic to cancer cells appear to have cytoprotective effects in non-cancerous cells¹⁰². In fact, non-cancerous cells are more resistant to high HDACi doses than cancer cells, and low doses have actually been shown to be both reno-^{238, 239} and neuroprotective^{240, 241}. Specifically, one possible mechanism for differential sensitivity to SAHA treatment has been related to the availability of ROS scavenging proteins. SAHA treatment increases expression levels of thioredoxin binding protein 2 (*TBP2*), resulting in a subsequent decrease in the availability of ROS scavenging proteins. Combined with the fact that SAHA also increases ROS generation in cancer cells, this may lead to preferential cancer cell death¹¹⁹. These studies indicate that the effects of HDACi treatment are both compound specific and context dependent.

Here, we have explored how m4PTB ameliorates injury in gentamicin-AKI in zebrafish larvae by examining effects on RTEC dedifferentiation/proliferation and leukocyte infiltration. Of course, there could be additional mechanisms. For example, HDACi have been shown to act as chemical chaperones²⁴² and to protect against oxidative stress^{243, 244}, representing other possible therapeutic targets for ameliorating AKI²⁴⁵. The Hukriede lab is currently investigating whether PTBA-class HDACi modulate oxidative stress during gentamicin-AKI in zebrafish.

Ultimately, comprehensive understanding of the mechanisms underlying how m4PTB mitigates renal injury will depend on characterizing HDAC isoform selectivity and downstream molecular targets.

Material modified and re-published with permission:

¹²⁶***Brilli LL**, *Swanhart LM, de Caestecker MP, Hukriede NA. HDAC inhibitors in kidney development and disease. *Pediatric nephrology*. 2013;28(10):1909-21. doi: 10.1007/s00467-012-2320-8. PubMed PMID: 23052657; PubMed Central PMCID: PMC3751322.

²¹⁵*Cianciolo Cosentino, C, *Skrypnyk, NI, ***Brilli, LL**, Chiba, T, Novitskaya, T, Woods, C, West, J, Korotchenko, VN, McDermott, L, Day, BW, Davidson, AJ, Harris, RC, de Caestecker, MP, Hukriede, NA: Histone deacetylase inhibitor enhances recovery after AKI. *Journal of the American Society of Nephrology : JASN*, 24: 943-953, 2013.

*Denotes equally contributing authors.

4.0 INTERSECTION OF M4PTB AND THE RETINOIC ACID PATHWAY IN AKI

4.1 HYPOTHESIS

We have shown that m4PTB ameliorates gentamicin-AKI in zebrafish larvae by promoting RTEC dedifferentiation and proliferation. To further characterize the underlying molecular mechanisms, we sought to identify active signaling pathways that promote renal regeneration post-AKI that could be affected by m4PTB treatment. Two lines of evidence led us to investigate how m4PTB impinges specifically on the RA pathway. First, HDACs/HDACi modulate RA signaling through direct interaction with corepressor complexes. Second, previous work in the Hukriede lab demonstrated that PTBA both stimulates RA target gene expression and requires intact RA signaling to expand the RPC population in the zebrafish embryo²⁰⁴. Therefore, we hypothesized that during AKI in zebrafish larvae, m4PTB also stimulates active RA signaling in the kidney.

4.2 RESULTS

4.2.1 RA signaling increases in the pronephros after gentamicin injection

We first characterized the role of RA signaling in gentamicin-AKI in zebrafish larvae, since this has not previously been evaluated. For this we used a zebrafish transgenic reporter, *Tg(12XRARE:EGFP)*¹⁶⁰. In this reporter line, activation of consensus RAREs drives EGFP expression, allowing RA signaling to be visualized and quantified in vivo by live imaging for EGFP^{159, 160}. Uninjured fish expressed basal levels of *egfp* mRNA in the retina and anterior spinal cord (Figure 21A), and a proportion of larvae retained *egfp* expression in the pronephric kidney through 4 dpf ($21\pm 8\%$, $n=9$ experiments, 12-16 larvae/group).

To evaluate the timing and location of RA activation after gentamicin-induced AKI, we first performed whole mount in situ hybridization to examine *egfp* expression in *Tg(12XRARE:EGFP)* larvae after gentamicin injection at 3 dpf. There was an increased proportion of fish with strong *egfp* expression throughout the pronephric kidney 6 hours after gentamicin injection (Figure 21A-B). Quantification of trunk *egfp* mRNA by qRT-PCR also demonstrated increased expression at 6 hpi (Figure 21-insets). We also evaluated trunk expression of *midkine a* (*mdka*), a known RAR target in mammals¹⁵². Consistent with the timing of increased RA reporter activation, *mdka* levels were increased at 6 hpi (1.0 ± 0.1 in uninjured controls vs. 1.7 ± 0.1 in gent-AKI, 15 larvae/group).

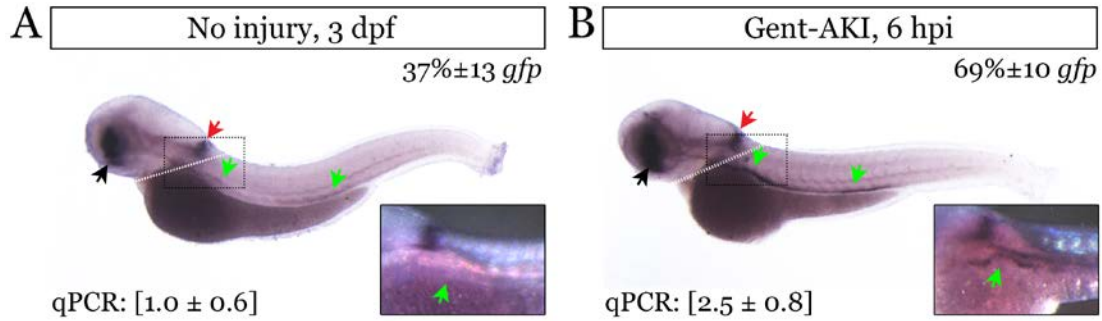


Figure 21: RA signaling is increased in zebrafish larval kidneys after AKI.

We injected *Tg(12XRARE:EGFP)* zebrafish larvae with 8ng of gentamicin at 3 dpf to induce renal injury. Whole mount in situ hybridization comparing *egfp* expression in uninjured controls (A) and gent-AKI larvae at 6 hpi. Colored arrows show domains of expression: retina (black), anterior spinal cord (red), and kidney (green). Higher magnification of the PT in the boxed region inset. Percent *egfp* quantifies the number of fish with strong, pan-renal expression (n=3 experiments at 3dpf, ≥ 12 larvae/group, mean \pm SEM). qRT-PCR for *egfp* mRNA for dissected trunk tissue posterior to the white dotted line are in brackets below the in situ image, mean fold change \pm SEM (n=3 experiments, 15 larvae/group). Normalized to β -actin and *sdha*²²¹.

Since these results indicate that RA signaling is rapidly activated in the kidney after gentamicin injection, we examined the localization and dynamics of RA signaling in the kidney in the first 24 hours after injury. Time-lapse confocal imaging in *Tg(12XRARE:EGFP)*; *Tg(cdh17:mCherry)* fish was used to visualize RA signaling in tubular epithelial cells, using loss of *cdh17:mCherry* expression as a marker of tubular cell dedifferentiation after injury^{160, 212}. Throughout the 24-hour imaging window, we observed heterogeneous populations of red, yellow, and green cells in the kidney. Consistent with our in situ hybridization studies, GFP fluorescence intensity decreased over time in the kidney of uninjured controls, and increased in gent-AKI fish. Specifically, we observed red cells (differentiated renal epithelial cells) that turned yellow (activation of RA signaling, overlay with mCherry) and eventually turned green (loss of mCherry expression) (Figure 22). These data indicate that RA signaling is rapidly activated in tubular epithelial cells that subsequently lose differentiation characteristics after gentamicin injection.

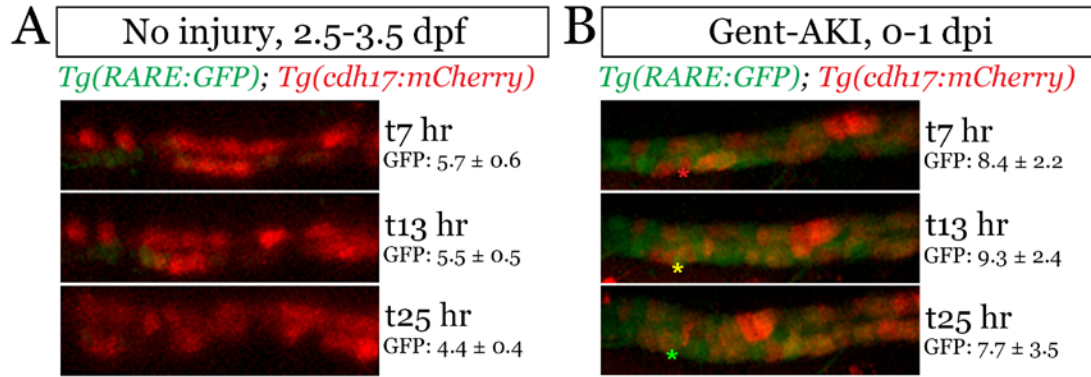


Figure 22: RA signaling increases in renal epithelial cells after AKI.

Single images from live time-lapse multi-photon imaging showing a region of the PT of uninjured (A) or gent-AKI (B) *Tg(12XRARE:GFP); Tg(cdh17:mCherry)* double transgenic fish. Imaging was performed for 21 hours beginning at 4 hours after gentamicin injection. Red indicates *cdh17*-positive, differentiated renal epithelial cells (example, red asterisk), green indicates RA reporter-positive cells (example, green asterisk), and yellow indicates double-positive cells (example, yellow asterisk). GFP values indicate average fluorescence intensity \pm SEM for the image stack at the indicated time point ($n=10$ uninjured and 6 gent-AKI nephrons)²²¹.

4.2.2 RA signaling is activated in injured tubular epithelial cells

To determine whether RA activation occurs in injured tubular cells, we evaluated Kim1 expression in *Tg(12XRARE:EGFP)* larvae after gentamicin-induced AKI. At 2 dpi, when we detected robust activation of Kim1 expression in PT cells (Figure 8), Kim1 colocalized with RARE:EGFP in RTECs (Figure 23). These data indicate that RA signaling is activated in a population of Kim1-positive injured RTECs in zebrafish larvae after gentamicin-AKI.

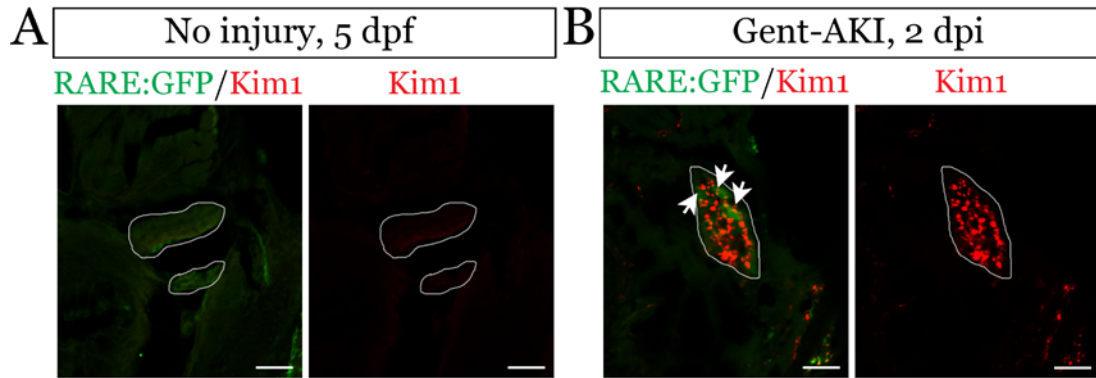


Figure 23: RA signaling is activated in Kim1-positive renal epithelium.

Immunofluorescence staining for Kim1 (red) and GFP (green) in the kidney of uninjured (A) and gent-AKI (B) *Tg(12XRARE:EGFP)* fish at 2 dpi. Examples of colocalization indicated by white arrows. Tubules are outlined in white. Scale bars, 20 μm ²²¹.

4.2.3 Inhibition of RA signaling impairs survival after AKI

To examine whether early activation of RA signaling is a critical step in renal regeneration processes post-AKI, we treated zebrafish larvae with Ro41-5253, a RAR antagonist that has been used to block RAR signaling in zebrafish^{160, 246, 247}. To determine an effective working dose, we treated *Tg(12XRARE:EGFP)* larvae with increasing concentrations of Ro41-5253 for 24 hours from 3 to 4 dpf. Treatment with 1 μM Ro41-5253 blocked all domains of *egfp* expression without negative effects on health (Figure 24A). Since we observed rapid activation of RA signaling within 24 hours of gentamicin injection, we next treated larvae with Ro41-5253 immediately after inducing renal injury. Ro41-5253-treated fish showed decreased survival after gentamicin injection compared to DMSO-treated fish (Figure 24B), indicating impaired recovery^{206, 215}. These data demonstrate that activating the RA pathway early after injury is critical for fish to survive after AKI.

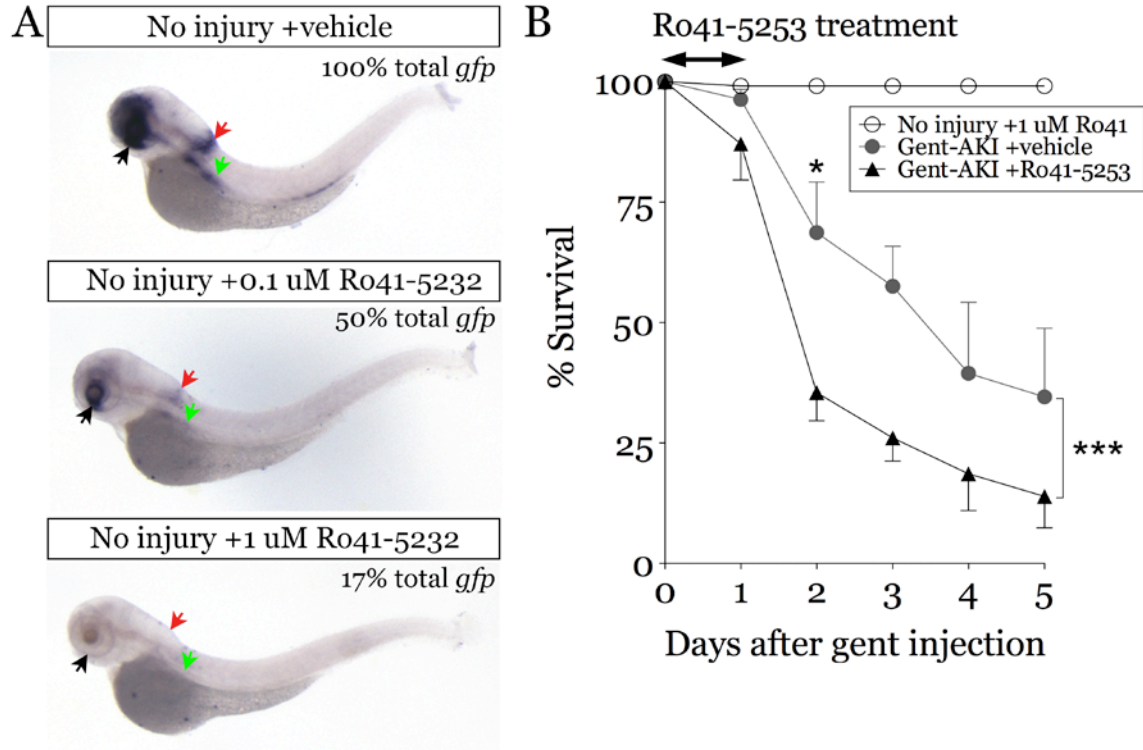


Figure 24: Ro41-5253 treatment inhibits RA signaling and impairs survival after AKI.

(A) Uninjured *Tg(12XRARE:EGFP)* larvae were treated with 1% DMSO vehicle, 0.1 μ M or 1 μ M Ro41-5253 from 3-4 dpf. Whole mount in situ hybridization was performed at 4 dpf to assess the ability of Ro41-5253 to block *egfp* expression. Colored arrows show domains of expression, including retina (black), anterior spinal cord (red), and kidney (green). Percent *egfp* quantifies the number of larvae that show visible *egfp* expression in any of these domains (n=3 experiments, 15 larvae/group). (B) Uninjured or gent-AKI larvae were treated with vehicle or 1 μ M Ro41-5253 from 3-4 dpf, and survival was assessed daily through 5 dpi (n=4 experiments, ≥ 20 larvae/group). 2-way ANOVA, ***P<0.0005. Bonferroni's correction for multiple comparisons between vehicle and Ro41-5253 treated larvae at the same time points: *P<0.05²²¹.

4.2.4 Inhibition of RA signaling impairs tubular regeneration after AKI

To examine the effects of inhibiting RA signaling on renal injury post-AKI, we harvested larvae after gentamicin injection and Ro41-5253 treatment and quantified *kim1* expression by qRT-PCR. Compared to DMSO, Ro41-5253 treatment did not significantly alter *kim1* mRNA levels at 1 dpi or 2 dpi (Figure 25A). Thus, decreased survival caused by RAR inhibition may not be mediated by increasing Kim1-responsive tubular injury.

Since the RA pathway is the central regulator of cell proliferation in other organ injury models in zebrafish^{180, 183}, and since renal tubular epithelial repair relies on the proliferation response of these cells after AKI in both mammals and zebrafish^{35, 215}, we asked whether inhibition of RA signaling affected proliferation dynamics in the kidney post-AKI by examining cells in S-phase by PCNA immunostaining. Ro41-5253-treated larvae showed a decrease in the number of PCNA-positive PT cells at 2 dpi (Figure 25B). These data indicate that RA signaling is critical for recovery and promotes PT cell proliferation in larval zebrafish post-AKI.

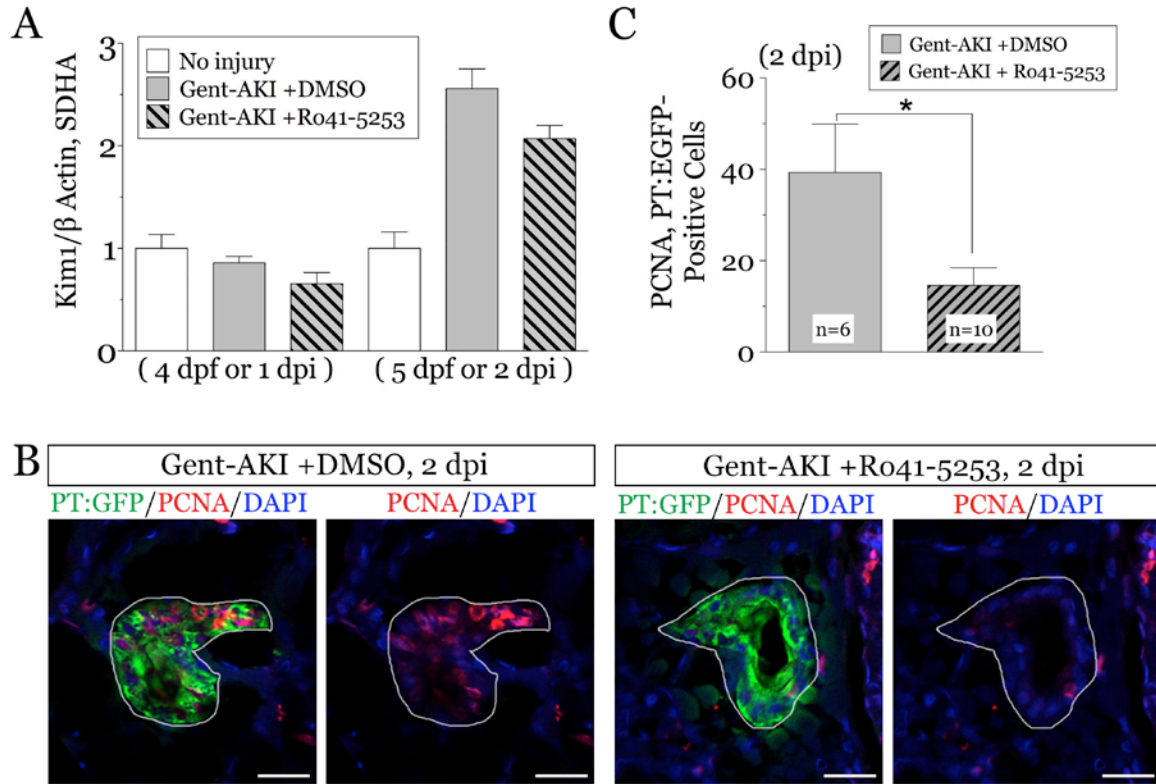


Figure 25: Blocking the RA pathway impairs tubular proliferation after AKI.

Zebrafish larvae were injected with 8ng gentamicin at 3 dpf to induce renal injury, followed by treatment with 1% DMSO vehicle or 0.5-1μM Ro41-5253 for 24 hours. (A) RNA was isolated from larval trunk tissue at 1 dpi and 2 dpi, followed by qRT-PCR to examine *kim1* mRNA expression. Graph is one representative experiment, shown as mean plus SD for 3 technical replicates (n=3 experiments at 1 dpi and n=4 experiments at 2 dpi, 15 larvae/group). Expression normalized to β -actin and *sdha*. (B) Immunofluorescence for PCNA (red) and GFP (green) in the PT of *Tg(PT:EGFP)* fish at 2 dpi. White lines outline the tubules. Scale bars, 20 μm. (C) PCNA-positive cells were quantified in the PT by examining serial sections. Data are expressed as mean \pm SEM; 2-tailed T test: *P<0.05. “n” represents the number of tubules analyzed per group²²¹.

4.2.5 Short-term ATRA treatment increases survival during AKI

Conversely, we examined whether increased RA signaling enhanced AKI recovery by treating fish with ATRA after gentamicin injection. We compared two treatment regimens: sustained 4nM ATRA treatment from 0-5 dpi, and 24-hour 4 nM ATRA from 0-1 dpi. Whereas long-term treatment impaired survival, short-term treatment improved survival (Figure 26). Careful considerations regarding dose and timing likely influence whether RA agonists will be effective AKI therapies.

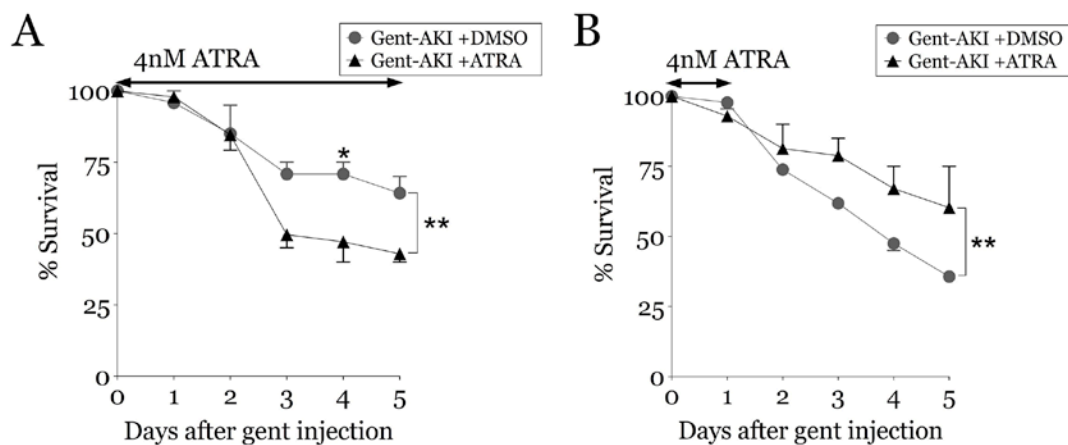


Figure 26: Effect of ATRA on survival after AKI depends on treatment duration.

(A) Larvae were injected with 8ng gentamicin at 3 dpf, followed by treatment with 1% DMSO vehicle or 4nM ATRA through 5 dpi. Survival was assessed daily through 5 dpi (n=2 experiments, 20-24 larvae per group). (B) Compound treatment with 1% DMSO vehicle or 4nM ATRA from 3-4 dpf only (n=2 experiments, 18-22 larvae/group). 2-way ANOVA, **P<0.005. Bonferroni's correction for multiple comparisons between DMSO and ATRA treated larvae at the same time points: *P<0.05.

4.2.6 Mechanism of m4PTB action requires intact RA signaling

Having determined that increased RA signaling early after AKI is critical for larval survival, we next assessed whether m4PTB treatment stimulated RA signaling. To do this, we treated groups

of *Tg(12XRARE:EGFP)* fish with DMSO, ATRA alone, m4PTB alone, or ATRA plus m4PTB at 4 dpf for 6-10 hours. We evaluated the effect of compound treatment on RA signaling by performing whole mount in situ hybridization and examining *egfp* mRNA expression (Figure 27A). To quantify these data, we counted the number of larvae that displayed strong *egfp* staining in the kidney/trunk region (Figure 27B). Compared to DMSO-treated controls, low-dose ATRA treatment moderately increased *egfp* expression. High-dose ATRA treatment further increased *egfp* staining intensity in all domains, most easily visualized in the kidney and trunk. However, m4PTB treatment alone had no effect on *egfp* expression compared to DMSO treatment. Further, co-treatment with m4PTB and low-dose ATRA did not increase expression over levels induced by ATRA alone. These data suggest that in uninjured larvae, m4PTB does not directly stimulate RARE-driven *egfp* expression, and does not synergize with ATRA in this reporter line.

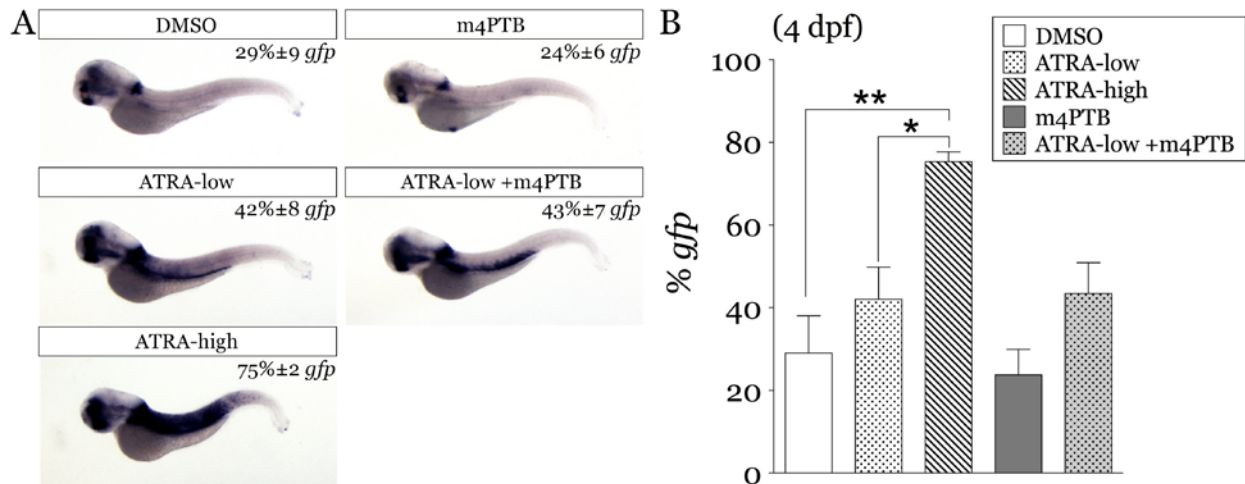


Figure 27: m4PTB does not synergize with ATRA to drive RARE:EGFP expression.

(A) Uninjured *Tg(12XRARE:EGFP)* larvae were treated with 1% DMSO vehicle, ATRA (low dose at 1-2nM, high dose at 4-10nM), m4PTB (1-4μM), or ATRA plus m4PTB. Treatment continued for 6-10 hours before fixation and subsequent whole mount in situ hybridization to examine *egfp* mRNA levels. (B) Percent *egfp* quantifies the number of larvae that show strong kidney/trunk *egfp* expression (n=3 experiments, 15 larvae/group). Data are expressed as mean ± SEM; 2-tailed T test: *P<0.05, **P<0.005.

Based on these results, we determined whether m4PTB's effects on RTEC proliferation

required an intact RA pathway. To do this, we utilized an inducible transgenic zebrafish line *Tg(hsp70l:RARA,cryaa:EGFP)*, here termed *Tg(hsp70:dnRARα)*, in which heat shock stimulates expression of a dominant-negative form of the human RA receptor alpha (DN-RARα)²⁴⁸. Since this line was used previously to study phenotypes during early development, we established a heat shock regimen in zebrafish larvae that would block RA signaling during the window of m4PTB activity. To evaluate the timing of DN-RARα protein activation, we heat shocked 4 dpf *Tg(hsp70:dnRARα)* larvae at 37°C for one hour and generated protein extracts after 0, 6, 12, or 24 hours. Single heat shock resulted in detectable DN-RARα protein from 0 to 6 hours (Figure 28). Importantly, compound treatment alone did not induce DN-RARα expression in this line (Figure 29). Since the effects of 4μM m4PTB treatment on histone acetylation are also abrogated between 6-12 hours (Figure 15), one-hour heat shock should reduce RA signaling during the same time period as m4PTB is active.

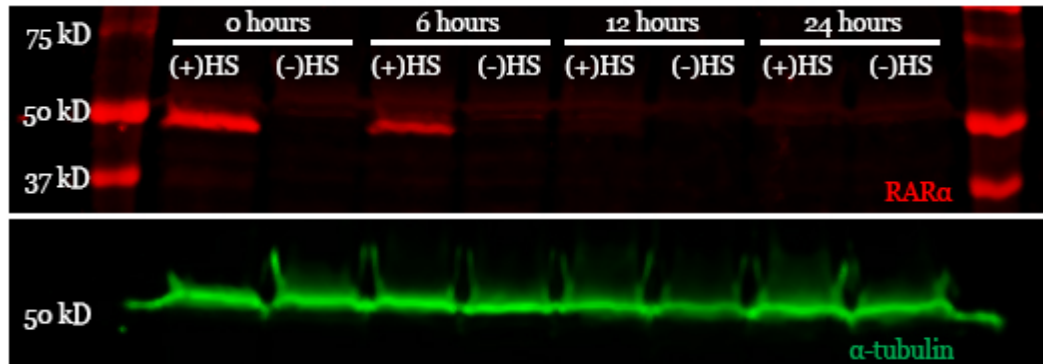


Figure 28: Time course of DN-RARα activation after heat shock.

Fluorescent western blot examining the stability of DN-RARα protein. Groups of *Tg(hsp70:dnRARα)* fish were heat shocked at 4 dpf for one hour at 37°C (+HS) and compared to non heat-shocked controls (-HS). Protein extracts were generated after 0, 6, 12, or 24 hours. DN-RARα protein could be detected through 6 hours after heat shock (red, top panel). α-tubulin demonstrates equal loading (green, bottom panel).

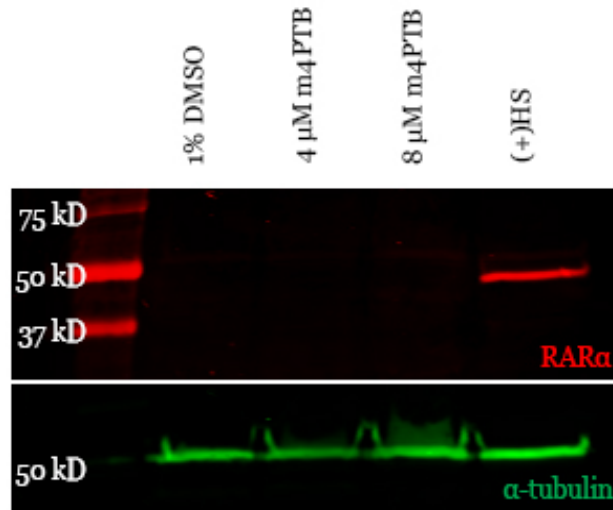


Figure 29: m4PTB treatment does not activate DN-RAR α expression.

Fluorescent western blot examining the effect of compound treatment on DN-RAR α induction in *Tg(hsp70:dnRAR α)* fish. Groups of transgenic larvae at 4 dpf were treated with 1% DMSO vehicle, m4PTB, or heat shocked for one hour at 37°C (+HS). Protein extracts were generated after 6 hours. DN-RAR α protein was detected only after heat shock (red, top panel). α -tubulin demonstrates equal loading (green, bottom panel).

We previously showed that m4PTB treatment increased RTEC proliferation both in uninjured larvae and after gentamicin injection (Figure 18). Therefore, we evaluated whether reducing RA signaling in this heat-inducible transgenic model would block m4PTB-stimulated RTEC proliferation. In uninjured *Tg(hsp70:dnRAR α)* larvae, we performed one-hour heat treatment at 4 dpf followed by 24-hour DMSO or m4PTB treatment. We quantified EdU S-phase proliferation at 5 dpf and compared proliferation to wildtype larvae treated with DMSO or m4PTB (Figure 30A). Proliferation rates were comparable between heat-shocked and non heat-shocked larvae treated with DMSO; however, larvae heat shocked before m4PTB treatment showed impaired RTEC proliferation compared to non heat-shocked controls (Figure 30B). Therefore in uninjured larvae, m4PTB requires RA signaling to stimulate RTEC proliferation. Similarly, we evaluated proliferation in this transgenic model after AKI. At 2.5 dpf, *Tg(hsp70:dnRAR α)* larvae were injected with gentamicin. At 2 dpi, larvae were heat shocked for one hour and treated with compound for 24 hours, followed by PCNA S-phase proliferation

analysis (Figure 30C). Post-AKI, m4PTB treatment significantly increased RTEC proliferation in non heat-shocked controls. When heat shock preceded compound treatment, m4PTB did not significantly increase RTEC proliferation (Figure 30D). Taken together, these data indicate that m4PTB does not directly stimulate the RA pathway, but rather its mechanism of action requires upstream RA signaling.

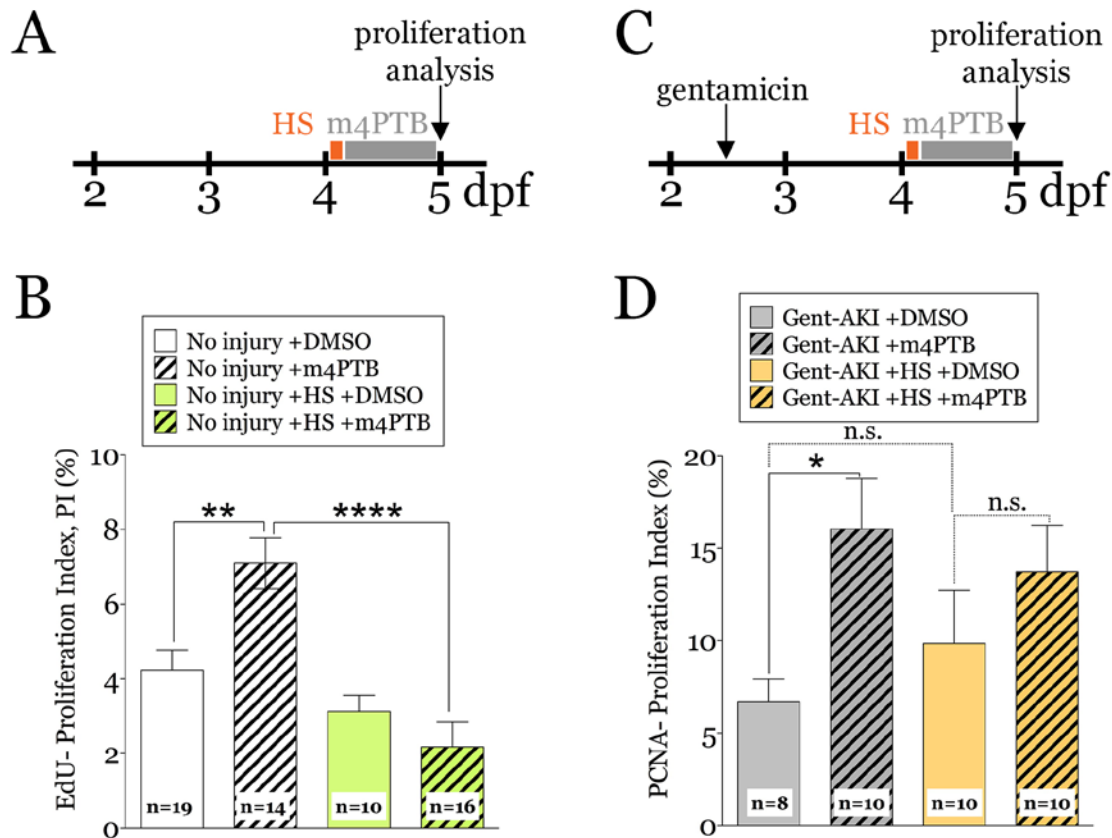


Figure 30: DN-RAR α induction impairs m4PTB-mediated RTEC proliferation.

(A) Experimental timeline. Uninjured *Tg(hsp70:dnRAR α)* larvae at 4 dpf were heat shocked for one hour at 37°C, followed by 24-hour treatment with 1% DMSO vehicle or 4 μ M m4PTB. 4 dpf wildtype larvae were not heat shocked and treated with DMSO m4PTB. Fish were treated with EdU and proliferation analysis was performed at 5 dpf. (B) EdU-positive cells were quantified by examining serial sections stained with anti-3G8. (C) Experimental timeline. *Tg(hsp70:dnRAR α)* larvae were injected with 8ng gentamicin at 2.5 dpf. At 2 dpi (4 dpf), larvae were heat shocked for one hour at 37°C. Following heat shock, larvae were treated with DMSO or m4PTB. After 24 hours at 3 dpi (5 dpf), larvae were fixed and PCNA proliferation analysis was performed. (D) PCNA-positive cells were quantified by examining serial sections stained with anti-3G8. Data are expressed as mean \pm SEM; 2-tailed T test: *P<0.05, **P<0.005, ***P<0.0005, ns not significant. “n” represents the number of tubules analyzed per group.

4.3 METHODS

4.3.1 Zebrafish husbandry

Zebrafish husbandry was performed as described in Chapter 2. In addition, embryos were used from the following published transgenic lines: *Tg(12XRARE-ef1a:EGFP)^{sk72 160}* and *Tg(hsp70:dnRAR α -acry:EGFP)²⁴⁸*. Positive *Tg(hsp70:dnRAR α -acry:EGFP)* larvae were identified at 2 dpf by examining for EGFP in the eye. For in vivo imaging and in situ hybridization, embryos were kept in E3 medium containing PTU after 24 hpf.

4.3.2 Gentamicin microinjection, chemical treatments, and heat shock

Gentamicin microinjection was performed as described in Chapter 2. For RA inhibition studies, zebrafish larvae were treated with 1uM Ro41-5253 (Enzo Life Sciences) in 1% DMSO diluted in E3 for 24 hours from 3 to 4 dpf, and then compound was washed out with several changes of E3. For survival assays, individual larvae were placed in wells of a 48 well plate after gentamicin microinjection and covered with E3 medium \pm Ro41-5253. Larvae viability was scored once per day on days 1-5 post injection. For heat shock treatments, groups of 4 dpf fish were arrayed in a 6 well plate and incubated with preheated E3 medium on a hot plate at 37°C. After one hour, the media was removed and the fish were returned to incubation at 28.5°C.

4.3.3 In situ hybridization

Zebrafish larvae were fixed in 4% paraformaldehyde for 24 hours and processed for whole mount in situ hybridization as previously described, using antisense RNA probe for *egfp*²⁰⁴. After staining, larvae were examined and scored based on intensity of colorimetric staining. Images are shown from one representative experiment.

4.3.4 DN-RAR α protein analysis

Cohorts of *Tg(hsp70:dnRAR α -acry:EGFP)* larvae were heat shocked at 4 dpf for one hour at 37°C and harvested for western blot. 25-30 larvae were pooled and transferred to cold PBST containing 0.1% tricaine for 10 minutes. This solution was removed, and 1x Laemmli buffer (Biorad) plus 5% 2-mercaptoethanol was added. SDS-PAGE and western blotting were performed as described previously²⁰⁴, with the following modifications for fluorescence imaging. Proteins were separated on a 10% polyacrylamide gel and transferred to PVDF Immobilon-FL membrane (Millipore) at 4°C for 30 minutes at 50V followed by 60 minutes at 100V. Membranes were incubated at 4°C overnight with 1:1,000 anti- α -tubulin (mouse, Sigma-Aldrich) and 1:750 anti-RAR α (rabbit, LifeSpan Biosciences) antibodies in Odyssey blocking buffer (LiCor) containing 0.2% Tween. The following day, membranes were incubated with goat anti-mouse 800CW and goat anti-rabbit 680RD secondary antibodies (LiCor) diluted at 1:15,000 in Odyssey blocking buffer for one hour at room temperature. Membranes were dried and kept in the dark until imaging using LiCor Odyssey CLx and Image Studio version 4.0 software. Original unmodified images are reported in Figure 32, Appendix A.

4.3.5 Histological analysis

Immunofluorescence was performed on cryosections as described in Chapter 2. To quantify PTEC proliferation, we counted the number of PCNA-positive cells in the PT, marked by PT:EGFP. Conditions for histology are summarized in Table 1, Appendix B.

4.3.6 RNA isolation and quantitative RT-PCR

Quantitative RT-PCR was performed as described in Chapter 2. Data shown in graphs are from one representative experiment with 3 technical replicates. Raw data for each replicate shown in Table 3, Appendix B. Primer sequences are listed in Table 2, Appendix B.

4.3.7 Live confocal zebrafish imaging

Time-lapse confocal imaging was performed as described in Chapter 2, with the following modifications. Image stacks were acquired using HCX IRAPO L 25X/0.95 water immersion objective, and were captured every 90 minutes for 21 hours.

4.3.8 Analysis of GFP fluorescence intensity

GFP fluorescence intensity activated by RA signaling in *Tg(12XRARE:EGFP); Tg(cdh17:mCherry)* larvae during live imaging experiments was quantified using the Intensity function in LAS AF Version 3.0.0 build 8134. First, a region of interest in the PT was created

using mCherry expression as a guide ($3350 \pm 160 \mu\text{M}^2$, mean \pm SEM). The average GFP intensity was then calculated in this region across an entire image stack in each nephron per larvae.

4.4 DISCUSSION

We have shown that after gentamicin injection in zebrafish larvae, RA signaling increases rapidly in populations of Kim1-positive injured RTECs that have down-regulated the renal differentiation marker Cadherin17. This response is essential for recovery, as chemical inhibition of RAR signaling immediately following gentamicin injection significantly decreases RTEC proliferation and larval survival. The role of RA signaling during renal development in zebrafish has been well characterized^{171, 172}, but this work provides insights into the critical role of RA signaling during zebrafish AKI.

Additional studies are required to define this role more clearly. First, our proliferation analysis after gentamicin injection and Ro51-5253 treatment implicates RA signaling during tubular regeneration. Further, we showed that RARE:EGFP-positive cells are injured and lose cadherin17:mCherry expression, suggesting that RA signaling may occur in dedifferentiated RTECs. However in live imaging experiments, it is important to take into account that photostability and cellular context affect fluorophore dynamics²⁴⁹. Although EGFP and mCherry have shown good photostability²⁵⁰, we plan to examine if Pax2a colocalizes with RARE:EGFP-positive RTECs, and if RAR inhibition decreases Pax2a levels. This would more definitively show that RA impinges on proliferation by modulating dedifferentiation.

In addition to proliferation and/or dedifferentiation, RA could have other positive effects during renal regeneration. In a zebrafish model of fin amputation, Blum and Begemann showed

that RA signaling not only modulates blastema proliferation, but it also increases *bcl2* expression effectively protecting against cell death¹⁸⁰. Specifically in the context of AKI, pre-treatment with ATRA before AKI induced by potassium dichromate in rats prevents oxidative damage and tubular cell death²⁵¹. Pax2 reactivation during injury also decreases RTEC apoptosis¹⁴, so RA could ultimately be playing a cytoprotective role by multiple mechanisms.

Although we demonstrated increased RA signaling in RTECs after gentamicin injection, these studies did not determine whether this was an autocrine or paracrine effect. In zebrafish gent-AKI, preliminary data suggests that Raldh2 levels increase in both RTECs and in surrounding peritubular cells, without changes in RAR expression. The implications of these findings are two-fold. First, both renal and non-renal cells may represent cellular sources of RA. Second, availability of ligand rather than signaling machinery may drive pathway activation, which is consistent with other reports¹⁵³. In line with these ideas, our collaborators in the de Caestecker lab observed increased RARE-hsp68-lacZ activity in both RTECs and macrophages in the kidney after IR-AKI in mice. This activity peaked 12-24 hours after injury, suggesting that rapid induction of RA signaling is conserved between zebrafish and mouse AKI. Further, they determined that paracrine RA signaling in RTECs from Raldh-positive macrophages was critical for mitigating injury, possibly through M2 alternative activation²²¹. In the future, we will evaluate whether Raldh2-positive leukocyte populations also mediate renal regeneration in zebrafish.

Taken together, data from zebrafish and mouse indicate therapeutic applicability for RA agonists during AKI. Low-dose ATRA in mice decreases injury, prevents fibrosis, and improves functional recovery during AKI²²¹, findings that corroborate our zebrafish studies that showed increased survival during AKI after short-term ATRA treatment. As is the case during

development, it appears that tight regulation of RA signaling is required during kidney disease: detrimental versus beneficial effects of RA agonists have been shown to vary based on dosage, timing, injury model, and compound²⁵². Therefore, treatment parameters must be carefully evaluated in order to demonstrate therapeutic potential in the clinical setting.

Ultimately, understanding the intrinsic role of RA in renal regeneration is motivated by attempting to dissect how PTBA-class HDACi mediate recovery during AKI. We have shown that m4PTB does not directly stimulate or synergize with ATRA to enhance *Tg(12XRARE:EGFP)* reporter expression. Several factors may explain these results. First, evaluating RARE-driven *egfp* mRNA by qRT-PCR, rather than by in situ hybridization, would provide a more quantitative analysis. Second, *Tg(12XRARE:EGFP)* fish may not comprehensively report all RA signaling in larvae. It would be informative to look directly at RA target genes, especially since PTBA was found to modulate the RA targets *cyp26a1* and *cmlc2* in zebrafish embryos²⁰⁴. Finally, effects of m4PTB could depend on context. We did not examine if m4PTB altered RARE:EGFP expression during injury. We also did not evaluate larval survival after ATRA/m4PTB co-treatment. For example, Chiba et al. saw no change in RA target gene expression after 1mg/kg ATRA in uninjured mice, yet they observed significant activation after AKI and ATRA treatment at the same dose, over levels induced by injury alone²²¹. These studies should be performed in the context of injury before concluding definitively that m4PTB does not enhance recovery in zebrafish AKI through enhancing RA signaling.

What our data suggest is that RA signaling is required possibly upstream of m4PTB action. Heat shock induction of DN-RAR α in zebrafish larvae blocked m4PTB's ability to stimulate RTEC proliferation. This effect was more pronounced in uninjured fish. In fact in gent-AKI fish, heat shock slightly increased RTEC proliferation in DMSO controls, although this

change was not significant. However, confounding factors may explain this observation, since heat shock has been shown to alter aspects of the injury environment including leukocyte migration²⁵³. Therefore, we are currently repeating these experiments in a chemical model using co-treatments with Ro41-5253 and m4PTB. Ultimately, m4PTB likely affects multiple pathways, and thorough understanding of how m4PTB mediates renal recovery will depend on a more global evaluation of m4PTB's HDAC and gene targets.

Material modified and re-published with permission:

²²¹*Chiba, T, *Skrypnyk, NI, ***Skvarca, LB**, Penchev, R, Zhang, KX, Rochon, ER, Fall, JL, Paueksakon, P, Yang, H, Alford, CE, Roman, BL, Zhang, MZ, Harris, RC, Hukriede, NA, de Caestecker, MP: Retinoic acid signaling coordinates macrophage-dependent injury and repair after AKI. *Journal of the American Society of Nephrology : JASN*, In press, 2015.

*Equally contributing authors.

5.0 GENERAL DISCUSSION

Collectively, these studies demonstrate the utility of gentamicin-induced AKI in zebrafish larvae as a tool for elucidating regenerative mechanisms in the kidney and contribute several insights to the AKI field. We show that the pronephric kidney in zebrafish expresses Kim1 and experiences leukocyte invasion after gentamicin injection, bolstering the case for conserved injury mechanisms between zebrafish and mammals. Together with the de Caestecker lab, we also show that the RA pathway mediates regenerative responses in RTECs that are critical for renal recovery in both zebrafish and mice²²¹.

Most significantly, this work defines a paradigm for AKI drug discovery in which the zebrafish plays a prominent role. PTBA-class HDACi were initially identified in zebrafish embryos due to effects during kidney organogenesis²⁰⁴. These effects translated to enhanced AKI recovery in zebrafish larvae by increasing dedifferentiation and proliferation of RTECs. In mouse AKI models, these compounds promote cell cycle progression, decrease inflammatory M1 macrophages, and mitigate fibrosis^{215, 236}. The translational nature of these findings justifies future studies in zebrafish to identify additional compounds and characterize their mechanisms in order to enhance the supply of new AKI treatments in the pipeline.

Of course, the ultimate goal is to develop effective treatments that can be used to treat patients who experience AKI. Despite our collaborators' elegant work in mice, several fundamental questions remain before these compounds are ready for human clinical trials.

Importantly, we have yet to identify the molecular target – or more likely, targets – of PTBA-class HDACi. Determining the isoform selectivity of these compounds will at least decrease the size of the proverbial haystack in which we must search for the pathways and genes they affect. In cancer cell lines, treatment with broad-spectrum HDACi alters the expression of 8-10% of all genes, a statistic that poignantly demonstrates the daunting nature of this task²⁵⁴. In the Hukriede lab, HDAC selectivity assays have shown that PTBA exhibits class I specificity. The most likely target appears to be HDAC8, the least-characterized family member in its class. Interestingly in terms of relevance to this work, genetic deletion of HDAC8 results in severe developmental cranial defects in mice and in a 46-fold induction of *Lhx1* expression²⁵⁵. The effects of HDAC8 repression on *Lhx1* were corroborated in vitro with the development of an HDAC8-specific inhibitor²⁵⁶. Since solubility issues have so far prohibited the use of these compounds in our zebrafish studies, the Hukriede lab is in the process of obtaining zebrafish HDAC8 mutant lines. Whether PTBA directly stimulates RTEC dedifferentiation in the context of AKI through repression of HDAC8 represents an exciting avenue of study.

Further, HDAC8 has been specifically linked to RA signaling. In neuroblastoma cells, co-treatment with ATRA and an HDAC8 inhibitor enhances tumor cell death, possibly through synergistic effects on CREB-mediated Caspase-8 activity²⁰¹. This study shows a potential link between HDAC8 and RA signaling in the context of cancer. Although we showed that it is unlikely that PTBA-class HDACi directly stimulate RA signaling in the zebrafish larval AKI-model, we demonstrated that upstream RA signaling is required. In the end, RA is simply one pathway that may be affected by PTBA treatment. Full characterization of PTBA's effects will require RNA-seq studies to analyze changes in the transcriptional profile.

These efforts are crucial not only to determine therapeutic mechanisms, but also to predict toxicity. In mouse, solubility rather than toxicity determines the maximum deliverable m4PTB dose (direct communication, M. de Caestecker). More generally, side effects of other HDACi include fatigue, nausea/vomiting, QT prolongation, and thrombocytopenia. Some negative effects may be due to direct cellular toxicity. In the kidney, SAHA was shown to induce apoptosis in 35% of rat PT cells in vitro²⁵⁷. In cultured mouse PT cells, TSA treatment upregulates the mitochondrial adapter protein p66sch. This increase is presumably linked to ROS generation, since knockdown of p66sch attenuates ROS production in treated cells²⁵⁸. In general, hydroxamic acids, such as SAHA and TSA, are subject to modification via sulfation, which leads to the buildup of highly reactive, toxic sulfate metabolites of the hydroxyl group²⁵⁹. For this reason, the therapeutic potential of hydroxamic acids may be limited, even though they are widely used for research purposes. Based on these studies, it may be warranted to monitor renal function in patients undergoing HDACi therapy, particularly if the treatment regimen involves those classes found to have cytotoxic effects.

One hypothesis for decreasing these toxicities includes the use of isoform-specific HDACi rather than pan inhibitors like SAHA and romidepsin¹⁰². To make this feasible, a high-throughput assay capable of testing the isoform selectivity of novel compounds is necessary. Bradner et al. have developed an elegant kinetic assay for HDACs 1 through 9, which has been validated by profiling 20 known HDACi currently used in either research or clinical settings¹¹⁴. This provides both researchers and clinicians with valuable information about the precise isoform selectivity of compounds so that mechanistic and off-target effects can be evaluated. If PTBA is truly specific to HDAC8 alone, this is promising in terms of limiting toxicities due to off-target effects.

Finally, the best candidate must be developed to clinical trials. Over 250 analogues have been generated in the PTBA class, some of which surpass m4PTB's effects on AKI recovery in both zebrafish and mice. Liver microsome studies, however, show that these analogues are rapidly metabolized, forming the PTBA parent compound that ultimately mediates their activity. Since metabolism differs from person to person, these prodrugs are second tier candidates for human therapies. In collaboration with Donna Huryn at the University of Pittsburgh Chemical Diversity Center, the Hukriede lab is now testing the next generation of PTBA analogues, designed as bioisosteres that are as stable as the parent compound, thus not requiring a prodrug for delivery. These ongoing studies will characterize molecular targets, toxicity, and metabolism and will determine whether future physicians will reach for PTBA-class HDACi as first-line therapy for their patients suffering from AKI.

Material modified and re-published with permission:

¹²⁶***Brilli LL**, *Swanhart LM, de Caestecker MP, Hukriede NA. HDAC inhibitors in kidney development and disease. *Pediatric nephrology*. 2013;28(10):1909-21. doi: 10.1007/s00467-012-2320-8. PubMed PMID: 23052657; PubMed Central PMCID: PMC3751322.

*Denotes equally contributing authors.

APPENDIX A

SUPPLEMENTAL FIGURES

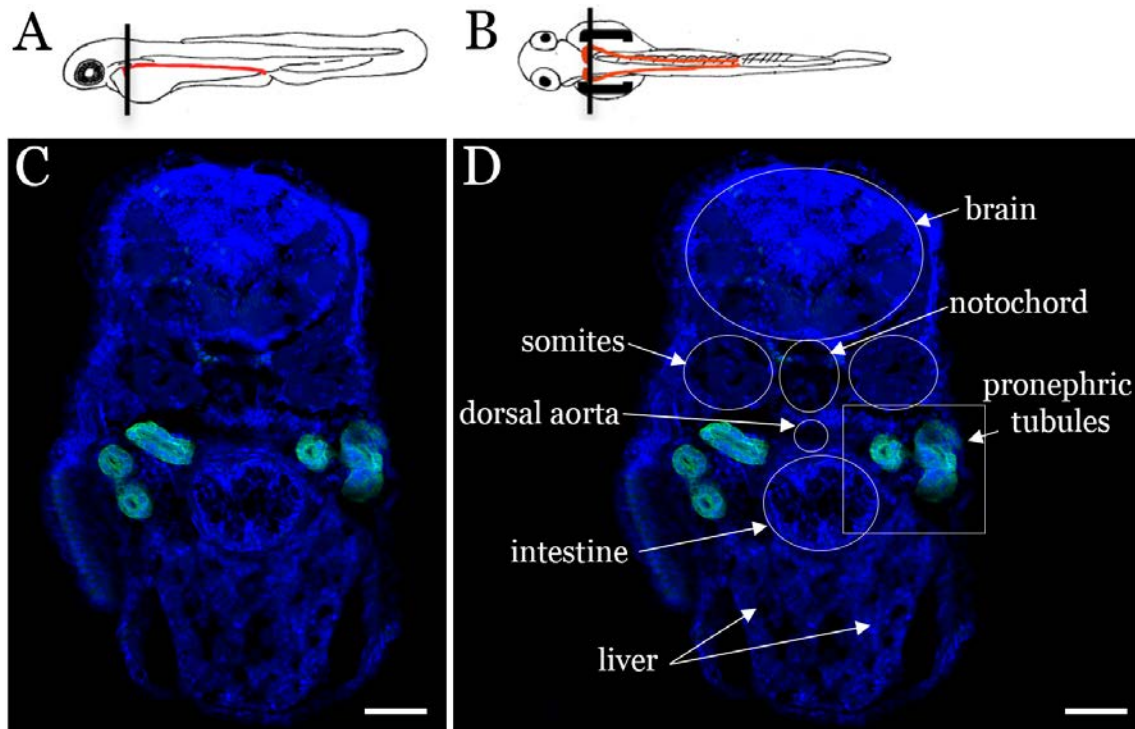


Figure 31: Anatomic orientation on transverse sections of zebrafish larvae.

(A-B) Sketch of lateral and dorsal views of zebrafish larvae. Pronephric tubules are colored in red. The black lines indicate the plane of section captured for immunofluorescence studies. Sketches drawn by C. Cosentino. (C-D) Transverse cryosection of uninjured *Tg(PT:EGFP)* zebrafish larvae at 5 dpf, stained with anti-GFP to mark pronephric tubules (green), and DAPI to mark nuclei (blue). Panel D shows the same image, with anatomic structures encircled and labeled for general orientation. White box shows the cropped region generally shown in figure panels throughout this document. Scale bars, 50 μm.

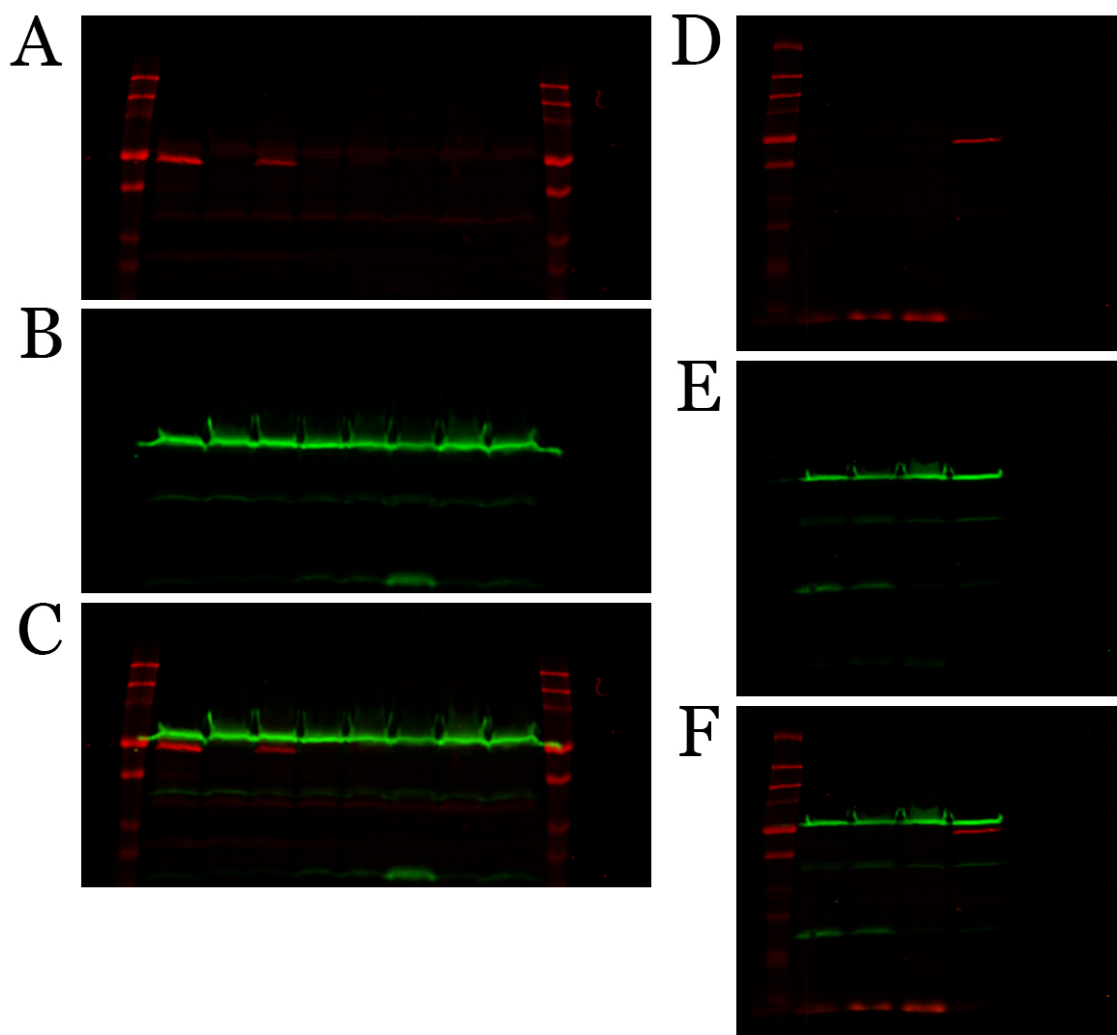


Figure 32: Fluorescence western raw images.

Unmodified fluorescent western blot images for Figure 28 (A-C) and Figure 29 (D-F). DN-RAR α protein was detected using anti-RAR α antibody (red, panels A and D), and anti- α -tubulin was used as a loading control (green, panels B and E). Merged images shown in panels C and F. Precision Plus Dual Color Protein Standard (Biorad) shows auto-fluorescence of the protein ladder visible in the red channel.

APPENDIX B

SUPPLEMENTAL TABLES

Table 1: Histology summary of antibodies and conditions.

Primary Antibodies						
<u>Antibody</u>	<u>Species</u>	<u>Conc.</u>	<u>Antigen Presentation</u>	<u>Fixation</u>	<u>Tissue Preparation</u>	<u>Source</u>
3G8	mouse	1:100	none	PFA	cryo	European Xenopus Resource Centre
Acetylated H4	rabbit	1:250	none	PFA + ProK	whole mount	Millipore
dendra2	mouse	1:100	none	PFA	cryo	Origene
GFP	rabbit	1:200	none	PFA	cryo	Invitrogen
GFP	chicken	1:100	none, citrate	PFA	cryo	Aves
Kim1	rat	1:100	none	PFA	cryo	R&D Systems
Na/K ATPase (α 6F)	mouse	1:50	none	Dent's + ProK	JB-4	Developmental Studies Hybridoma Bank
Pax2a	rabbit	1:100	citrate	PFA	cryo	GeneTex
PCNA	mouse	1:3000	citrate	PFA	cryo	Sigma

Secondary Antibodies			
<u>Antibody</u>	<u>Species</u>	<u>Conc.</u>	<u>Source</u>
Alexa fluor 488	goat anti-mouse	1:1000	Invitrogen
Alexa fluor 488	goat anti-rabbit	1:1000	Invitrogen
Alexa fluor 555	goat anti-chicken	1:1000	Invitrogen
Alexa fluor 568	donkey anti-rabbit	1:1000	Invitrogen
Alexa fluor 594	goat anti-rat	1:1000	Invitrogen
Cy3	goat anti-mouse	1:500	Jackson Laboratories

Table 2: qRT-PCR primer sequences.

<u>Gene</u>	<u>Forward Primer Sequence</u>	<u>Reverse Primer Sequence</u>
<i>kim1</i>	CGCTAGAAGTAAGGCAGAA	CACTGTTCGTATTCGCTTTC
<i>gfp</i>	GAAGTTCATCTGCACCAC	ATGGCGGACTTGAAGAAG
<i>mdka</i>	AACAAACCCAAAGGAAAGAAAGGC	CCGCTCGTGCTGAACAAC
<i>β actin</i>	CGTGCTGTCTTCCCATCCA	TCACCAACGTAGCTGTCTTTCTG
<i>sdha</i>	GAGTCTCCAATCAGTATCCAGTAGTAGA	CACTGTGTGCGAGCGTGTG

Table 3: Raw qRT-PCR data for zebrafish studies.

Raw qRT-PCR data for Figure 8										
<i>kim1</i>	<u>No injury, 4dpf</u>		<u>2ng Gent-AKI, 1dpi</u>		<u>4ng Gent-AKI, 1dpi</u>		<u>6ng Gent-AKI, 1dpi</u>		<u>8ng Gent-AKI, 1dpi</u>	
	Fold Change	StdDev	Fold Change	StdDev	Fold Change	StdDev	Fold Change	StdDev	Fold Change	StdDev
Replicate 1	1.000	0.248	0.829	0.257	2.037	1.205	1.894	0.798	2.343	0.971
Replicate 2	1.000	0.146	1.401	0.371	2.017	0.158	1.964	0.317	2.258	0.307
Replicate 3	1.000	0.462	2.238	0.891	3.915	0.685	3.045	0.430	2.871	0.583
Replicate 4	1.000	0.113	0.874	0.114	1.274	0.094	1.993	0.328	1.527	0.274
<i>kim1</i>	<u>No injury, 5dpf</u>		<u>2ng Gent-AKI, 2dpi</u>		<u>4ng Gent-AKI, 2dpi</u>		<u>6ng Gent-AKI, 2dpi</u>		<u>8ng Gent-AKI, 2dpi</u>	
	Fold Change	StdDev	Fold Change	StdDev	Fold Change	StdDev	Fold Change	StdDev	Fold Change	StdDev
Replicate 1	1.000	0.125	1.027	0.127	1.072	0.144	1.346	0.065	2.633	0.189
Replicate 2	1.000	0.250	1.263	0.278	1.044	0.198	1.986	0.167	1.761	0.322
Replicate 3	1.000	0.233	0.977	0.097	1.674	0.313	2.345	0.501	1.716	0.523
Replicate 4	1.000	0.138	1.337	0.257	1.963	0.191	2.552	0.452	2.235	0.319
Replicate 5	1.000	0.426	2.056	0.531	1.857	0.307	3.767	0.585	2.811	0.684
Replicate 6	1.000	0.120	2.381	0.347	2.428	0.220	3.042	0.247	2.682	0.286
Replicate 7	1.000	0.176	1.127	0.085	1.560	0.167	1.989	0.203	2.577	0.123

Raw qRT-PCR data for Figure 21				
<i>gfp</i>	<u>No injury, 3dpf</u>		<u>Gent-AKI, 6hpi</u>	
	Fold Change	StdDev	Fold Change	StdDev
Replicate 1	1.000	0.167	0.957	0.106
Replicate 2	1.000	0.353	2.570	0.462
Replicate 3	1.000	0.273	4.086	0.730

Raw qRT-PCR data for Figure 25						
<i>kim1</i>	<u>No injury, 4dpf</u>		<u>Gent-AKI +DMSO, 1dpi</u>		<u>Gent-AKI +Ro41, 1dpi</u>	
	Fold Change	StdDev	Fold Change	StdDev	Fold Change	StdDev
Replicate 1	1.000	0.158	0.879	0.086	1.393	0.233
Replicate 2	1.000	0.136	0.858	0.063	0.655	0.109
Replicate 3	1.000	0.146	0.631	0.074	0.538	0.137
<i>kim1</i>	<u>No injury, 5dpf</u>		<u>Gent-AKI +DMSO, 2dpi</u>		<u>Gent-AKI +Ro41, 2dpi</u>	
	Fold Change	StdDev	Fold Change	StdDev	Fold Change	StdDev
Replicate 1	1.000	0.129	2.707	0.291	3.308	0.305
Replicate 2	1.000	0.158	2.557	0.185	2.068	0.129
Replicate 3	1.000	0.042	5.183	0.215	2.536	0.299
Replicate 4	1.000	0.194	3.933	0.260	2.765	0.121

BIBLIOGRAPHY

1. Dressler, GR: The cellular basis of kidney development. *Annu Rev Cell Dev Biol*, 22: 509-529, 2006.
2. Drummond, IA, Davidson, AJ: Zebrafish kidney development. *Methods in cell biology*, 100: 233-260, 2010.
3. Tsang, TE, Shawlot, W, Kinder, SJ, Kobayashi, A, Kwan, KM, Schughart, K, Kania, A, Jessell, TM, Behringer, RR, Tam, PP: Lim1 activity is required for intermediate mesoderm differentiation in the mouse embryo. *Developmental biology*, 223: 77-90, 2000.
4. Bouchard, M, Souabni, A, Mandler, M, Neubuser, A, Busslinger, M: Nephric lineage specification by Pax2 and Pax8. *Genes Dev*, 16: 2958-2970, 2002.
5. al-Awqati, Q, Goldberg, MR: Architectural patterns in branching morphogenesis in the kidney. *Kidney international*, 54: 1832-1842, 1998.
6. Mendelsohn, C, Batourina, E, Fung, S, Gilbert, T, Dodd, J: Stromal cells mediate retinoid-dependent functions essential for renal development. *Development*, 126: 1139-1148, 1999.
7. Batourina, E, Gim, S, Bello, N, Shy, M, Clagett-Dame, M, Srinivas, S, Costantini, F, Mendelsohn, C: Vitamin A controls epithelial/mesenchymal interactions through Ret expression. *Nat Genet*, 27: 74-78, 2001.
8. Dressler, GR: Advances in early kidney specification, development and patterning. *Development*, 136: 3863-3874, 2009.
9. Little, MH, McMahon, AP: Mammalian kidney development: principles, progress, and projections. *Cold Spring Harbor perspectives in biology*, 4, 2012.
10. Reidy, KJ, Rosenblum, ND: Cell and molecular biology of kidney development. *Seminars in nephrology*, 29: 321-337, 2009.
11. Drummond, I: Making a zebrafish kidney: a tale of two tubes. *Trends Cell Biol*, 13: 357-365, 2003.

12. Wingert, RA, Davidson, AJ: The zebrafish pronephros: a model to study nephron segmentation. *Kidney international*, 73: 1120-1127, 2008.
13. Diep, CQ, Peng, Z, Ukah, TK, Kelly, PM, Daigle, RV, Davidson, AJ: Development of the zebrafish mesonephros. *Genesis*, 53: 257-269, 2015.
14. Cirio, MC, de Groh, ED, de Caestecker, MP, Davidson, AJ, Hukriede, NA: Kidney regeneration: common themes from the embryo to the adult. *Pediatric nephrology*, 29: 553-564, 2014.
15. Al-Awqati, Q, Oliver, JA: Stem cells in the kidney. *Kidney international*, 61: 387-395, 2002.
16. Bertram, JF, Douglas-Denton, RN, Diouf, B, Hughson, MD, Hoy, WE: Human nephron number: implications for health and disease. *Pediatric nephrology*, 26: 1529-1533, 2011.
17. Bertram, JF: Estimating glomerular number: why we do it and how. *Clinical and experimental pharmacology & physiology*, 40: 785-788, 2013.
18. Bellomo, R, Ronco, C, Kellum, JA, Mehta, RL, Palevsky, P, Acute Dialysis Quality Initiative, w: Acute renal failure - definition, outcome measures, animal models, fluid therapy and information technology needs: the Second International Consensus Conference of the Acute Dialysis Quality Initiative (ADQI) Group. *Critical care*, 8: R204-212, 2004.
19. Mehta, RL, Kellum, JA, Shah, SV, Molitoris, BA, Ronco, C, Warnock, DG, Levin, A, Acute Kidney Injury, N: Acute Kidney Injury Network: report of an initiative to improve outcomes in acute kidney injury. *Critical care*, 11: R31, 2007.
20. Uchino, S, Bellomo, R, Goldsmith, D, Bates, S, Ronco, C: An assessment of the RIFLE criteria for acute renal failure in hospitalized patients. *Critical care medicine*, 34: 1913-1917, 2006.
21. Fang, Y, Ding, X, Zhong, Y, Zou, J, Teng, J, Tang, Y, Lin, J, Lin, P: Acute kidney injury in a Chinese hospitalized population. *Blood purification*, 30: 120-126, 2010.
22. Hoste, EA, Clermont, G, Kersten, A, Venkataraman, R, Angus, DC, De Bacquer, D, Kellum, JA: RIFLE criteria for acute kidney injury are associated with hospital mortality in critically ill patients: a cohort analysis. *Critical care*, 10: R73, 2006.
23. Cruz, DN, Bolgan, I, Perazella, MA, Bonello, M, de Cal, M, Corradi, V, Polanco, N, Ocampo, C, Nalesso, F, Piccinni, P, Ronco, C, North East Italian Prospective Hospital Renal Outcome Survey on Acute Kidney Injury, I: North East Italian Prospective Hospital Renal Outcome Survey on Acute Kidney Injury (NEiPHROS-AKI): targeting the problem with the RIFLE Criteria. *Clinical journal of the American Society of Nephrology : CJASN*, 2: 418-425, 2007.
24. Ostermann, M, Chang, RW: Acute kidney injury in the intensive care unit according to RIFLE. *Critical care medicine*, 35: 1837-1843; quiz 1852, 2007.

25. Bagshaw, SM, George, C, Bellomo, R, Committe, ADM: A comparison of the RIFLE and AKIN criteria for acute kidney injury in critically ill patients. *Nephrol Dial Transplant*, 23: 1569-1574, 2008.
26. Flowers, NT, Croft, JB: Hospitalization discharge diagnoses for kidney disease - United States, 1980-2005 (Reprinted from MMWR, vol 57, pg 309-312, 2008). *Jama-J Am Med Assoc*, 299: 2144-2145, 2008.
27. Ali, T, Khan, I, Simpson, W, Prescott, G, Townend, J, Smith, W, Macleod, A: Incidence and outcomes in acute kidney injury: a comprehensive population-based study. *Journal of the American Society of Nephrology : JASN*, 18: 1292-1298, 2007.
28. Chertow, GM, Burdick, E, Honour, M, Bonventre, JV, Bates, DW: Acute kidney injury, mortality, length of stay, and costs in hospitalized patients. *Journal of the American Society of Nephrology : JASN*, 16: 3365-3370, 2005.
29. Uchino, S, Kellum, JA, Bellomo, R, Doig, GS, Morimatsu, H, Morgera, S, Schetz, M, Tan, I, Bouman, C, Macedo, E, Gibney, N, Tolwani, A, Ronco, C, Beginning, Ending Supportive Therapy for the Kidney, I: Acute renal failure in critically ill patients: a multinational, multicenter study. *Jama*, 294: 813-818, 2005.
30. Murugan, R, Kellum, JA: Acute kidney injury: what's the prognosis? *Nature reviews Nephrology*, 7: 209-217, 2011.
31. Waikar, SS, Liu, KD, Chertow, GM: Diagnosis, epidemiology and outcomes of acute kidney injury. *Clinical journal of the American Society of Nephrology : CJASN*, 3: 844-861, 2008.
32. Lieberthal, W, Nigam, SK: Acute renal failure. II. Experimental models of acute renal failure: imperfect but indispensable. *American journal of physiology Renal physiology*, 278: F1-F12, 2000.
33. Langenberg, C, Wan, L, Egi, M, May, CN, Bellomo, R: Renal blood flow in experimental septic acute renal failure. *Kidney international*, 69: 1996-2002, 2006.
34. Wan, L, Bagshaw, SM, Langenberg, C, Saotome, T, May, C, Bellomo, R: Pathophysiology of septic acute kidney injury: what do we really know? *Critical care medicine*, 36: S198-203, 2008.
35. Bonventre, JV, Yang, L: Cellular pathophysiology of ischemic acute kidney injury. *The Journal of clinical investigation*, 121: 4210-4221, 2011.
36. Conger, JD, Schrier, RW: Renal hemodynamics in acute renal failure. *Annual review of physiology*, 42: 603-614, 1980.
37. Sharfuddin, AA, Molitoris, BA: Pathophysiology of ischemic acute kidney injury. *Nature reviews Nephrology*, 7: 189-200, 2011.

38. Verma, SK, Molitoris, BA: Renal endothelial injury and microvascular dysfunction in acute kidney injury. *Seminars in nephrology*, 35: 96-107, 2015.
39. Lieberthal, W, Nigam, SK: Acute renal failure. I. Relative importance of proximal vs. distal tubular injury. *The American journal of physiology*, 275: F623-631, 1998.
40. Li, L, Zepeda-Orozco, D, Black, R, Lin, F: Autophagy is a component of epithelial cell fate in obstructive uropathy. *The American journal of pathology*, 176: 1767-1778, 2010.
41. Lieberthal, W, Koh, JS, Levine, JS: Necrosis and apoptosis in acute renal failure. *Seminars in nephrology*, 18: 505-518, 1998.
42. Saikumar, P, Venkatachalam, MA: Role of apoptosis in hypoxic/ischemic damage in the kidney. *Seminars in nephrology*, 23: 511-521, 2003.
43. Kimura, T, Takabatake, Y, Takahashi, A, Kaimori, JY, Matsui, I, Namba, T, Kitamura, H, Niimura, F, Matsusaka, T, Soga, T, Rakugi, H, Isaka, Y: Autophagy protects the proximal tubule from degeneration and acute ischemic injury. *Journal of the American Society of Nephrology : JASN*, 22: 902-913, 2011.
44. Imamura, R, Isaka, Y, Sandoval, RM, Ori, A, Adamsky, S, Feinstein, E, Molitoris, BA, Takahara, S: Intravital two-photon microscopy assessment of renal protection efficacy of siRNA for p53 in experimental rat kidney transplantation models. *Cell transplantation*, 19: 1659-1670, 2010.
45. Molitoris, BA, Dagher, PC, Sandoval, RM, Campos, SB, Ashush, H, Fridman, E, Brafman, A, Faerman, A, Atkinson, SJ, Thompson, JD, Kalinski, H, Skaliter, R, Erlich, S, Feinstein, E: siRNA targeted to p53 attenuates ischemic and cisplatin-induced acute kidney injury. *Journal of the American Society of Nephrology : JASN*, 20: 1754-1764, 2009.
46. Safirstein, RL: Acute renal failure: from renal physiology to the renal transcriptome. *Kidney international Supplement*: S62-66, 2004.
47. Nicholson, DW: From bench to clinic with apoptosis-based therapeutic agents. *Nature*, 407: 810-816, 2000.
48. Hartman, HA, Lai, HL, Patterson, LT: Cessation of renal morphogenesis in mice. *Developmental biology*, 310: 379-387, 2007.
49. Kuure, S, Vuolteenaho, R, Vainio, S: Kidney morphogenesis: cellular and molecular regulation. *Mechanisms of development*, 92: 31-45, 2000.
50. Humphreys, BD, Valerius, MT, Kobayashi, A, Mugford, JW, Soeung, S, Duffield, JS, McMahon, AP, Bonventre, JV: Intrinsic epithelial cells repair the kidney after injury. *Cell stem cell*, 2: 284-291, 2008.
51. Benigni, A, Morigi, M, Remuzzi, G: Kidney regeneration. *Lancet*, 375: 1310-1317, 2010.

52. Witzgall, R, Brown, D, Schwarz, C, Bonventre, JV: Localization of proliferating cell nuclear antigen, vimentin, c-Fos, and clusterin in the postischemic kidney. Evidence for a heterogenous genetic response among nephron segments, and a large pool of mitotically active and dedifferentiated cells. *The Journal of clinical investigation*, 93: 2175-2188, 1994.
53. Imgrund, M, Grone, E, Grone, HJ, Kretzler, M, Holzman, L, Schlondorff, D, Rothenpieler, UW: Re-expression of the developmental gene Pax-2 during experimental acute tubular necrosis in mice 1. *Kidney international*, 56: 1423-1431, 1999.
54. Villanueva, S, Cespedes, C, Vio, CP: Ischemic acute renal failure induces the expression of a wide range of nephrogenic proteins. *American journal of physiology Regulatory, integrative and comparative physiology*, 290: R861-870, 2006.
55. Terada, Y, Tanaka, H, Okado, T, Shimamura, H, Inoshita, S, Kuwahara, M, Sasaki, S: Expression and function of the developmental gene Wnt-4 during experimental acute renal failure in rats. *Journal of the American Society of Nephrology : JASN*, 14: 1223-1233, 2003.
56. Lin, SL, Li, B, Rao, S, Yeo, EJ, Hudson, TE, Nowlin, BT, Pei, H, Chen, L, Zheng, JJ, Carroll, TJ, Pollard, JW, McMahon, AP, Lang, RA, Duffield, JS: Macrophage Wnt7b is critical for kidney repair and regeneration. *Proceedings of the National Academy of Sciences of the United States of America*, 107: 4194-4199, 2010.
57. Yang, L, Besschetnova, TY, Brooks, CR, Shah, JV, Bonventre, JV: Epithelial cell cycle arrest in G2/M mediates kidney fibrosis after injury. *Nature medicine*, 16: 535-543, 531p following 143, 2010.
58. Sutton, TA, Kelly, KJ, Mang, HE, Plotkin, Z, Sandoval, RM, Dagher, PC: Minocycline reduces renal microvascular leakage in a rat model of ischemic renal injury. *American journal of physiology Renal physiology*, 288: F91-97, 2005.
59. Kelly, KJ, Williams, WW, Jr., Colvin, RB, Meehan, SM, Springer, TA, Gutierrez-Ramos, JC, Bonventre, JV: Intercellular adhesion molecule-1-deficient mice are protected against ischemic renal injury. *The Journal of clinical investigation*, 97: 1056-1063, 1996.
60. Matsumoto, M, Makino, Y, Tanaka, T, Tanaka, H, Ishizaka, N, Noiri, E, Fujita, T, Nangaku, M: Induction of renoprotective gene expression by cobalt ameliorates ischemic injury of the kidney in rats. *Journal of the American Society of Nephrology : JASN*, 14: 1825-1832, 2003.
61. Takada, M, Nadeau, KC, Shaw, GD, Marquette, KA, Tilney, NL: The cytokine-adhesion molecule cascade in ischemia/reperfusion injury of the rat kidney. Inhibition by a soluble P-selectin ligand. *The Journal of clinical investigation*, 99: 2682-2690, 1997.
62. Sharfuddin, AA, Sandoval, RM, Berg, DT, McDougal, GE, Campos, SB, Phillips, CL, Jones, BE, Gupta, A, Grinnell, BW, Molitoris, BA: Soluble thrombomodulin protects ischemic kidneys. *Journal of the American Society of Nephrology : JASN*, 20: 524-534, 2009.

63. Humphreys, BD, Lin, SL, Kobayashi, A, Hudson, TE, Nowlin, BT, Bonventre, JV, Valerius, MT, McMahon, AP, Duffield, JS: Fate tracing reveals the pericyte and not epithelial origin of myofibroblasts in kidney fibrosis. *The American journal of pathology*, 176: 85-97, 2010.
64. Schrimpf, C, Xin, C, Campanholle, G, Gill, SE, Stallcup, W, Lin, SL, Davis, GE, Gharib, SA, Humphreys, BD, Duffield, JS: Pericyte TIMP3 and ADAMTS1 modulate vascular stability after kidney injury. *Journal of the American Society of Nephrology : JASN*, 23: 868-883, 2012.
65. Chen, YT, Chang, FC, Wu, CF, Chou, YH, Hsu, HL, Chiang, WC, Shen, J, Chen, YM, Wu, KD, Tsai, TJ, Duffield, JS, Lin, SL: Platelet-derived growth factor receptor signaling activates pericyte-myofibroblast transition in obstructive and post-ischemic kidney fibrosis. *Kidney international*, 80: 1170-1181, 2011.
66. Venkatachalam, MA, Weinberg, JM, Kriz, W, Bidani, AK: Failed Tubule Recovery, AKI-CKD Transition, and Kidney Disease Progression. *Journal of the American Society of Nephrology : JASN*, 2015.
67. Lin, SL, Chang, FC, Schrimpf, C, Chen, YT, Wu, CF, Wu, VC, Chiang, WC, Kuhnert, F, Kuo, CJ, Chen, YM, Wu, KD, Tsai, TJ, Duffield, JS: Targeting endothelium-pericyte cross talk by inhibiting VEGF receptor signaling attenuates kidney microvascular rarefaction and fibrosis. *The American journal of pathology*, 178: 911-923, 2011.
68. Nelson, PJ, Rees, AJ, Griffin, MD, Hughes, J, Kurts, C, Duffield, J: The renal mononuclear phagocytic system. *Journal of the American Society of Nephrology : JASN*, 23: 194-203, 2012.
69. Jang, HR, Rabb, H: Immune cells in experimental acute kidney injury. *Nature reviews Nephrology*, 11: 88-101, 2015.
70. Wu, H, Chen, G, Wyburn, KR, Yin, J, Bertolino, P, Eris, JM, Alexander, SI, Sharland, AF, Chadban, SJ: TLR4 activation mediates kidney ischemia/reperfusion injury. *The Journal of clinical investigation*, 117: 2847-2859, 2007.
71. Wolfs, TG, Buurman, WA, van Schadewijk, A, de Vries, B, Daemen, MA, Hiemstra, PS, van 't Veer, C: In vivo expression of Toll-like receptor 2 and 4 by renal epithelial cells: IFN-gamma and TNF-alpha mediated up-regulation during inflammation. *Journal of immunology*, 168: 1286-1293, 2002.
72. Li, L, Huang, L, Sung, SS, Vergis, AL, Rosin, DL, Rose, CE, Jr., Lobo, PI, Okusa, MD: The chemokine receptors CCR2 and CX3CR1 mediate monocyte/macrophage trafficking in kidney ischemia-reperfusion injury. *Kidney international*, 74: 1526-1537, 2008.
73. Awad, AS, Rouse, M, Huang, L, Vergis, AL, Reutershan, J, Cathro, HP, Linden, J, Okusa, MD: Compartmentalization of neutrophils in the kidney and lung following acute ischemic kidney injury. *Kidney international*, 75: 689-698, 2009.

74. Thornton, MA, Winn, R, Alpers, CE, Zager, RA: An evaluation of the neutrophil as a mediator of in vivo renal ischemic-reperfusion injury. *The American journal of pathology*, 135: 509-515, 1989.
75. Rabb, H, Mendiola, CC, Dietz, J, Saba, SR, Issekutz, TB, Abanilla, F, Bonventre, JV, Ramirez, G: Role of CD11a and CD11b in ischemic acute renal failure in rats. *The American journal of physiology*, 267: F1052-1058, 1994.
76. Ricardo, SD, van Goor, H, Eddy, AA: Macrophage diversity in renal injury and repair. *The Journal of clinical investigation*, 118: 3522-3530, 2008.
77. Cao, Q, Harris, DC, Wang, Y: Macrophages in Kidney Injury, Inflammation, and Fibrosis. *Physiology*, 30: 183-194, 2015.
78. Lee, S, Huen, S, Nishio, H, Nishio, S, Lee, HK, Choi, BS, Ruhrberg, C, Cantley, LG: Distinct macrophage phenotypes contribute to kidney injury and repair. *Journal of the American Society of Nephrology : JASN*, 22: 317-326, 2011.
79. Jo, SK, Sung, SA, Cho, WY, Go, KJ, Kim, HK: Macrophages contribute to the initiation of ischaemic acute renal failure in rats. *Nephrol Dial Transplant*, 21: 1231-1239, 2006.
80. Zhang, MZ, Yao, B, Yang, S, Jiang, L, Wang, S, Fan, X, Yin, H, Wong, K, Miyazawa, T, Chen, J, Chang, I, Singh, A, Harris, RC: CSF-1 signaling mediates recovery from acute kidney injury. *The Journal of clinical investigation*, 122: 4519-4532, 2012.
81. Sola, A, Weigert, A, Jung, M, Vinuesa, E, Brecht, K, Weis, N, Brune, B, Borregaard, N, Hotter, G: Sphingosine-1-phosphate signalling induces the production of Lcn-2 by macrophages to promote kidney regeneration. *The Journal of pathology*, 225: 597-608, 2011.
82. Schmidt, IM, Hall, IE, Kale, S, Lee, S, He, CH, Lee, Y, Chupp, GL, Moeckel, GW, Lee, CG, Elias, JA, Parikh, CR, Cantley, LG: Chitinase-like protein Brp-39/YKL-40 modulates the renal response to ischemic injury and predicts delayed allograft function. *Journal of the American Society of Nephrology : JASN*, 24: 309-319, 2013.
83. Lech, M, Grobmayr, R, Ryu, M, Lorenz, G, Hartter, I, Mulay, SR, Susanti, HE, Kobayashi, KS, Flavell, RA, Anders, HJ: Macrophage phenotype controls long-term AKI outcomes--kidney regeneration versus atrophy. *Journal of the American Society of Nephrology : JASN*, 25: 292-304, 2014.
84. Kim, MG, Boo, CS, Ko, YS, Lee, HY, Cho, WY, Kim, HK, Jo, SK: Depletion of kidney CD11c+ F4/80+ cells impairs the recovery process in ischaemia/reperfusion-induced acute kidney injury. *Nephrol Dial Transplant*, 25: 2908-2921, 2010.
85. Ranganathan, PV, Jayakumar, C, Ramesh, G: Netrin-1-treated macrophages protect the kidney against ischemia-reperfusion injury and suppress inflammation by inducing M2 polarization. *American journal of physiology Renal physiology*, 304: F948-957, 2013.

86. Butcher, BW, Liu, KD: Fluid overload in AKI: epiphenomenon or putative effect on mortality? *Current opinion in critical care*, 18: 593-598, 2012.
87. Vaara, ST, Korhonen, AM, Kaukonen, KM, Nisula, S, Inkinen, O, Hoppu, S, Laurila, JJ, Mildh, L, Reinikainen, M, Lund, V, Parviainen, I, Pettilä, V, Group, FS: Fluid overload is associated with an increased risk for 90-day mortality in critically ill patients with renal replacement therapy: data from the prospective FINNAKI study. *Critical care*, 16: R197, 2012.
88. Zhang, Z: Biomarkers, diagnosis and management of sepsis-induced acute kidney injury: a narrative review. *Heart, lung and vessels*, 7: 64-73, 2015.
89. Oh, HJ, Shin, DH, Lee, MJ, Koo, HM, Doh, FM, Kim, HR, Han, JH, Park, JT, Han, SH, Yoo, TH, Choi, KH, Kang, SW: Early initiation of continuous renal replacement therapy improves patient survival in severe progressive septic acute kidney injury. *Journal of critical care*, 27: 743 e749-718, 2012.
90. Lo, LJ, Go, AS, Chertow, GM, McCulloch, CE, Fan, D, Ordonez, JD, Hsu, CY: Dialysis-requiring acute renal failure increases the risk of progressive chronic kidney disease. *Kidney international*, 76: 893-899, 2009.
91. Uchino, S, Bellomo, R, Bagshaw, SM, Goldsmith, D: Transient azotaemia is associated with a high risk of death in hospitalized patients. *Nephrol Dial Transplant*, 25: 1833-1839, 2010.
92. Kellum, JA, Angus, DC: Patients are dying of acute renal failure. *Critical care medicine*, 30: 2156-2157, 2002.
93. Kjellstrand, CM, Ebben, J, Davin, T: Time of death, recovery of renal function, development of chronic renal failure and need for chronic hemodialysis in patients with acute tubular necrosis. *Transactions - American Society for Artificial Internal Organs*, 27: 45-50, 1981.
94. Liano, F, Felipe, C, Tenorio, MT, Rivera, M, Abaira, V, Saez-de-Urturi, JM, Ocana, J, Fuentes, C, Severiano, S: Long-term outcome of acute tubular necrosis: a contribution to its natural history. *Kidney international*, 71: 679-686, 2007.
95. Coca, SG, Singanamala, S, Parikh, CR: Chronic kidney disease after acute kidney injury: a systematic review and meta-analysis. *Kidney international*, 81: 442-448, 2012.
96. Chawla, LS, Kimmel, PL: Acute kidney injury and chronic kidney disease: an integrated clinical syndrome. *Kidney international*, 82: 516-524, 2012.
97. Venkatachalam, MA, Griffin, KA, Lan, R, Geng, H, Saikumar, P, Bidani, AK: Acute kidney injury: a springboard for progression in chronic kidney disease. *American journal of physiology Renal physiology*, 298: F1078-1094, 2010.

98. Humphreys, BD, Xu, F, Sabbisetti, V, Grgic, I, Naini, SM, Wang, N, Chen, G, Xiao, S, Patel, D, Henderson, JM, Ichimura, T, Mou, S, Soeung, S, McMahon, AP, Kuchroo, VK, Bonventre, JV: Chronic epithelial kidney injury molecule-1 expression causes murine kidney fibrosis. *The Journal of clinical investigation*, 123: 4023-4035, 2013.
99. Basile, DP: The endothelial cell in ischemic acute kidney injury: implications for acute and chronic function. *Kidney international*, 72: 151-156, 2007.
100. Rifkin, DE, Coca, SG, Kalantar-Zadeh, K: Does AKI truly lead to CKD? *Journal of the American Society of Nephrology : JASN*, 23: 979-984, 2012.
101. Chen, S, Bellew, C, Yao, X, Stefkova, J, Dipp, S, Saifudeen, Z, Bachvarov, D, El-Dahr, SS: Histone deacetylase (HDAC) activity is critical for embryonic kidney gene expression, growth, and differentiation. *The Journal of biological chemistry*, 286: 32775-32789, 2011.
102. Bush, EW, McKinsey, TA: Protein acetylation in the cardiorenal axis: the promise of histone deacetylase inhibitors. *Circ Res*, 106: 272-284, 2010.
103. Glozak, MA, Sengupta, N, Zhang, X, Seto, E: Acetylation and deacetylation of non-histone proteins. *Gene*, 363: 15-23, 2005.
104. Gui, CY, Ngo, L, Xu, WS, Richon, VM, Marks, PA: Histone deacetylase (HDAC) inhibitor activation of p21WAF1 involves changes in promoter-associated proteins, including HDAC1. *Proceedings of the National Academy of Sciences of the United States of America*, 101: 1241-1246, 2004.
105. Smith, CL: A shifting paradigm: histone deacetylases and transcriptional activation. *BioEssays : news and reviews in molecular, cellular and developmental biology*, 30: 15-24, 2008.
106. Nusinzon, I, Horvath, CM: Histone deacetylases as transcriptional activators? Role reversal in inducible gene regulation. *Sci STKE*, 2005: re11, 2005.
107. Gregoret, I, Lee, Y-M, Goodson, HV: Molecular Evolution of the Histone Deacetylase Family: Functional Implications of Phylogenetic Analysis. *Journal of molecular biology*, 338: 17-31, 2004.
108. Haberland, M, Montgomery, RL, Olson, EN: The many roles of histone deacetylases in development and physiology: implications for disease and therapy. *Nat Rev Genet*, 10: 32-42, 2009.
109. Chen, S, El-Dahr, SS: Histone deacetylases in kidney development: implications for disease and therapy. *Pediatric nephrology*, 2012.
110. Stanya, KJ, Kao, HY: New insights into the functions and regulation of the transcriptional corepressors SMRT and N-CoR. *Cell Div*, 4: 7, 2009.

111. Watson, PJ, Fairall, L, Santos, GM, Schwabe, JW: Structure of HDAC3 bound to co-repressor and inositol tetrakisphosphate. *Nature*, 481: 335-340, 2012.
112. Li, X: Epigenetics and autosomal dominant polycystic kidney disease. *Biochimica et biophysica acta*, 1812: 1213-1218, 2011.
113. Yoshida, M, Matsuyama, A, Komatsu, Y, Nishino, N: From discovery to the coming generation of histone deacetylase. *Current Medicinal Chemistry*, 10: 2351-2358, 2003.
114. Bradner, JE, West, N, Grachan, ML, Greenberg, EF, Haggarty, SJ, Tandy, W, Mazitschek, R: Chemical phylogenetics of histone deacetylases. *Nature Chemical Biology*, 6: 238-243, 2010.
115. Hubbert, C, Guardiola, A, Shao, R, Kawaguchi, Y, Ito, A, Nixon, A, Yoshida, M, Wang, XF, Yao, TP: HDAC6 is a microtubule-associated deacetylase. *Nature*, 417: 455-458, 2002.
116. Kawaguchi, Y, Kovacs, JJ, McLaurin, A, Vance, JM, Ito, A, Yao, TP: The deacetylase HDAC6 regulates aggresome formation and cell viability in response to misfolded protein stress. *Cell*, 115: 727-738, 2003.
117. Kwon, S, Zhang, Y, Matthias, P: The deacetylase HDAC6 is a novel critical component of stress granules involved in the stress response. *Genes Dev*, 21: 3381-3394, 2007.
118. Boyault, C, Zhang, Y, Fritah, S, Caron, C, Gilquin, B, Kwon, SH, Garrido, C, Yao, TP, Vourc'h, C, Matthias, P, Khochbin, S: HDAC6 controls major cell response pathways to cytotoxic accumulation of protein aggregates. *Genes Dev*, 21: 2172-2181, 2007.
119. Marks, PA, Breslow, R: Dimethyl sulfoxide to vorinostat: development of this histone deacetylase inhibitor as an anticancer drug. *Nature biotechnology*, 25: 84-90, 2007.
120. Bieliauskas, AV, Pflum, MK: Isoform-selective histone deacetylase inhibitors. *Chem Soc Rev*, 37: 1402-1413, 2008.
121. Furumai, R, Matsuyama, A, Kobashi, N, Lee, KH, Nishiyama, M, Nakajima, H, Tanaka, A, Komatsu, Y, Nishino, N, Yoshida, M, Horinouchi, S: FK228 (depsipeptide) as a natural prodrug that inhibits class I histone deacetylases. *Cancer research*, 62: 4916-4921, 2002.
122. Bolden, JE, Peart, MJ, Johnstone, RW: Anticancer activities of histone deacetylase inhibitors. *Nat Rev Drug Discov*, 5: 769-784, 2006.
123. Minucci, S, Pelicci, PG: Histone deacetylase inhibitors and the promise of epigenetic (and more) treatments for cancer. *Nat Rev Cancer*, 6: 38-51, 2006.
124. Batshaw, ML, MacArthur, RB, Tuchman, M: Alternative pathway therapy for urea cycle disorders: twenty years later. *The Journal of pediatrics*, 138: S46-54; discussion S54-45, 2001.

125. Jain, S, Zain, J: Romidepsin in the treatment of cutaneous T-cell lymphoma. *J Blood Med*, 2: 37-47, 2011.
126. Brilli, LL, Swanhart, LM, de Caestecker, MP, Hukriede, NA: HDAC inhibitors in kidney development and disease. *Pediatric nephrology*, 28: 1909-1921, 2013.
127. Marks, PA: Discovery and development of SAHA as an anticancer agent. *Oncogene*, 26: 1351-1356, 2007.
128. Ornoy, A: Valproic acid in pregnancy: how much are we endangering the embryo and fetus? *Reprod Toxicol*, 28: 1-10, 2009.
129. Nervi, C, Borello, U, Fazi, F, Buffa, V, Pelicci, PG, Cossu, G: Inhibition of histone deacetylase activity by trichostatin A modulates gene expression during mouse embryogenesis without apparent toxicity. *Cancer research*, 61: 1247-1249, 2001.
130. Iwano, M, Neilson, EG: Mechanisms of tubulointerstitial fibrosis. *Current Opinion in Nephrology and Hypertension*, 13: 279-284, 2004.
131. Zeisberg, M, Neilson, EG: Mechanisms of tubulointerstitial fibrosis. *J Am Soc Nephrol*, 21: 1819-1834, 2010.
132. Marumo, T, Hishikawa, K, Yoshikawa, M, Fujita, T: Epigenetic regulation of BMP7 in the regenerative response to ischemia. *J Am Soc Nephrol*, 19: 1311-1320, 2008.
133. Advani, A, Huang, Q, Thai, K, Advani, SL, White, KE, Kelly, DJ, Yuen, DA, Connelly, KA, Marsden, PA, Gilbert, RE: Long-term administration of the histone deacetylase inhibitor vorinostat attenuates renal injury in experimental diabetes through an endothelial nitric oxide synthase-dependent mechanism. *The American journal of pathology*, 178: 2205-2214, 2011.
134. Gilbert, RE, Huang, Q, Thai, K, Advani, SL, Lee, K, Yuen, DA, Connelly, KA, Advani, A: Histone deacetylase inhibition attenuates diabetes-associated kidney growth: potential role for epigenetic modification of the epidermal growth factor receptor. *Kidney international*, 79: 1312-1321, 2011.
135. Imai, N, Hishikawa, K, Marumo, T, Hirahashi, J, Inowa, T, Matsuzaki, Y, Okano, H, Kitamura, T, Salant, D, Fujita, T: Inhibition of histone deacetylase activates side population cells in kidney and partially reverses chronic renal injury. *Stem Cells*, 25: 2469-2475, 2007.
136. Noh, H, Oh, EY, Seo, JY, Yu, MR, Kim, YO, Ha, H, Lee, HB: Histone deacetylase-2 is a key regulator of diabetes- and transforming growth factor-beta1-induced renal injury. *American journal of physiology Renal physiology*, 297: F729-739, 2009.
137. Van Beneden, K, Geers, C, Pauwels, M, Mannaerts, I, Verbeelen, D, van Grunsven, LA, Van den Branden, C: Valproic acid attenuates proteinuria and kidney injury. *Journal of the American Society of Nephrology : JASN*, 22: 1863-1875, 2011.

138. Pang, M, Zhuang, S: Histone deacetylase: a potential therapeutic target for fibrotic disorders. *J Pharmacol Exp Ther*, 335: 266-272, 2010.
139. Kinugasa, F, Noto, T, Matsuoka, H, Urano, Y, Sudo, Y, Takakura, S, Mutoh, S: Prevention of renal interstitial fibrosis via histone deacetylase inhibition in rats with unilateral ureteral obstruction. *Transpl Immunol*, 23: 18-23, 2010.
140. Yoshikawa, M, Hishikawa, K, Marumo, T, Fujita, T: Inhibition of histone deacetylase activity suppresses epithelial-to-mesenchymal transition induced by TGF-beta1 in human renal epithelial cells. *J Am Soc Nephrol*, 18: 58-65, 2007.
141. Chen, J, Chen, JK, Nagai, K, Plieth, D, Tan, M, Lee, TC, Threadgill, DW, Neilson, EG, Harris, RC: EGFR signaling promotes TGFbeta-dependent renal fibrosis. *J Am Soc Nephrol*, 23: 215-224, 2012.
142. Kuratsune, M, Masaki, T, Hirai, T, Kiribayashi, K, Yokoyama, Y, Arakawa, T, Yorioka, N, Kohno, N: Signal transducer and activator of transcription 3 involvement in the development of renal interstitial fibrosis after unilateral ureteral obstruction. *Nephrology (Carlton)*, 12: 565-571, 2007.
143. Marumo, T, Hishikawa, K, Yoshikawa, M, Hirahashi, J, Kawachi, S, Fujita, T: Histone deacetylase modulates the proinflammatory and -fibrotic changes in tubulointerstitial injury. *American journal of physiology Renal physiology*, 298, 2009.
144. Vukicevic, S, Basic, V, Rogic, D, Basic, N, Shih, MS, Shepard, A, Jin, D, Dattatreya Murthy, B, Jones, W, Dorai, H, Ryan, S, Griffiths, D, Maliakal, J, Jelic, M, Pastorcic, M, Stavljenic, A, Sampath, TK: Osteogenic protein-1 (bone morphogenetic protein-7) reduces severity of injury after ischemic acute renal failure in rat. *J Clin Invest*, 102: 202-214, 1998.
145. Morrissey, J, Hruska, K, Guo, G, Wang, S, Chen, Q, Klahr, S: Bone morphogenetic protein-7 improves renal fibrosis and accelerates the return of renal function. *J Am Soc Nephrol*, 13 Suppl 1: S14-21, 2002.
146. Zeisberg, M, Hanai, J, Sugimoto, H, Mammoto, T, Charytan, D, Strutz, F, Kalluri, R: BMP-7 counteracts TGF-beta1-induced epithelial-to-mesenchymal transition and reverses chronic renal injury. *Nature medicine*, 9: 964-968, 2003.
147. Hsing, CH, Lin, CF, So, E, Sun, DP, Chen, TC, Li, CF, Yeh, CH: alpha2-Adrenoceptor agonist dexmedetomidine protects septic acute kidney injury through increasing BMP-7 and inhibiting HDAC2 and HDAC5. *American journal of physiology Renal physiology*, 303: F1443-1453, 2012.
148. Oliver, JA, Maarouf, O, Cheema, FH, Martens, TP, Al-Awqati, Q: The renal papilla is a niche for adult kidney stem cells. *J Clin Invest*, 114: 795-804, 2004.

149. Oliver, JA, Klinakis, A, Cheema, FH, Friedlander, J, Sampogna, RV, Martens, TP, Liu, C, Efstratiadis, A, Al-Awqati, Q: Proliferation and migration of label-retaining cells of the kidney papilla. *J Am Soc Nephrol*, 20: 2315-2327, 2009.
150. Wolbach, SB, Howe, PR: Tissue Changes Following Deprivation of Fat-Soluble a Vitamin. *The Journal of experimental medicine*, 42: 753-777, 1925.
151. Blomhoff, R, Blomhoff, HK: Overview of retinoid metabolism and function. *Journal of neurobiology*, 66: 606-630, 2006.
152. Balmer, JE, Blomhoff, R: Gene expression regulation by retinoic acid. *Journal of lipid research*, 43: 1773-1808, 2002.
153. Cunningham, TJ, Duester, G: Mechanisms of retinoic acid signalling and its roles in organ and limb development. *Nature reviews Molecular cell biology*, 16: 110-123, 2015.
154. Duester, G: Retinoic acid synthesis and signaling during early organogenesis. *Cell*, 134: 921-931, 2008.
155. Larson, RS, Tallman, MS: Retinoic acid syndrome: manifestations, pathogenesis, and treatment. *Best practice & research Clinical haematology*, 16: 453-461, 2003.
156. Mark, M, Ghyselinck, NB, Chambon, P: Function of retinoic acid receptors during embryonic development. *Nuclear receptor signaling*, 7: e002, 2009.
157. Gilardi, F, Desvergne, B: RXRs: collegial partners. *Sub-cellular biochemistry*, 70: 75-102, 2014.
158. Benbrook, DM, Chambon, P, Rochette-Egly, C, Asson-Batres, MA: History of retinoic acid receptors. *Sub-cellular biochemistry*, 70: 1-20, 2014.
159. Mandal, A, Rydeen, A, Anderson, J, Sorrell, MR, Zygmunt, T, Torres-Vazquez, J, Waxman, JS: Transgenic retinoic acid sensor lines in zebrafish indicate regions of available embryonic retinoic acid. *Developmental dynamics : an official publication of the American Association of Anatomists*, 242: 989-1000, 2013.
160. Waxman, JS, Yelon, D: Zebrafish retinoic acid receptors function as context-dependent transcriptional activators. *Dev Biol*, 352: 128-140, 2011.
161. Rossant, J, Zirngibl, R, Cado, D, Shago, M, Giguere, V: Expression of a retinoic acid response element-hsplacZ transgene defines specific domains of transcriptional activity during mouse embryogenesis. *Genes Dev*, 5: 1333-1344, 1991.
162. Shimozono, S, Iimura, T, Kitaguchi, T, Higashijima, S, Miyawaki, A: Visualization of an endogenous retinoic acid gradient across embryonic development. *Nature*, 496: 363-366, 2013.

163. le Maire, A, Bourguet, W: Retinoic acid receptors: structural basis for coregulator interaction and exchange. *Sub-cellular biochemistry*, 70: 37-54, 2014.
164. Kumar, S, Duester, G: Retinoic acid controls body axis extension by directly repressing Fgf8 transcription. *Development*, 141: 2972-2977, 2014.
165. Studer, M, Popperl, H, Marshall, H, Kuroiwa, A, Krumlauf, R: Role of a conserved retinoic acid response element in rhombomere restriction of Hoxb-1. *Science*, 265: 1728-1732, 1994.
166. Clagett-Dame, M, Knutson, D: Vitamin A in reproduction and development. *Nutrients*, 3: 385-428, 2011.
167. Das, BC, Thapa, P, Karki, R, Das, S, Mahapatra, S, Liu, TC, Torregroza, I, Wallace, DP, Kambhampati, S, Van Veldhuizen, P, Verma, A, Ray, SK, Evans, T: Retinoic acid signaling pathways in development and diseases. *Bioorganic & medicinal chemistry*, 22: 673-683, 2014.
168. Rhinn, M, Dolle, P: Retinoic acid signalling during development. *Development*, 139: 843-858, 2012.
169. Cartry, J, Nichane, M, Ribes, V, Colas, A, Riou, JF, Pieler, T, Dolle, P, Bellefroid, EJ, Umbhauer, M: Retinoic acid signalling is required for specification of pronephric cell fate. *Developmental biology*, 299: 35-51, 2006.
170. Kim, D, Dressler, GR: Nephrogenic factors promote differentiation of mouse embryonic stem cells into renal epithelia. *Journal of the American Society of Nephrology : JASN*, 16: 3527-3534, 2005.
171. Wingert, RA, Selleck, R, Yu, J, Song, HD, Chen, Z, Song, A, Zhou, Y, Thisse, B, Thisse, C, McMahon, AP, Davidson, AJ: The cdx genes and retinoic acid control the positioning and segmentation of the zebrafish pronephros. *PLoS genetics*, 3: 1922-1938, 2007.
172. Wingert, RA, Davidson, AJ: Zebrafish nephrogenesis involves dynamic spatiotemporal expression changes in renal progenitors and essential signals from retinoic acid and irx3b. *Developmental dynamics : an official publication of the American Association of Anatomists*, 240: 2011-2027, 2011.
173. Vilar, J, Gilbert, T, Moreau, E, Merlet-Benichou, C: Metanephros organogenesis is highly stimulated by vitamin A derivatives in organ culture. *Kidney international*, 49: 1478-1487, 1996.
174. Mendelsohn, C, Lohnes, D, Decimo, D, Lufkin, T, LeMeur, M, Chambon, P, Mark, M: Function of the retinoic acid receptors (RARs) during development (II). Multiple abnormalities at various stages of organogenesis in RAR double mutants. *Development*, 120: 2749-2771, 1994.

175. Wilson, JG, Warkany, J: Malformations in the genito-urinary tract induced by maternal vitamin A deficiency in the rat. *The American journal of anatomy*, 83: 357-407, 1948.
176. Lelievre-Pegorier, M, Vilar, J, Ferrier, ML, Moreau, E, Freund, N, Gilbert, T, Merlet-Benichou, C: Mild vitamin A deficiency leads to inborn nephron deficit in the rat. *Kidney international*, 54: 1455-1462, 1998.
177. Goodyer, P, Kurpad, A, Rekha, S, Muthayya, S, Dwarkanath, P, Iyengar, A, Philip, B, Mhaskar, A, Benjamin, A, Maharaj, S, Laforte, D, Raju, C, Phadke, K: Effects of maternal vitamin A status on kidney development: a pilot study. *Pediatric nephrology*, 22: 209-214, 2007.
178. Maden, M, Hind, M: Retinoic acid, a regeneration-inducing molecule. *Developmental dynamics : an official publication of the American Association of Anatomists*, 226: 237-244, 2003.
179. Gudas, LJ: Emerging roles for retinoids in regeneration and differentiation in normal and disease states. *Biochim Biophys Acta*, 1821: 213-221, 2012.
180. Blum, N, Begemann, G: Retinoic acid signaling controls the formation, proliferation and survival of the blastema during adult zebrafish fin regeneration. *Development*, 139: 107-116, 2012.
181. Mathew, LK, Sengupta, S, Franzosa, JA, Perry, J, La Du, J, Andreasen, EA, Tanguay, RL: Comparative expression profiling reveals an essential role for raldh2 in epimorphic regeneration. *J Biol Chem*, 284: 33642-33653, 2009.
182. Maden, M: Retinoic acid in the development, regeneration and maintenance of the nervous system. *Nature reviews Neuroscience*, 8: 755-765, 2007.
183. Kikuchi, K, Holdway, JE, Major, RJ, Blum, N, Dahn, RD, Begemann, G, Poss, KD: Retinoic acid production by endocardium and epicardium is an injury response essential for zebrafish heart regeneration. *Dev Cell*, 20: 397-404, 2011.
184. Lee, MY, Lu, A, Gudas, LJ: Transcriptional regulation of Rex1 (zfp42) in normal prostate epithelial cells and prostate cancer cells. *Journal of cellular physiology*, 224: 17-27, 2010.
185. Bushue, N, Wan, YJ: Retinoid pathway and cancer therapeutics. *Advanced drug delivery reviews*, 62: 1285-1298, 2010.
186. Lazzeri, E, Peired, AJ, Lasagni, L, Romagnani, P: Retinoids and glomerular regeneration. *Seminars in nephrology*, 34: 429-436, 2014.
187. Mallipattu, SK, He, JC: The beneficial role of retinoids in glomerular disease. *Frontiers in medicine*, 2: 16, 2015.

188. Han, SY, So, GA, Jee, YH, Han, KH, Kang, YS, Kim, HK, Kang, SW, Han, DS, Han, JY, Cha, DR: Effect of retinoic acid in experimental diabetic nephropathy. *Immunology and cell biology*, 82: 568-576, 2004.
189. Perez de Lema, G, Lucio-Cazana, FJ, Molina, A, Luckow, B, Schmid, H, de Wit, C, Moreno-Manzano, V, Banas, B, Mampaso, F, Schlondorff, D: Retinoic acid treatment protects MRL/lpr lupus mice from the development of glomerular disease. *Kidney international*, 66: 1018-1028, 2004.
190. Suzuki, A, Ito, T, Imai, E, Yamato, M, Iwatani, H, Kawachi, H, Hori, M: Retinoids regulate the repairing process of the podocytes in puromycin aminonucleoside-induced nephrotic rats. *Journal of the American Society of Nephrology : JASN*, 14: 981-991, 2003.
191. Wagner, J, Dechow, C, Morath, C, Lehrke, I, Amann, K, Waldherr, R, Floege, J, Ritz, E: Retinoic acid reduces glomerular injury in a rat model of glomerular damage. *Journal of the American Society of Nephrology : JASN*, 11: 1479-1487, 2000.
192. Ratnam, KK, Feng, X, Chuang, PY, Verma, V, Lu, TC, Wang, J, Jin, Y, Farias, EF, Napoli, JL, Chen, N, Kaufman, L, Takano, T, D'Agati, VD, Klotman, PE, He, JC: Role of the retinoic acid receptor-alpha in HIV-associated nephropathy. *Kidney international*, 79: 624-634, 2011.
193. Zhang, J, Pippin, JW, Vaughan, MR, Krofft, RD, Taniguchi, Y, Romagnani, P, Nelson, PJ, Liu, ZH, Shankland, SJ: Retinoids augment the expression of podocyte proteins by glomerular parietal epithelial cells in experimental glomerular disease. *Nephron Experimental nephrology*, 121: e23-37, 2012.
194. Peired, A, Angelotti, ML, Ronconi, E, la Marca, G, Mazzinghi, B, Sisti, A, Lombardi, D, Giocaliere, E, Della Bona, M, Villanelli, F, Parente, E, Ballerini, L, Sagrinati, C, Wanner, N, Huber, TB, Liapis, H, Lazzeri, E, Lasagni, L, Romagnani, P: Proteinuria impairs podocyte regeneration by sequestering retinoic acid. *Journal of the American Society of Nephrology : JASN*, 24: 1756-1768, 2013.
195. Kishimoto, K, Kinoshita, K, Hino, S, Yano, T, Nagare, Y, Shimazu, H, Nozaki, Y, Sugiyama, M, Ikoma, S, Funauichi, M: Therapeutic effect of retinoic acid on unilateral ureteral obstruction model. *Nephron Experimental nephrology*, 118: e69-78, 2011.
196. Menegola, E, Di Renzo, F, Broccia, ML, Giavini, E: Inhibition of histone deacetylase as a new mechanism of teratogenesis. *Birth Defects Res C Embryo Today*, 78: 345-353, 2006.
197. Altucci, L, Gronemeyer, H: The promise of retinoids to fight against cancer. *Nat Rev Cancer*, 1: 181-193, 2001.
198. Berg, WJ, Schwartz, LH, Amsterdam, A, Mazumdar, M, Vlamis, V, Law, TM, Nanus, DM, Motzer, RJ: A phase II study of 13-cis-retinoic acid in patients with advanced renal cell carcinoma. *Invest New Drugs*, 15: 353-355, 1997.

199. Wang, XF, Qian, DZ, Ren, M, Kato, Y, Wei, Y, Zhang, L, Fansler, Z, Clark, D, Nakanishi, O, Pili, R: Epigenetic modulation of retinoic acid receptor beta2 by the histone deacetylase inhibitor MS-275 in human renal cell carcinoma. *Clin Cancer Res*, 11: 3535-3542, 2005.
200. Touma, SE, Goldberg, JS, Moench, P, Guo, X, Tickoo, SK, Gudas, LJ, Nanus, DM: Retinoic acid and the histone deacetylase inhibitor trichostatin a inhibit the proliferation of human renal cell carcinoma in a xenograft tumor model. *Clin Cancer Res*, 11: 3558-3566, 2005.
201. Rettig, I, Koenke, E, Trippel, F, Mueller, WC, Burhenne, J, Kopp-Schneider, A, Fabian, J, Schober, A, Fernekorn, U, von Deimling, A, Deubzer, HE, Milde, T, Witt, O, Oehme, I: Selective inhibition of HDAC8 decreases neuroblastoma growth in vitro and in vivo and enhances retinoic acid-mediated differentiation. *Cell death & disease*, 6: e1657, 2015.
202. Jiang, M, Zhu, K, Grenet, J, Lahti, JM: Retinoic acid induces caspase-8 transcription via phospho-CREB and increases apoptotic responses to death stimuli in neuroblastoma cells. *Biochim Biophys Acta*, 1783: 1055-1067, 2008.
203. Pili, R, Salumbides, B, Zhao, M, Altio, S, Qian, D, Zwiebel, J, Carducci, MA, Rudek, MA: Phase I study of the histone deacetylase inhibitor entinostat in combination with 13-cis retinoic acid in patients with solid tumours. *Br J Cancer*, 106: 77-84, 2012.
204. de Groh, ED, Swanhart, LM, Cosentino, CC, Jackson, RL, Dai, W, Kitchens, CA, Day, BW, Smithgall, TE, Hukriede, NA: Inhibition of histone deacetylase expands the renal progenitor cell population. *J Am Soc Nephrol*, 21: 794-802, 2010.
205. Howe, K, Clark, MD, Torroja, CF, Torrance, J, Berthelot, C, Muffato, M, Collins, JE, Humphray, S, McLaren, K, Matthews, L, McLaren, S, Sealy, I, Caccamo, M, Churcher, C, Scott, C, Barrett, JC, Koch, R, Rauch, GJ, White, S, Chow, W, Kilian, B, Quintais, LT, Guerra-Assuncao, JA, Zhou, Y, Gu, Y, Yen, J, Vogel, JH, Eyre, T, Redmond, S, Banerjee, R, Chi, J, Fu, B, Langley, E, Maguire, SF, Laird, GK, Lloyd, D, Kenyon, E, Donaldson, S, Sehra, H, Almeida-King, J, Loveland, J, Trevanion, S, Jones, M, Quail, M, Willey, D, Hunt, A, Burton, J, Sims, S, McLay, K, Plumb, B, Davis, J, Clee, C, Oliver, K, Clark, R, Riddle, C, Elliot, D, Threadgold, G, Harden, G, Ware, D, Begum, S, Mortimore, B, Kerry, G, Heath, P, Phillimore, B, Tracey, A, Corby, N, Dunn, M, Johnson, C, Wood, J, Clark, S, Pelan, S, Griffiths, G, Smith, M, Glithero, R, Howden, P, Barker, N, Lloyd, C, Stevens, C, Harley, J, Holt, K, Panagiotidis, G, Lovell, J, Beasley, H, Henderson, C, Gordon, D, Auger, K, Wright, D, Collins, J, Raisen, C, Dyer, L, Leung, K, Robertson, L, Ambridge, K, Leongamornlert, D, McGuire, S, Gilderthorp, R, Griffiths, C, Manthavadi, D, Nichol, S, Barker, G, Whitehead, S, Kay, M, Brown, J, Murnane, C, Gray, E, Humphries, M, Sycamore, N, Barker, D, Saunders, D, Wallis, J, Babbage, A, Hammond, S, Mashregi-Mohammadi, M, Barr, L, Martin, S, Wray, P, Ellington, A, Matthews, N, Ellwood, M, Woodmansey, R, Clark, G, Cooper, J, Tromans, A, Grafham, D, Skuce, C, Pandian, R, Andrews, R, Harrison, E, Kimberley, A, Garnett, J, Fosker, N, Hall, R, Garner, P, Kelly, D, Bird, C, Palmer, S, Gehring, I, Berger, A, Dooley, CM, Ersan-Urun, Z, Eser, C, Geiger, H, Geisler, M, Karotki, L, Kirn, A,

- Konantz, J, Konantz, M, Oberlander, M, Rudolph-Geiger, S, Teucke, M, Lanz, C, Raddatz, G, Osoegawa, K, Zhu, B, Rapp, A, Widaa, S, Langford, C, Yang, F, Schuster, SC, Carter, NP, Harrow, J, Ning, Z, Herrero, J, Searle, SM, Enright, A, Geisler, R, Plasterk, RH, Lee, C, Westerfield, M, de Jong, PJ, Zon, LI, Postlethwait, JH, Nusslein-Volhard, C, Hubbard, TJ, Roest Crollius, H, Rogers, J, Stemple, DL: The zebrafish reference genome sequence and its relationship to the human genome. *Nature*, 496: 498-503, 2013.
206. Cianciolo Cosentino, C, Roman, BL, Drummond, IA, Hukriede, NA: Intravenous microinjections of zebrafish larvae to study acute kidney injury. *J Vis Exp*, 2010.
 207. Hentschel, DM, Park, KM, Cilenti, L, Zervos, AS, Drummond, I, Bonventre, JV: Acute renal failure in zebrafish: a novel system to study a complex disease. *American journal of physiology Renal physiology*, 288: F923-929, 2005.
 208. Diep, CQ, Ma, D, Deo, RC, Holm, TM, Naylor, RW, Arora, N, Wingert, RA, Bollig, F, Djordjevic, G, Lichman, B, Zhu, H, Ikenaga, T, Ono, F, Englert, C, Cowan, CA, Hukriede, NA, Handin, RI, Davidson, AJ: Identification of adult nephron progenitors capable of kidney regeneration in zebrafish. *Nature*, 470: 95-100, 2011.
 209. Keightley, MC, Wang, CH, Pazhakh, V, Lieschke, GJ: Delineating the roles of neutrophils and macrophages in zebrafish regeneration models. *Int J Biochem Cell Biol*, 56: 92-106, 2014.
 210. Novoa, B, Figueras, A: Zebrafish: model for the study of inflammation and the innate immune response to infectious diseases. *Advances in experimental medicine and biology*, 946: 253-275, 2012.
 211. Zon, LI, Peterson, RT: In vivo drug discovery in the zebrafish. *Nat Rev Drug Discov*, 4: 35-44, 2005.
 212. Sanker, S, Cirio, MC, Vollmer, LL, Goldberg, ND, McDermott, LA, Hukriede, NA, Vogt, A: Development of high-content assays for kidney progenitor cell expansion in transgenic zebrafish. *Journal of biomolecular screening*, 18: 1193-1202, 2013.
 213. Karasawa, T, Wang, Q, David, LL, Steyger, PS: Calreticulin binds to gentamicin and reduces drug-induced ototoxicity. *Toxicological sciences : an official journal of the Society of Toxicology*, 124: 378-387, 2011.
 214. Lopez-Novoa, JM, Quiros, Y, Vicente, L, Morales, AI, Lopez-Hernandez, FJ: New insights into the mechanism of aminoglycoside nephrotoxicity: an integrative point of view. *Kidney international*, 79: 33-45, 2011.
 215. Cianciolo Cosentino, C, Skrypnik, NI, Brilli, LL, Chiba, T, Novitskaya, T, Woods, C, West, J, Korotchenko, VN, McDermott, L, Day, BW, Davidson, AJ, Harris, RC, de Caestecker, MP, Hukriede, NA: Histone deacetylase inhibitor enhances recovery after AKI. *Journal of the American Society of Nephrology : JASN*, 24: 943-953, 2013.

216. Ichimura, T, Bonventre, JV, Bailly, V, Wei, H, Hession, CA, Cate, RL, Sanicola, M: Kidney injury molecule-1 (KIM-1), a putative epithelial cell adhesion molecule containing a novel immunoglobulin domain, is up-regulated in renal cells after injury. *J Biol Chem*, 273: 4135-4142, 1998.
217. Nielsen, SE, Schjoedt, KJ, Astrup, AS, Tarnow, L, Lajer, M, Hansen, PR, Parving, HH, Rossing, P: Neutrophil Gelatinase-Associated Lipocalin (NGAL) and Kidney Injury Molecule 1 (KIM1) in patients with diabetic nephropathy: a cross-sectional study and the effects of lisinopril. *Diabetic medicine : a journal of the British Diabetic Association*, 27: 1144-1150, 2010.
218. Vanmassenhove, J, Vanholder, R, Nagler, E, Van Biesen, W: Urinary and serum biomarkers for the diagnosis of acute kidney injury: an in-depth review of the literature. *Nephrol Dial Transplant*, 28: 254-273, 2013.
219. Charlton, JR, Portilla, D, Okusa, MD: A basic science view of acute kidney injury biomarkers. *Nephrol Dial Transplant*, 29: 1301-1311, 2014.
220. Singh, AP, Junemann, A, Muthuraman, A, Jaggi, AS, Singh, N, Grover, K, Dhawan, R: Animal models of acute renal failure. *Pharmacological reports : PR*, 64: 31-44, 2012.
221. Chiba, T, Skrypnik, NI, Skvarca, LB, Penchev, R, Zhang, KX, Rochon, ER, Fall, JL, Pauksakon, P, Yang, H, Alford, CE, Roman, BL, Zhang, MZ, Harris, RC, Hukriede, NA, de Caestecker, MP: Retinoic acid signaling coordinates macrophage-dependent injury and repair after AKI. *Journal of the American Society of Nephrology : JASN*, In press, 2015.
222. Humphreys, BD, Czerniak, S, DiRocco, DP, Hasnain, W, Cheema, R, Bonventre, JV: Repair of injured proximal tubule does not involve specialized progenitors. *Proceedings of the National Academy of Sciences of the United States of America*, 108: 9226-9231, 2011.
223. Maeshima, A, Maeshima, K, Nojima, Y, Kojima, I: Involvement of Pax-2 in the action of activin A on tubular cell regeneration. *Journal of the American Society of Nephrology : JASN*, 13: 2850-2859, 2002.
224. Drummond, IA, Majumdar, A, Hentschel, H, Elger, M, Solnica-Krezel, L, Schier, AF, Neuhauss, SC, Stemple, DL, Zwartkruis, F, Rangini, Z, Driever, W, Fishman, MC: Early development of the zebrafish pronephros and analysis of mutations affecting pronephric function. *Development*, 125: 4655-4667, 1998.
225. Kitaguchi, T, Kawakami, K, Kawahara, A: Transcriptional regulation of a myeloid-lineage specific gene lysozyme C during zebrafish myelopoiesis. *Mechanisms of development*, 126: 314-323, 2009.
226. Ellett, F, Pase, L, Hayman, JW, Andrianopoulos, A, Lieschke, GJ: mpeg1 promoter transgenes direct macrophage-lineage expression in zebrafish. *Blood*, 117: e49-56, 2011.

227. Murayama, E, Kissa, K, Zapata, A, Mordelet, E, Briolat, V, Lin, HF, Handin, RI, Herbomel, P: Tracing hematopoietic precursor migration to successive hematopoietic organs during zebrafish development. *Immunity*, 25: 963-975, 2006.
228. Harvie, EA, Green, JM, Neely, MN, Huttenlocher, A: Innate immune response to *Streptococcus iniae* infection in zebrafish larvae. *Infection and immunity*, 81: 110-121, 2013.
229. Dong, X, Swaminathan, S, Bachman, LA, Croatt, AJ, Nath, KA, Griffin, MD: Resident dendritic cells are the predominant TNF-secreting cell in early renal ischemia-reperfusion injury. *Kidney international*, 71: 619-628, 2007.
230. Westerfield, M: *The zebrafish book : a guide for the laboratory use of zebrafish (Brachydanio rerio)*, Eugene, OR, M. Westerfield, 1993.
231. Mahler, J, Filippi, A, Driever, W: DeltaA/DeltaD regulate multiple and temporally distinct phases of notch signaling during dopaminergic neurogenesis in zebrafish. *The Journal of neuroscience : the official journal of the Society for Neuroscience*, 30: 16621-16635, 2010.
232. Johnson, CS, Holzemer, NF, Wingert, RA: Laser ablation of the zebrafish pronephros to study renal epithelial regeneration. *Journal of visualized experiments : JoVE*, 2011.
233. Wang, Y, Sun, ZH, Zhou, L, Li, Z, Gui, JF: Grouper tshbeta promoter-driven transgenic zebrafish marks proximal kidney tubule development. *PloS one*, 9: e97806, 2014.
234. Zhou, W, Hildebrandt, F: Inducible podocyte injury and proteinuria in transgenic zebrafish. *Journal of the American Society of Nephrology : JASN*, 23: 1039-1047, 2012.
235. Hutchinson, TH, Bogi, C, Winter, MJ, Owens, JW: Benefits of the maximum tolerated dose (MTD) and maximum tolerated concentration (MTC) concept in aquatic toxicology. *Aquatic toxicology*, 91: 197-202, 2009.
236. Novitskaya, T, McDermott, L, Zhang, KX, Chiba, T, Pauksakon, P, Hukriede, NA, de Caestecker, MP: A PTBA small molecule enhances recovery and reduces postinjury fibrosis after aristolochic acid-induced kidney injury. *American journal of physiology Renal physiology*, 306: F496-504, 2014.
237. Wynn, TA: Fibrosis under arrest. *Nature medicine*, 16: 523-525, 2010.
238. Pang, M, Kothapally, J, Mao, H, Tolbert, E, Ponnusamy, M, Chin, YE, Zhuang, S: Inhibition of histone deacetylase activity attenuates renal fibroblast activation and interstitial fibrosis in obstructive nephropathy. *American journal of physiology Renal physiology*, 297: F996-F1005, 2009.
239. Arany, I, Herbert, J, Herbert, Z, Safirstein, RL: Restoration of CREB function ameliorates cisplatin cytotoxicity in renal tubular cells. *American journal of physiology Renal physiology*, 294: F577-581, 2008.

240. Kim, HJ, Rowe, M, Ren, M, Hong, JS, Chen, PS, Chuang, DM: Histone deacetylase inhibitors exhibit anti-inflammatory and neuroprotective effects in a rat permanent ischemic model of stroke: multiple mechanisms of action. *J Pharmacol Exp Ther*, 321: 892-901, 2007.
241. Shein, NA, Grigoriadis, N, Alexandrovich, AG, Simeonidou, C, Lourbopoulos, A, Polyzoidou, E, Trembovler, V, Mascagni, P, Dinarello, CA, Shohami, E: Histone deacetylase inhibitor ITF2357 is neuroprotective, improves functional recovery, and induces glial apoptosis following experimental traumatic brain injury. *Faseb J*, 23: 4266-4275, 2009.
242. Bouche-careilh, M, Hutt, DM, Szajner, P, Flotte, TR, Balch, WE: Histone deacetylase inhibitor (HDACi) suberoylanilide hydroxamic acid (SAHA)-mediated correction of alpha1-antitrypsin deficiency. *J Biol Chem*, 287: 38265-38278, 2012.
243. Shimazu, T, Hirschey, MD, Newman, J, He, W, Shirakawa, K, Le Moan, N, Grueter, CA, Lim, H, Saunders, LR, Stevens, RD, Newgard, CB, Farese, RV, Jr., de Cabo, R, Ulrich, S, Akassoglou, K, Verdin, E: Suppression of oxidative stress by beta-hydroxybutyrate, an endogenous histone deacetylase inhibitor. *Science*, 339: 211-214, 2013.
244. Chen, Y, He, R, Chen, Y, D'Annibale, MA, Langley, B, Kozikowski, AP: Studies of benzamide- and thiol-based histone deacetylase inhibitors in models of oxidative-stress-induced neuronal death: identification of some HDAC3-selective inhibitors. *ChemMedChem*, 4: 842-852, 2009.
245. Himmelfarb, J, McMonagle, E, Freedman, S, Klenzak, J, McMenamin, E, Le, P, Pupim, LB, Ikizler, TA, The, PG: Oxidative stress is increased in critically ill patients with acute renal failure. *Journal of the American Society of Nephrology : JASN*, 15: 2449-2456, 2004.
246. Bohnsack, BL, Kasprick, DS, Kish, PE, Goldman, D, Kahana, A: A zebrafish model of axenfeld-riege syndrome reveals that pitx2 regulation by retinoic acid is essential for ocular and craniofacial development. *Investigative ophthalmology & visual science*, 53: 7-22, 2012.
247. Lengerke, C, Wingert, R, Beeretz, M, Grauer, M, Schmidt, AG, Konantz, M, Daley, GQ, Davidson, AJ: Interactions between Cdx genes and retinoic acid modulate early cardiogenesis. *Developmental biology*, 354: 134-142, 2011.
248. Waxman, JS, Keegan, BR, Roberts, RW, Poss, KD, Yelon, D: Hoxb5b acts downstream of retinoic acid signaling in the forelimb field to restrict heart field potential in zebrafish. *Dev Cell*, 15: 923-934, 2008.
249. Chudakov, DM, Matz, MV, Lukyanov, S, Lukyanov, KA: Fluorescent proteins and their applications in imaging living cells and tissues. *Physiological reviews*, 90: 1103-1163, 2010.

250. Hebisch, E, Knebel, J, Landsberg, J, Frey, E, Leisner, M: High variation of fluorescence protein maturation times in closely related *Escherichia coli* strains. *PloS one*, 8: e75991, 2013.
251. Perez, A, Ramirez-Ramos, M, Calleja, C, Martin, D, Namorado, MC, Sierra, G, Ramirez-Ramos, ME, Paniagua, R, Sanchez, Y, Arreola, L, Reyes, JL: Beneficial effect of retinoic acid on the outcome of experimental acute renal failure. *Nephrol Dial Transplant*, 19: 2464-2471, 2004.
252. Zhou, TB, Drummen, GP, Qin, YH: The controversial role of retinoic Acid in fibrotic diseases: analysis of involved signaling pathways. *International journal of molecular sciences*, 14: 226-243, 2012.
253. Lam, PY, Harvie, EA, Huttenlocher, A: Heat shock modulates neutrophil motility in zebrafish. *PloS one*, 8: e84436, 2013.
254. Glaser, KB, Staver, MJ, Waring, JF, Stender, J, Ulrich, RG, Davidsen, SK: Gene expression profiling of multiple histone deacetylase (HDAC) inhibitors: defining a common gene set produced by HDAC inhibition in T24 and MDA carcinoma cell lines. *Molecular cancer therapeutics*, 2: 151-163, 2003.
255. Haberland, M, Mokalled, MH, Montgomery, RL, Olson, EN: Epigenetic control of skull morphogenesis by histone deacetylase 8. *Genes Dev*, 23: 1625-1630, 2009.
256. Saha, A, Pandian, GN, Sato, S, Taniguchi, J, Hashiya, K, Bando, T, Sugiyama, H: Synthesis and biological evaluation of a targeted DNA-binding transcriptional activator with HDAC8 inhibitory activity. *Bioorganic & medicinal chemistry*, 21: 4201-4209, 2013.
257. Dong, G, Wang, L, Wang, CY, Yang, T, Kumar, MV, Dong, Z: Induction of apoptosis in renal tubular cells by histone deacetylase inhibitors, a family of anticancer agents. *J Pharmacol Exp Ther*, 325: 978-984, 2008.
258. Arany, I, Clark, JS, Ember, I, Juncos, LA: Epigenetic modifiers exert renal toxicity through induction of p66shc. *Anticancer Research*, 31: 3267-3272, 2011.
259. Mulder, GJ, Meerman, JH: Sulfation and glucuronidation as competing pathways in the metabolism of hydroxamic acids: the role of N,O-sulfonation in chemical carcinogenesis of aromatic amines. *Environ Health Perspect*, 49: 27-32, 1983.